



OPEN

Compartmental Models Driven by Renewal Processes: Survival Analysis and Applications to SVIS Epidemic Models

Divine Wanduku¹✉ & Md Mahmud Hasan²

Compartmental models with exponentially distributed lifetime stages assume a constant hazard rate, limiting their scope. This study develops a theoretical framework for systems with general lifetime distributions, modeled as transition rates in a renewal process. Applications are provided for the SVIS (Susceptible-Vaccinated-Infected-Susceptible) disease epidemic model to investigate the impacts of hazard rate functions (HRFs) on disease control. The novel SVIS model is formulated as a non-autonomous nonlinear system (NANLS) of ordinary differential equations (ODEs), with coefficients defined by HRFs. Key statistical properties and the *basic reproduction number* (\mathfrak{R}_0) are derived, and conditions for the system's asymptotic autonomy are established for specific lifetime distributions. Four HRF behaviors—*monotonic, bathtub, reverse bathtub, and constant*—are analyzed to determine conditions for disease eradication and the asymptotic population under these scenarios. Sensitivity analysis examines how HRF behaviors shape system trajectories. Numerical simulations illustrate the influence of diverse lifetime models on vaccine efficacy and immunity, offering insights for effective disease management.

Keywords Hazard rate function, Jump Process, Non-autonomous ODE, Renewal process, Asymptotically autonomous system, SVIS model, Random interjump times

Compartmental dynamic models expressed as systems of differential equations (d.e.s) have a long history of application to investigate biological, epidemiological, biochemical and social dynamical systems etc. (cf.¹⁻⁹), which represent the evolution of systems of biochemical reactions between chemical species; represent the transmission dynamics of a communicable disease in a population; represent ecological interactions between biological species, such as, *predator-prey* systems; represent the connectivity dynamics between nodes in a complex social network, where links are the social ties between subjects socializing in the network etc.

For example, for an M species ecological system, where X_i is the i^{th} specie, and the vector $X(t) = (X_1(t), X_2(t), \dots, X_M(t))$ are all species, then a model for the average dynamic interactions between the M species is expressed either as an *autonomous nonlinear system* (ANLS),

$$dX(t) = f(X(t))dt = [A(X(t))X(t)]dt, \quad (1.1)$$

or *non-autonomous nonlinear system* (NANLS),

$$dX(t) = f(t, X(t))dt = [A(t, X(t))X(t)]dt, \quad (1.2)$$

where f is the vector of nonlinear rate functions for the system expressed further for the ANLS in (1.1) as the product of the matrix function $A(X(t)) \in \mathbb{R}^{M \times M}$ with constant coefficients and the vector $X(t)$; and expressed in NANLS in (1.2) as the product of the matrix function $A(t, X(t)) \in \mathbb{R}^{M \times M}$ with coefficients that are continuous functions of time t and the vector $X(t)$. The systems (1.1)-(1.2) can take either *homogeneous or non-homogeneous forms* (cf.¹).

¹Department of Mathematical Sciences, Georgia Southern University, 65 Georgia Ave, Room 3309, Statesboro, Georgia 30460, USA. ²Department of Biostatistics, Data Science and Epidemiology, School of Public Health, Augusta University, 1120, 15th Street, Augusta, GA 30912, USA. ✉email: dwanduku@georgiasouthern.edu; wandukudivine@yahoo.com

An example of the ANLS in (1.1) is the classic SVIS epidemic model (cf.¹⁰) with $M = 3$ states: susceptible S , vaccinated V , and infected I states; the vaccination confers partial artificial immunity; and includes vital dynamics; and for a fixed population with size N i.e. $N = S(t) + I(t) + V(t)$, the dynamics is given by,

$$\begin{aligned} dS(t) &= \left[\alpha_{ND}N - \beta_{IS}\frac{I(t)}{N}S(t) - \alpha_{SV}S(t) + \alpha_{VS}V(t) + \alpha_{IS}I(t) - \alpha_{ND}S(t) \right] dt, \\ dV(t) &= \left[\alpha_{SV}S(t) - \beta_{IV}\frac{I(t)}{N}V(t) - \alpha_{VS}V(t) - \alpha_{ND}V(t) \right] dt, \\ dI(t) &= \left[\beta_{IS}\frac{I(t)}{N}S(t) + \beta_{IV}\frac{I(t)}{N}V(t) - \alpha_{IS}I(t) - \alpha_{ND}I(t) \right] dt, \end{aligned} \quad (1.3)$$

where α_{ij} is an exponential conversion rate from state i to j , $i, j \in \{S, V, I\}$; and β_{IV} and β_{IS} are exponential disease transmission rates from state I to either state S or state V , respectively; and α_{ND} is both the birth and death rates.

Underlying the ANLS (1.3) is a special type of *jump process* called a *Markov jump process* or a *continuous time Markov chain (CTMC)*; and in particular, a *birth-and-death process* (cf.^{3,7}), that assumes that only *single* transitions among the 3 states in the compartments (S, V, I), occur over random interjump times τ_{ij} , between states $i, j \forall i, j \in \{S, V, I\}, i \neq j$ that are *exponentially distributed* with non-homogeneous exponential rates. Moreover, the infinitesimal generator transition rate matrix is derived from (1.3) (see^{3,5,7} for examples of the underlying CTMC). For instance, the interaction between a single susceptible individual 1_S , and a given number of infectious individuals $I(t)$ over a small time interval $[t, t + \Delta t]$, occurs at the exponential rate $\beta_{IS}\frac{I(t)}{N}\Delta t$; and this leads to an infection, and addition of a single infectious individual 1_I . This is denoted by the reaction rate equations $1_S + I(t) \xrightarrow{\beta_{IS}\frac{I(t)}{N}\Delta t} I(t) + 1_I$. Similarly, the interaction between a single vaccinated individual 1_V and $I(t)$, leads to infection, denoted by $1_V + I(t) \xrightarrow{\beta_{IV}\frac{I(t)}{N}\Delta t} I(t) + 1_I$. Recall^{4,6}, this sort of interaction between susceptible and infectious individuals, or interactions between a predator and prey, that requires homogeneous mixing between two species is called *mass-action kinetics or interactions*.

The mathematical principles for deriving the *mass-action exponential rates* $\beta_{IS}\frac{I(t)}{N}$ and $\beta_{IV}\frac{I(t)}{N}$ over the small time interval $[t, t + \Delta t]$ are *homogeneous mixing* and the *Binomial-Poisson hierarchical or mixed distribution model* explained in [Theorem 3.1^{11–13}]. In this paper, the transition events between the species S , V , and I denoted by $S(t) \rightarrow I(t)$ & $V(t) \rightarrow I(t)$, where the arrows “ \rightarrow ” point to the direction of transition from one state to another, occur by *mass-action contact (MAC)*. And the random interjump times until a single susceptible or a vaccinated individual gets infected, are denoted by τ_{SI}^{MAC} and τ_{VI}^{MAC} . That is, given that $I(t)$ individuals present at the beginning of the interval $[t, t + \Delta t]$, then

$$\tau_{SI}^{MAC}|I(t) \sim \text{Exponential}(\beta_{IS}\frac{I(t)}{N})\Delta t, \quad \tau_{VI}^{MAC}|I(t) \sim \text{Exponential}(\beta_{IV}\frac{I(t)}{N})\Delta t.$$

While the assumption that the random interjump times τ_{SI}^{MAC} and τ_{VI}^{MAC} are exponentially distributed is justified by assuming the MAC principle, the random interjump times for the following single transition events between the states S , V , and I , that do not require MAC, need not be exponentially distributed (cf.^{14–16}). For example, the time until a susceptible individual is vaccinated τ_{VS} ; the time until an infectious individual recovers from infection τ_{IS} ; the time until an individual is born τ_{BS} ; and the time until an individual dies τ_{XD} (where $B \equiv \text{birth}$, $D \equiv \text{death}$, and $X \in \{S, V, I\}$); over the time interval $[t, t + \Delta t]$, represent events that do not require MAC, and need not be exponentially distributed. In this paper, the transition events mentioned above that do not require MAC are denoted by $S(t) \leftrightarrow V(t)$, $I(t) \rightarrow S(t)$, $\text{birth} \rightarrow S(t)$, and $X(t) \rightarrow \text{death}$, $\forall X \in \{S, V, I\}$, (where the double arrow “ \leftrightarrow ” signifies transition in either directions between the two different states); and these events are called *non-mass-action-contact transition events (non-MAC)*.

Indeed, in (1.3) the assumption of the state $V(t)$ returning to the state $S(t)$ with loss of immunity (denoted by the event $V(t) \rightarrow S(t)$) at the exponential rate α_{VS} per vaccinated individual, signifies that the interjump time, τ_{VS} , until the vaccinated person loses immunity is $\tau_{VS} \sim \text{Exponential}(\alpha_{VS})$. Clearly, this further suggests that the hazard rate function (HRF) for τ_{VS} , denoted by, $\alpha_{\tau_{VS}}(t) = \alpha_{VS}$ is constant, which is unrealistic for representing the lifetime of a vaccine with limited efficacy. In fact, a lifetime model with a monotonic increasing HRF would be more suitable for the immunity lifetime of a vaccine with lower efficacy as depicted in Figure 1. That is, Figure 1 (a) depicts the unrealistic constant rate $\alpha_{VS}V(t)$ of artificial immunity rate for a vaccine with low efficacy in the Markovian model (1.3), compared with the plausible rate $\alpha_{\tau_{VS}}(t)V(t)$ in Figure 1 (b), where $\alpha_{\tau_{VS}}(t)$ is the HRF of the *Lindley distribution* with shape parameters $\theta = 0.75$ (cf.¹⁷).

The question remains how to incorporate more suitable lifetime distributions for the interjump times between the *non-MAC* transition events in a compartmental dynamic model. The second question is how adding the non-

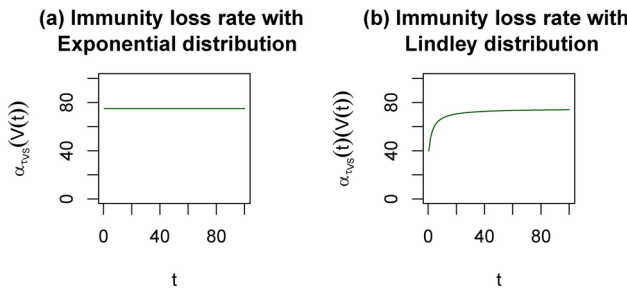


Fig. 1. Shows the unrealistic loss of artificial immunity rate in the Markovian model (1.3), where it is assumed the vaccines has low efficacy. That is, (a) shows a constant rate $\alpha_{VS} V(t)$ in the Markovian model (1.3), where α_{VS} the HRF of the *Exponential distribution* with parameter $\theta = 0.75$; and (b) shows a monotonically increasing rate $\alpha_{VS}(t)V(t)$ expected for a vaccine with low efficacy, where $\alpha_{VS}(t)$ is the HRF of the *Lindley distribution* with shape parameter $\theta = 0.75$. This example, it is assumed that $V(t) = 100, \forall t \in [0, 100]$.

exponentially distributed interjump times modifies and impacts the asymptotic properties of the compartmental model, in particular, the control mechanisms in the system.

A number of authors have considered non-Markovian models for epidemic dynamics with non-exponential lifetime distributions to represent interjump times for various transition events in epidemic dynamics. For instance, in the studies^{15,16} the analysis of deterministic *mean-field* approximations for stochastic models representing epidemic dynamics in human network population structures, where the underlying stochastic disease transmission and recovery processes are non-Markovian is considered. In the study¹⁸, some general non-Markovian stochastic epidemic models are considered, and focus to analyze the asymptotic behavior of the epidemic dynamics in large population sizes. In the study¹⁹, a *renewal process* in a physiologically structured population with application to cell growth is presented. Also see the studies^{14,20,21} that considered derivatives of the exponential distribution.

It is not surprising that when interjump times are no longer exponentially distributed, then the new model for the average dynamics in the system is a NANLS d.e.s, and no longer ANLS of d.e.s. (cf.¹⁴). In this study, the interjump times for the non-MAC events are arbitrary with HRFs that exhibit either *a monotonic, a unimodal, a bathtub, an inverted bathtub, or a constant shape* (cf.^{22,23}). Moreover, the mean-field dynamic equations for the underlying non-Markovian jump processes in the compartmental model are NANLS of d.e.s.

For most compartmental epidemic models (e.g. SIS, SIR, SEIRS models etc.) that are ANLS of o.d.e.s, the control mechanisms (e.g. disease eradication and disease persistence) in the system are investigated by examining the qualitative properties of the equilibria (cf.^{24,25}). On the other hand, epidemic models with NANLS of o.d.e.s (cf.²⁶) have no equilibria. However, under special assumptions of the uniform convergence of the rate functions of the NANLS of o.d.e.s, the NANLS are asymptotically autonomous (cf.^{27,28}), and so insights about the control mechanisms for the NANLS may be drawn asymptotically in the limiting ANLS.

Without losing primary focus on every non-Markovian compartmental model with non-exponentially distributed lifetime stages, this study utilizes the *mean-field dynamics* for the SVIS epidemic dynamics in (1.3) as a special example to elucidate the importance of the statistical properties (e.g. HRFs) of the survival lifetime distributions in the epidemic dynamics. For example, the new SVIS model with general lifetime distribution for the vaccination stage will represent a complex vaccination strategy where a single individual either receives (a) $n > 1$ doses of a given vaccine with distinct immunity lifetimes, or (b) $n > 1$ distinct doses of different vaccines with unique immunity lifetimes. In this complex scenario, the reliability of the vaccination immunity is a *competing risk* (cf.²⁹). In addition, it is shown that when the interjump times for the non-MAC events in the system are no longer exponentially distributed, then a NANLS for the SVIS model (1.3) is obtained, where the system coefficients are HRFs of the interjump times for the non-MAC transition events in the system. Furthermore, the HRFs are selected from a family of functions exhibiting various shapes (e.g. monotonic, unimodal, bathtub, constant) that are ultimately bounded with a uniform constant limit over time, and as a result, the SVIS NANLS model becomes asymptotically a SVIS ANLS model. Moreover, the equilibrium states of the asymptotic SVIS ANLS model, which depend on the asymptotic behaviors of the HRFs are investigated. In fact, by examining the zero-rate trajectory of the NANLS SVIS model, the behaviors of the HRFs and their impacts on the asymptotic steady states are completely characterized. In this study (1) the mathematical and statistical justifications, and a step-by-step approach to incorporate different lifetime distributions for the interjump times for non-MAC events in a compartmental dynamic system are given. (2) The importance of the qualitative behaviors of the HRFs to determine the existence of an ADFE (Asymptotic disease-free equilibrium) for disease eradication is given.

This work is organized as follows. In Section 2, a general model for a renewal process in a dynamic two compartments system is given, and the transition rates for single events over interjump times in the process are derived. In Section 3, the SVIS epidemic model with random interjump times for the non-MAC transition events is derived. In Section 4, the model validation results are given. In Section 5, different types of HRF behaviors are discussed in a dynamic system. In Section 6, the steady states of the asymptotic ANLS SVIS model are given. In Section 7, the sensitivity of the trajectories of the NANLS SVIS system to the qualitative behaviors of the HRFs is characterized. In section 9, numerical simulation results are given. The following notations are used in this study.

Notation 1.1

- (1.) **SVIS**-Susceptible-Vaccinated-Infectious-Susceptible; **HRF** - Hazard rate function; **ADFE** -Asymptotic disease-free equilibrium; **NANLS** - Non-autonomous nonlinear system ; **ANLS** - Autonomous nonlinear system; **o.d.e.s** - Ordinary differential equations; **SVIS** - Susceptible-vaccinated- infectious-susceptible; **CHRF** - Cumulative hazard rate function; **ZRSF** - Zero-rate solution function; **CTMC**- Continuous time Markov chain.
- (2.) *Lindley*(\cdots) abbreviates the **Lindley Distribution** (cf.¹⁷); *Gamma*(\cdots) abbreviates the **Gamma Distribution** (cf.³⁰); *EWFD*(\cdots) abbreviates the **Exponentiated Weibull Family Distribution** (cf.³¹); *EHLD*(\cdots) abbreviates the **Exponentiated Half-Logistic Distribution** (cf.³²); *GPGWD*(\cdots) abbreviates the **Generalized Power Generalized Weibull Distribution** (cf.³³).

Derivation of a jump process for a two compartment dynamic ecological system via the renewal theory

Consider a two compartment population e.g. a species in an ecological environment, or chemical species in a chemical kinetic reaction, composed of two compartments/states $s_i, i = 1, 2$, and at any instant, every individual in the population is in only one of the two states. For example, in a SIS disease epidemic, state s_1 may be the susceptible state (S); s_2 may be the infectious state (I). Also, suppose the two states $s_i, i = 1, 2$ are interrelated, such that, in any small time interval $[t, t + \Delta t]$, an individual in one state s_i may change state to the other state s_j , where $i \neq j$. That is, the two categorical states *communicate* with each other. A *single* transition event where an individual from state s_i changes state to state s_j is denoted by $s_i \rightarrow s_j$. Thus, there are two possible distinct single transitional events $s_i \rightarrow s_j$, and $s_j \rightarrow s_i, i \neq j$ between the two states.

Let $\{C_{ij}(t), t \geq 0\}$ be a general counting process, where $C_{ij}(t)$ is the number of single transition events of type $s_i \rightarrow s_j, i \neq j$ over the interval $[0, t)$. Furthermore, suppose T_k^{ij} is the time that the k^{th} transition event $s_i \rightarrow s_j, i \neq j$ occurred (i.e. the time until the k^{th} individual in state s_i converts to state $s_j, i \neq j$). Clearly, both $C_{ij}(t)$ and T_k^{ij} are random variables, and the collection $\{T_k^{ij}, k \geq 1\}$ are jump times for the counting process $\{C_{ij}(t), t \geq 0\}$, where $\lim_{k \rightarrow \infty} T_k^{ij} = \infty$, and $C_{ij}(t) = \sum_{k=1}^{\infty} \mathbb{I}_{[T_k^{ij}, \infty)}(t)$.

For a special class of *renewal process* for the dynamics, the time until the next jump for the event, $s_i \rightarrow s_j, i \neq j$ occurs (i.e. the time between the $(k-1)^{\text{th}}$ jump and the k^{th} jump), is denoted by τ_{ij}^k , and it is given by $\tau_{ij}^k = T_k^{ij} - T_{k-1}^{ij}$. τ_{ij}^k is also called the *inter-jump time* for the process $\{C_{ij}(t), t \geq 0\}$. It is assumed that all inter-jump times $\tau_{ij}^k, \forall k \geq 1$ are *independent and belong to the same distribution family, but not identically distributed*, since the distribution of τ_{ij}^k depends on the state of the system. Let the inter-jump time τ_{ij}^k be a general lifetime random variable with cumulative density function (CDF) $F_{\tau_{ij}^k}(t), t \geq 0$.

In addition, observe that the time of the n^{th} jump $T_n^{ij} = \sum_{k=1}^n \tau_{ij}^k$; and the distribution of $T_n^{ij} \sim \text{CONV}_{k=1}^n(F_{\tau_{ij}^k}) \equiv F_{\tau_{ij}} * F_{\tau_{ij}} * \dots * F_{\tau_{ij}}^n$, where $\text{CONV}_{k=1}^n(F_{\tau_{ij}^k})$ denotes a convolution of the n CDFs $F_{\tau_{ij}^k}, k = 1, 2, \dots, n$. Furthermore, at anytime $t > 0$, and for $n > 0$ number of transition events, it follows that

$$\mathbb{P}(C_{ij}(t) \geq n) = \mathbb{P}(T_n^{ij} \leq t) = \text{CONV}_{k=1}^n(F_{\tau_{ij}^k})(t), \quad (2.1)$$

and the function $R(t)$ obtained by computing the expected value $R(t) = \mathbb{E}[C_{ij}(t)]$ is called the *renewal function* for the process $\{C_{ij}(t), t \geq 0\}$.

While the inter-jump times $\tau_{ij}^k \sim F_{\tau_{ij}^k}, \forall k \geq 1$ of the counting process need not be IID (Independent Identically Distributed) and *exponentially distributed* as in a *Poisson process* (cf.³⁴), there exists a link between the exponential distribution and the inter-jump times τ_{ij}^k via the *cumulative hazard rate function (CHRF)* of τ_{ij}^k (note that this statement is true for any non-negative random variable. See any text on survival analysis e.g.²²). That is, let $\alpha_{\tau_{ij}^k}(t)$ be the *HRF* for τ_{ij}^k at any instant $t > 0$. Then over the time interval $[0, t)$,

$$\mathbb{P}(\tau_{ij}^k > t) = e^{-A_{ij}^k(t)}, \quad A_{ij}^k(t) = \int_0^t \alpha_{\tau_{ij}^k}(u) du, \quad (2.2)$$

where $A_{ij}^k(t)$ is the CHRF of τ_{ij}^k . That is, assuming the HRF $\alpha_{\tau_{ij}^k}(t)$ for τ_{ij}^k is known, then from (2.2), the CDF $F_{\tau_{ij}^k}(t)$ at time $t > 0$ is equal to the CDF $F_{\text{Exp}(A_{ij}^k(t))}(t)$ for the exponential distribution with the non-homogeneous rate $A_{ij}^k(t)$, i.e.

$$F_{\tau_{ij}^k}(t) = \mathbb{P}(\tau_{ij}^k \leq t) = 1 - e^{-A_{ij}^k(t)} = F_{\text{Exp}(A_{ij}^k(t))}(t). \quad (2.3)$$

Note that the relationship in (2.3) between the distribution $F_{\tau_{ij}^k}(t)$ and the exponential distribution $F_{\text{Exp}(A_{ij}^k(t))}(t)$ does not suggest that the distribution of τ_{ij}^k is the exponential distribution, since the intensity

$A_{ij}^k(t)$ depends on the HRF of τ_{ij}^k . Instead, the relation in (2.3) suggests the following: (1.) a probability generator for τ_{ij}^k is the exponential distribution with intensity given by the CHRF of τ_{ij}^k ; and (2.) there is confirmation for the earlier assumption of independent interjump times that the counting process $\{C_{ij}(t), t \geq 0\}$ along with the family of jump times $\{T_k^{ij}, k \geq 1\}$ defines a process where the time until the next jump exhibits the *no-memory property*, and therefore a *Markov renewal process* (cf.³⁵).

Using (2.3), the rate for each transition event $s_i \rightarrow s_j, i \neq j$ to occur is obtained in the following by applying the *birth-and-death process* (cf.³⁴) of a CTMC, where it is assumed that only a single transition between the states $s_i, s_j, i \neq j$ occurs in a small time interval of length Δt . Suppose $S_i(t)$ is the number of individuals in each state $s_i, i = 1, 2$ at time t (note that $S_i(t)$ is a quantitative variable and s_i is a categorical variable). Without loss of generality (w.l.o.g.), assume that $S_i(t)$ is discrete. Let $g_{s_i s_j}(S_i(t))$ be the rate of a single transition event $s_i \rightarrow s_j, i \neq j, \forall i, j = 1, 2$. The stochastic process $\{(S_1(t), S_2(t)), t \geq 0\}$ will represent the number of individuals in each state at time t , and the transition rates for each event $s_i \rightarrow s_j, i \neq j, \forall i, j = 1, 2$ is exhibited in Figure 2. Over any small time interval $[t, t + \Delta t]$, if the events $s_i \rightarrow s_j$, and $s_j \rightarrow s_i, i \neq j, \forall i, j = 1, 2$ occur, then the possible outcomes for the number of individuals $S_i(t)$ either increases or decreases by one individual, i.e., either $S_i \rightarrow S_i + 1$ or $S_i \rightarrow S_i - 1$. Note that based on the assumptions above, the following discrete time approximation of the continuous time jump process $\{(S_1(t), S_2(t)), t \geq 0\}$ in relationship with the counting process $\{C_{ij}(t), t \geq 0\}$ is obtained (cf.¹¹).

$$\begin{aligned} S_1(t + \Delta t) &= S_1(t) - C_{12}(\Delta t) + C_{21}(\Delta t) \\ S_2(t + \Delta t) &= S_2(t) - C_{21}(\Delta t) + C_{12}(\Delta t), \end{aligned} \quad (2.4)$$

where $C_{12}(\Delta t)$ and $C_{21}(\Delta t)$ are independent, and both random variables $C_{21}(\Delta t) - C_{12}(\Delta t)$ and $C_{12}(\Delta t) - C_{21}(\Delta t)$ have the same support $\{-1, 0, 1\}$. The infinitesimal generator transition probabilities for the stochastic process $\{(S_1(t), S_2(t)), t \geq 0\}$ is derived subsequently.

Let $(\Omega, (\mathfrak{F}_t)_{t \geq 0}, \mathbb{P})$ be a complete probability space, where $(\mathfrak{F}_t)_{t \geq 0}$ is a filtration, and for all $t \geq 0$, \mathfrak{F}_t is the smallest sigma algebra generated by all random vectors $(S_1(t), S_2(t))$, $\forall t \geq 0$ denoted by $\mathfrak{F}_t = \sigma((S_1(r), S_2(r)) : r \in [0, t])$. From (2.3)-(2.4), it is easy to see that $\{(S_1(t), S_2(t)), t \geq 0\}$ is a jump process that generalizes a *continuous time Markov chain*, and for each state $(S_i(t), S_j(t))$, it follows that $\mathbb{P}((S_i(t + \Delta t), S_j(t + \Delta t)) | \mathfrak{F}_t) = \mathbb{P}((S_i(t + \Delta t), S_j(t + \Delta t)) | (S_i(t), S_j(t))), \forall i \neq j$. Moreover, from (2.2) and (2.4), note that $\int_t^{t+\Delta t} \alpha_{\tau_{ij}^k}(u) du = A_{ij}^k(t + \Delta t) - A_{ij}^k(t)$, and it is easy to see that the infinitesimal generator transition probabilities for the jump process are given by

$$\begin{aligned} \mathbb{P}[S_i(t + \Delta t) - S_i(t) = m, S_j(t + \Delta t) - S_j(t) = l | (S_i(t), S_j(t))] \\ = \begin{cases} \alpha_{\tau_{ij}}(t) S_i(t) \Delta t + o(\Delta t), & (m, l) = (-1, 1) \\ \alpha_{\tau_{ji}}(t) S_j(t) \Delta t + o(\Delta t), & (m, l) = (1, -1) \\ 1 - \sum_{j \neq i} \alpha_{\tau_{ij}}(t) S_i(t) \Delta t + o(\Delta t), & (m, l) = (0, 0), \\ o(\Delta t), & \text{otherwise.} \end{cases} \end{aligned} \quad (2.5)$$

The following example illustrates and explains further how (2.2), (2.3) and (2.4) have been used to obtain (2.5).

Example 2.1 Applying the distribution of the interjump times in (2.3), and using the counting process in (2.4), it follows in (2.5) that when $m = -1$ and $l = 1$,

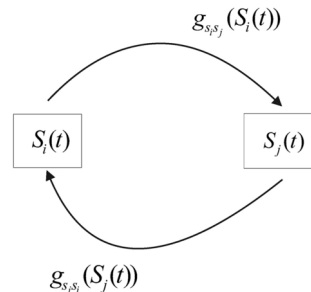


Fig. 2. Shows the framework for the transition dynamics between the two states $s_i, i = 1, 2$ of the system, where $S_i(t)$ is the number of individuals in state s_i . Also, $g_{s_i s_j}(S_i(t)), \forall i \neq j \in \{1, 2\}$ is the transition rate for the event $s_i \rightarrow s_j, i \neq j$, where τ_{ij} is the random time until the next transition occurs.

$$\begin{aligned}
& \mathbb{P}(S_i(t + \Delta t) - S_i(t) = m, S_j(t + \Delta t) - S_j(t) = l | (S_i(t), S_j(t))) \\
& = \mathbb{P}(S_i(t + \Delta t) - S_i(t) = -1, S_j(t + \Delta t) - S_j(t) = 1 | (S_i(t), S_j(t))) \\
& = \mathbb{P}(C_{21}(\Delta t) = 0, C_{12}(\Delta t) = 1 | (S_1(t), S_2(t))) \\
& = \mathbb{P}(C_{21}(\Delta t) = 0 | (S_1(t), S_2(t))) \times \mathbb{P}(C_{12}(\Delta t) = 1 | (S_1(t), S_2(t))) \\
& = \mathbb{P}(C_{12}(\Delta t) = 1 | (S_1(t), S_2(t))) \\
& = \mathbb{P}(\tau_{12}^k \leq t + \Delta t, \tau_{12}^k > t, (S_1(t), S_2(t))) \\
& = 1 - e^{-[A_{12}^k(t + \Delta t) - A_{12}^k(t)]S_1(t)} = 1 - e^{-\left(\int_t^{t + \Delta t} \alpha_{\tau_{12}}(u) du\right)S_1(t)} \\
& \approx \alpha_{\tau_{12}}(t)S_1(t)\Delta t + o(\Delta t).
\end{aligned} \tag{2.6}$$

Thus, in Figure 2, it follows from (2.5) that the conversion rates $g_{s_i s_j}(S_i(t)) = \alpha_{\tau_{ij}}(t)S_i(t)$, and $g_{s_j s_i}(S_j(t)) = \alpha_{\tau_{ji}}(t)S_j(t)$, $\forall i \neq j \in \{1, 2\}$. Furthermore, the average increment for the process $\{(S_1(t), S_2(t)), t \geq 0\}$ over the interval $[t, t + \Delta t]$ is given by

$$\begin{aligned}
\mathbb{E}[S_i(t + \Delta t) - S_i(t) | (S_i(t), S_j(t))] & = [-g_{s_i s_j}(S_i(t)) + g_{s_j s_i}(S_j(t))] \Delta t, \\
\mathbb{E}[S_j(t + \Delta t) - S_j(t) | (S_i(t), S_j(t))] & = [-g_{s_j s_i}(S_j(t)) + g_{s_i s_j}(S_i(t))] \Delta t.
\end{aligned} \tag{2.7}$$

From (2.7), when only the average or mean field dynamics of the jump process $\{(S_1(t), S_2(t)), t \geq 0\}$ is of interest, and no random fluctuations in $[t, t + \Delta t]$ are considered, then by applying the following approximation of the derivative of the smooth average value of (2.7) over time i.e.

$$\begin{aligned}
\lim_{\Delta t \rightarrow 0} \frac{1}{\Delta t} \mathbb{E}[S_i(t + \Delta t) - S_i(t)] & = \lim_{\Delta t \rightarrow 0} \frac{1}{\Delta t} \mathbb{E}[\mathbb{E}[S_i(t + \Delta t) - S_i(t) | (S_i(t), S_j(t))]] \\
& \approx \frac{d\mathbb{E}[S_i(t)]}{dt},
\end{aligned} \tag{2.8}$$

the mean-field dynamics for the system is given by

$$\begin{aligned}
\frac{d\mathbb{E}[S_i(t)]}{dt} & = [-g_{s_i s_j}\mathbb{E}(S_i(t)) + g_{s_j s_i}\mathbb{E}(S_j(t))], \\
\frac{d\mathbb{E}[S_j(t)]}{dt} & = [-g_{s_j s_i}\mathbb{E}(S_j(t)) + g_{s_i s_j}\mathbb{E}(S_i(t))].
\end{aligned} \tag{2.9}$$

To minimize complex notations in the rest of the paper, the deterministic functions $\mathbb{E}[S_i(t)]$ and $\mathbb{E}[S_j(t)]$ will be denoted by the corresponding variables $S_i(t)$, and $S_j(t)$, respectively, without the expectation operator. That is, (2.9) will be rewritten as follows.

$$\begin{aligned}
\frac{dS_i(t)}{dt} & = [-g_{s_i s_j}(S_i(t)) + g_{s_j s_i}(S_j(t))] \\
& = -\alpha_{\tau_{ij}}(t)S_i(t) + \alpha_{\tau_{ji}}(t)S_j(t), \\
\frac{dS_j(t)}{dt} & = [-g_{s_j s_i}(S_j(t)) + g_{s_i s_j}(S_i(t))] \\
& = -\alpha_{\tau_{ji}}(t)S_j(t) + \alpha_{\tau_{ij}}(t)S_i(t).
\end{aligned} \tag{2.10}$$

Remark 2.1 While the jump process in Section 2 has been derived for the dynamics of a two compartment ecological population s_i , $i = 1, 2$, the technique and ideas are easily generalized, inductively, to derive the dynamics for any ecological population with more than two states e.g. SIR, SEIRS, or SVIS epidemic models. The next section provides an application of the SVIS model.

Application to a theoretical SVIS model with general lifetime distributions

In this section, the transition rates for the single events and the interjump times of the renewal process in Section 2 are applied to derive the average dynamics of a SVIS disease epidemic.

Assumptions of the SVIS model

Assumption 3.1 (a1.) Consider a population of a given total size $N(t)$ at time t , that is composed of susceptibles S , vaccinated V with partial artificial immunity and infectious I , where

$$N(t) = S(t) + V(t) + I(t), t \geq 0, \quad N(0) = S(0) + V(0) + I(0) > 0, \tag{3.1}$$

where initially $V(0) \geq 0$, $S(0) > 0$ and $I(0) > 0$. At this point, the population in (3.1) is deterministic, and later when a random population is mentioned, the state of the stochastic process will be conditioned on (3.1) at any time.

- (a2.) There is homogeneous mixing between all species S, V, I , and as explained in Section 1, there is MAC in the transition events $S(t) \rightarrow I(t)$ & from $V(t) \rightarrow I(t)$. Moreover, in the small time interval $[t, t + \Delta t]$, the interjump times until the next susceptible or vaccinated individual is infected are random variables denoted by $\tau_{SI}^{MAC}(\Delta t)$ and $\tau_{VI}^{MAC}(\Delta t)$. That is, given $I(t)$ individuals present during the interval $[t, t + \Delta t]$, then

$$\begin{aligned}\tau_{SI}^{MAC}(\Delta t)|I(t) &\sim \text{Exponential}(\beta_{IS} \frac{I(t)}{N})\Delta t, \\ \tau_{VI}^{MAC}(\Delta t)|I(t) &\sim \text{Exponential}(\beta_{IV} \frac{I(t)}{N})\Delta t.\end{aligned}\quad (3.2)$$

- (a3.) There is an influx or birth of susceptible individuals at a constant exponential rate B . As described in Section 1, it is assumed that the single transition events from $S(t) \rightarrow V(t)$, $S(t) \leftarrow V(t)$, $I(t) \rightarrow S(t)$, $B \rightarrow S(t)$, where $B = \text{influx}$; $I(t) \rightarrow DD$, where $DD = \text{disease related death}$; and $X(t) \rightarrow ND$, $\forall X \in \{S, V, I\}$, where $ND = \text{natural death}$, are *non-mass-action-contact transition events* and denoted by “non-MAC”.
 (a4.) It is assumed that only single non-MAC transitions mentioned in (a3.) occur in any small time interval $[t, t + \Delta t]$; and the interjump times until the next non-MAC transition event for each type in (a3.) are random variables. That is, let τ_{ij}^k be the random interjump times between the $(k - 1)^{\text{th}}$ and k^{th} single transition from state i to state j , $\forall i, j \in \{S, V, I\}$, over the interval $[t, t + \Delta t]$. Note, in the rest of the derivation of the SVIS model, the k in τ_{ij}^k is omitted, that is, the random variable τ_{ij} will denote τ_{ij}^k , $\tau_{ij}^k \sim \tau_{ij}$, and it will be understood that τ_{ij} is referring to the interjump time until the k^{th} transition occurs. Moreover, τ_{ii} denotes the amount of time in the event that an individual in state i remains only in state i . Thus, for (a3.), the random interjump times until the next (or the k^{th}) non-MAC transition events $S(t) \rightarrow V(t)$, $V(t) \rightarrow S(t)$, and $I(t) \rightarrow S(t)$ occur are denoted by τ_{SV} , τ_{VS} and τ_{IS} , respectively; and for the event $B \rightarrow S(t)$, the random interjump time until the next transition event occurs is denoted by τ_{NB} . Also, for the event $I(t) \rightarrow DD$, the random interjump time until the next transition occurs is denoted by τ_{IDD} . In addition, for the event $X(t) \rightarrow ND$, $\forall X \in \{S, V, I\}$, the random interjump time until the next transition occurs is denoted by τ_{XND} . Moreover, since it is assumed that natural death causes are uniform across all states S, V, I , then $\tau_{XND} \equiv \tau_{ND}$.
 (a5.) It is also assumed that in the interval $[t, t + \Delta t]$, all of the random interjump times in (a4.) i.e. τ_{ij}^k , $k \geq 1$, for each transition event category $i \rightarrow j$, where $i, j \in \{S, V, I\}$, $i \neq j$, are independent variables, and depend on the state $S(t)$, $V(t)$ and $I(t)$ at time t . That is, the underlying counting process for the number of transitions for the event $i \rightarrow j$ is a *Markov renewal process* (cf. 34,35).
 (a6.) For every single transition event $i \rightarrow j$ from state i to state j , $\forall i, j \in \{S, V, I\}$ over the interval $[t, t + \Delta t]$, it is assumed that $g_{ij}(i(t))\Delta t$ is the transition rate, where the exact form of $g_{ij}(i(t))$ is to be determined using the random interjump time τ_{ij} . That is, for each non-MAC transition event in (a3.), there exists a transition rate defined as follows. For the transition event $S(t) \rightarrow V(t)$, $g_{SV}(S(t))$ denotes the instantaneous transition rate, and for the transition event $V(t) \rightarrow S(t)$, $g_{VS}(V(t))$ denotes the instantaneous transition rate. For the event $I(t) \rightarrow S(t)$, the rate is $g_{IS}(I(t))$; and for $B \rightarrow S(t)$, the rate is $g_{BS}(N(t))$; also, for $I(t) \rightarrow DD$, the rate is $g_{IDD}(I(t))$; and for $X(t) \rightarrow ND$, $\forall X \in \{S, V, I\}$, the rate is $g_{XND}(X(t))$. Also, for the MAC events in (a2.), i.e. $S(t) \rightarrow I(t)$, the rate is $g_{SI}(S(t))$ and from $V(t) \rightarrow I(t)$, the rate is $g_{VI}(V(t))$. The transition rates are depicted in Figure 3.
 (a7.) It is assumed that there are $m > 0$ vaccines available for the disease, which have similar effects, and prescriptions are the same, regardless of the specific vaccine, such that a susceptible person receives the required number of doses for complete immunity, from any of the m vaccines. Furthermore, a fully vaccinated person receives n doses of any of the m vaccines, where the doses can be a mixture of the different vaccines. For example, during the early stages of the COVID-19 pandemic, where COVID-19 vaccines were newly developed, a fully vaccinated person received two doses of either the *Pfizer* or *Moderna* vaccines; or a single dose of the *Johnson & Johnson* vaccine. Moreover, a third dose was administered for those vaccinated with either *Pfizer* or *Moderna* vaccines, which was considered an immunity booster. Furthermore, the booster could be from any of the vaccines *Pfizer* or *Moderna* or *Johnson & Johnson* (cf. 36).

Hence, it is assumed that a partially vaccinated individual has received at least one of n number of required doses of the m vaccines; and a fully vaccinated person has received all n doses of the vaccines. Furthermore, it is assumed that each dose of the available vaccines has a separate immunity lifetime efficacy.

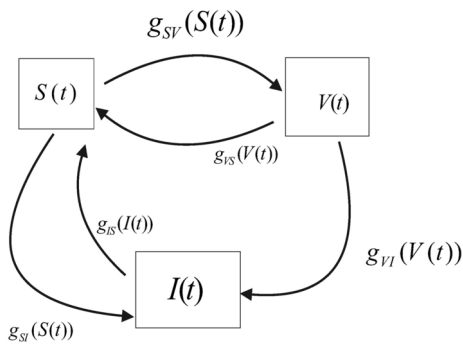


Fig. 3. Shows the framework for the SVIS model with general conversion rates $g_{ij}(t)$, $\forall i, j \in \{S, V, I\}$ for transition events $i \rightarrow j$, where τ_{ij} is the random time until the next transition occurs.

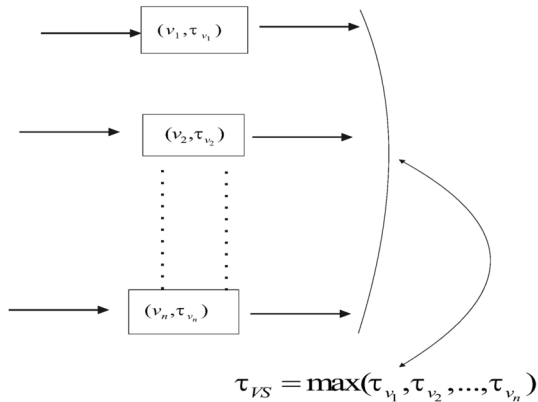


Fig. 4. Shows the parallel system vaccination strategy for the V state, where for each $k \in \{1, 2, \dots, n\}$, the pair (v_k, τ_{v_k}) denotes the k^{th} dose of the vaccine v_k and the efficacy lifetime τ_{v_k} of the k^{th} dose. Thus, since every susceptible person receives at most one of the n doses, the immunity lifetime of a vaccinated person is a competing risk and given by the random variable $\tau_{vs} = \max\{\tau_{v_1}, \tau_{v_2}, \dots, \tau_{v_n}\}$.

Indeed, each dose of the m vaccines is denoted by v_j , $j = 1, 2, \dots, n$, where $n > 0$. It is not necessary to label the specific vaccine the dose is obtained from. Moreover, each vaccine dose confers partial immunity to the individual vaccinated. That is, the effective immunity lifetime of the j^{th} dose v_j , $j = 1, 2, \dots, n$ in any vaccinated individual is denoted by τ_{v_j} . Thus, it is easy to see that the reliability of the vaccination immunity obtained from the n recommended doses, to confer protection against infection is a *competing risk* (cf.²³) in a parallel vaccination immunity lifetime model exhibited in Figure 4; and the random time until the immunity wanes, and the individual returns to the susceptible state $S(t)$ is given by the random variable,

$$\tau_{vs} = \max\{\tau_{v_1}, \tau_{v_2}, \dots, \tau_{v_n}\}. \quad (3.3)$$

- (a8.) The following additional assumptions are made to reduce the complexity in the vaccinated state $V(t)$ in reference to (a7.). **(i.)** Meanwhile the ages of immunity effectiveness with respect to vaccine dosages are represented and preserved by the random variables τ_{v_j} , $\forall j$ in (3.3), the multi-population age structure compartmentalization of the vaccinated state $V(t)$ with respect to vaccine type (of the m vaccines), and with respect to the age of immunity effectiveness is not considered. **(ii.)** The variable infectivity or reinfectivity rates of the vaccinated population due to the varied partial immunity protection levels conferred by the vaccines is not considered.

Also, there is no vertical transmission of the disease; individuals recover from the disease with very negligible acquired immunity and as a result there is no reinfection; the incubation of the disease lapses over a relatively short time that can be ignored. Refer to exemplary literature^{37,38} for more complex multi-population representations of the vaccinated state.

The following notation will be used to derive the rate equations.

Remark 3.1

- (a.) Note that while the minimal model complexity obtained by reducing the heterogeneities in the vaccinated population as stated in Assumption 3.1 (a8.), seems to penalize the microscopic evaluation of the disease dynamics, the statistical proprieties of the most essential components of $V(t)$, by age of immunity effectiveness, and by the number of doses of the m vaccines received are preserved by the parameters of the lifetime distributions of τ_{v_j} , $\forall j \in \{1, 2, \dots, n\}$ in (3.3).
- (b.) The following general notations for conditional probabilities for lifetime random variables with memory and memory-less properties are used. If τ_a and τ_b are two lifetime random variables with memory-less property and no memory-less property, respectively, then the conditional survival functions over the time interval $(t_1, t_2]$ is denoted by

$$\begin{aligned} P_{\tau_a}(t_2|t_1) &= P(\tau_a > t_2|\tau_a > t_1) = P(\tau_a > t_2 - t_1) = P_{\tau_a}(t_2 - t_1), \\ P_{\tau_b}(t_2|t_1) &= P(\tau_b > t_2|\tau_b > t_1) = \frac{P(\tau_b > t_2)}{P(\tau_b > t_1)} = \frac{P_{\tau_b}(t_2)}{P_{\tau_b}(t_1)}. \end{aligned} \quad (3.4)$$

- (c.) Note from (3.4), for any lifetime random variable with no memory-less property τ_b , the derivative of the conditional probability distribution

$$\frac{d}{dt} (P_{\tau_b}(t|r)) = \frac{d}{dt} \left(\frac{P_{\tau_b}(t)}{P_{\tau_b}(r)} \right) = \frac{P'_{\tau_b}(t)}{P_{\tau_b}(r)} = -P_{\tau_b}(t|r)\alpha_{\tau_b}(t), \quad (3.5)$$

where $\alpha_{\tau_b}(t)$ is the *hazard rate function (HRF)* of τ_b .

The following can be deduced from Assumption 3.1 (a2.). From (3.4), the random interjump times for the MAC-transition events

$$\begin{aligned} \tau_{SI}^{MAC}(\Delta t)|I(t) \sim \text{Exponential}(\beta_{IS} \frac{I(t)}{N})\Delta t, \iff P_{\tau_{SI}^{MAC}|I(t)}(t_2|t_1) &= e^{-\int_{t_1}^{t_2} [\beta_{IS} \frac{I(u)}{N(u)}] du}, \\ \tau_{VI}^{MAC}(\Delta t)|I(t) \sim \text{Exponential}(\beta_{IV} \frac{I(t)}{N})\Delta t \iff P_{\tau_{VI}^{MAC}|I(t)}(t_2|t_1) &= e^{-\int_{t_1}^{t_2} [\beta_{IV} \frac{I(u)}{N(u)}] du}. \end{aligned} \quad (3.6)$$

From Assumption 3.1 (a3. & a4.), the interjump times between “birth” or “influx” at constant exponential rate B implies that $\tau_{NB} \sim \text{Exponential}(B)$, and hence in (a6.), $g_{NB}(N(t)) = B$ (constant birth or influx rate).

The other transition rates $g_{ij}(i(t))$ in (a6.), exhibited in Figure 3 are derived later.

From Assumption 3.1 (a7.), the survival function for τ_{VS} , representing the probability that the next newly vaccinated individual remains artificially immune over the interval $(0, s]$ is given by

$$P_{\tau_{VS}}(s) = P(\tau_{VS} > s) = 1 - \left[\prod_{j=1}^n P(\tau_{v_j} \leq s) \right], \quad (3.7)$$

and from (3.4), the probability that the next newly vaccinated individual at time t remains immune over the interval $(t, t + s]$ is given by

$$P(\tau_{VS} > s + t | \tau_{VS} > t) = \frac{P_{\tau_{VS}}(s + t)}{P_{\tau_{VS}}(t)} = P_{\tau_{VS}}(s + t | t). \quad (3.8)$$

Note that for a population conditioned at anytime to the total value $N(t) = S(t) + V(t) + I(t)$, where $S(t)$, $V(t)$, $I(t)$ are given values at time t , the transition rates between the states S , V , I in the disease dynamics are deterministic, while the random times between transition events that involve MAC or non-MAC have lifetime distributions. In the following, by conditioning on the state of the population at time t , i.e. $(S(t), V(t), I(t))$, a common probabilistic approach is applied to derive the average dynamics for the rates at which each state in $(S(t), V(t), I(t))$ changes with time.

Derivation of the SVIS model

While it is convenient to write the transition rates directly between the three states S , V , I using (2.5)-(2.10), it is more convincing to apply the survival functions of the interjump times in Assumption 3.1, to obtain the very transition rates in (2.5) and the average dynamics in (2.10). That is, for any given small time interval $[t, t + \Delta t]$,

it is assumed that the state at time $S(t)$, $V(t)$, $I(t)$ is given or deterministic, whereas the survival over the interval depends on the distribution of the interjump times. This method for deriving differential equation models that describe only the average dynamics, has been explored in the literature (cf.^{14,20,39}).

Define the following. **(b1)** From Assumption 3.1 (**a4.**), τ_{SS} is lifetime until a susceptible exits the state i.e. until either infected, vaccinated or dies naturally. The probability that the susceptible individual remains susceptible over the interval $(r, t]$ is defined using (3.4) by

$$P_{\tau_{SS}}(t|r) = P_{\tau_{SV}}(t|r)P_{\tau_{SI}^{MAC}|I(t)}(t|r)P_{\tau_{SN}D}(t|r), \quad (3.9)$$

where, $P_{\tau_{SV}}(t|r)$, $P_{\tau_{SI}}(t|r)$ and $P_{\tau_{SN}D}(t|r)$ are conditional survival probabilities for τ_{SV} , τ_{SI} and $\tau_{SN}D$ over $(r, t]$ defined in (**a1.-a7.**), respectively, and from (3.6) $P_{\tau_{SI}^{MAC}|I(t)}(t|r) = e^{-\int_r^t (\beta_{IS} \frac{I(r)}{N(r)}) dr}$. Furthermore, the total susceptible population $S(t)$ present at time t , taking into consideration all conversion rates in Figure 3 into the S state, defined in Assumption 3.1 (**a3.-a7.**), given the initial amount $S(0)$ and constant birth rate $g_{NB}(N(t)) = B$ is given by

$$S(t) = S(0)P_{\tau_{SS}}(t|0) + \int_0^t [B + g_{VS}(V(r)) + g_{IS}(I(r))]P_{\tau_{SS}}(t|r)dr. \quad (3.10)$$

It is easy to see that differentiating (3.10) with respect to time t and rearranging like terms leads to

$$\begin{aligned} S'(t) &= \left[S(0)P'_{\tau_{SV}}(t|0)P_{\tau_{SI}^{MAC}|I(t)}(t|0)P_{\tau_{SN}D}(t|0) + S(0)P_{\tau_{SV}}(t|0)P'_{\tau_{SI}^{MAC}|I(t)}(t|0)P_{\tau_{SN}D}(t|0) \right. \\ &\quad + S(0)P_{\tau_{SV}}(t|0)P_{\tau_{SI}^{MAC}|I(t)}(t|0)P'_{\tau_{SN}D}(t|0) \Big] \\ &\quad + \left[\int_0^t [B + g_{VS}(V(r)) + g_{IS}(I(r))]P'_{\tau_{SV}}(t|r)P_{\tau_{SI}^{MAC}|I(t)}(t|r)P_{\tau_{SN}D}(t|r)dr \right. \\ &\quad + \int_0^t [B + g_{VS}(V(r)) + g_{IS}(I(r))]P_{\tau_{SV}}(t|r)P'_{\tau_{SI}^{MAC}|I(t)}(t|r)P_{\tau_{SN}D}(t|r)dr \\ &\quad \left. + \int_0^t [B + g_{VS}(V(r)) + g_{IS}(I(r))]P_{\tau_{SV}}(t|r)P_{\tau_{SI}^{MAC}|I(t)}(t|r)P'_{\tau_{SN}D}(t|r)dr \right]. \end{aligned} \quad (3.11)$$

Applying (3.5) in (3.11), and rearranging like terms, leads to the following.

$$S'(t) = \left[B + g_{VS}(V(t)) + g_{IS}(I(t)) - \beta_{IS} \frac{I(t)}{N(t)} S(t) - \alpha_{\tau_{SV}}(t)S(t) - \alpha_{\tau_{ND}}(t)S(t) \right]. \quad (3.12)$$

It is easy to see from (3.12) and Figure 3 that the conversion rate functions in (**a6.**) $g_{SV}(S(t)) = \alpha_{\tau_{SV}}(t)S(t)$, $g_{SN}D(S(t)) = \alpha_{\tau_{ND}}(t)S(t)$, and $g_{SI}(S(t)) = \beta_{IS} \frac{I(t)}{N(t)} S(t)$.

The equation for the $V(t)$ state is similarly derived as for $S(t)$. In (**a1.-a7.**), τ_{VV} is lifetime until a vaccinated individual exits the state i.e. either loses immunity, gets infected or dies naturally. The probability that the vaccinated individual remains immune over the interval $(r, t]$ is defined using (3.4) by

$$P_{\tau_{VV}}(t|r) = P_{\tau_{VS}}(t|r)P_{\tau_{VI}^{MAC}|I(t)}(t|r)P_{\tau_{IN}D}(t|r) \quad (3.13)$$

where, $P_{\tau_{VS}}(t|r)$, $P_{\tau_{VI}^{MAC}|I(t)}(t|r)$ and $P_{\tau_{IN}D}(t|r)$ are conditional survival probabilities for τ_{VS} , τ_{VI}^{MAC} and $\tau_{IN}D$ over $(r, t]$ defined in (**a1.-a7.**), respectively, and from (3.6), $P_{\tau_{VI}^{MAC}|I(t)}(t|r) = e^{-\int_r^t (\beta_{IV} \frac{I(r)}{N(r)}) dr}$. Furthermore, the vaccinated population $V(t)$ at time t , taking into consideration all conversion rates in Figure 3 into the V state, defined in Assumption 3.1 (**a3.-a7.**), given that the initial amount $V(0) \geq 0$ is

$$V(t) = V(0)P_{\tau_{VV}}(t|0) + \int_0^t [g_{SV}(S(r))]P_{\tau_{VV}}(t|r)dr, \quad (3.14)$$

Since from Assumption 3.1 (**a4.-a7.**), the conditional probability in (3.13) is a product of conditional probabilities for both the exponential lifetime distribution and other general lifetime random variables τ_{VS} , and τ_{ND} , it follows that differentiating (3.14) with respect to time t and rearranging like terms leads to

$$\begin{aligned}
V'(t) = & \left[V(0)P'_{\tau_{VS}}(t|0)P_{\tau_{VI}}(t|r)P_{\tau_{IND}}(t|r) + V(0)P_{\tau_{VS}}(t|r)P'_{\tau_{VI}}P_{\tau_{IND}}(t|r)(t|0) \right. \\
& + V(0)P_{\tau_{VS}}(t|r)P_{\tau_{VI}}P'_{\tau_{IND}}(t|r)(t|0) \Big] + g_{SV}(S(t)) + \int_0^t [g_{SV}(S(r))]P'_{\tau_{VS}}(t|r)P_{\tau_{VI}}(t|r)P_{\tau_{IND}}(t|r)dr \\
& + \int_0^t [g_{SV}(S(r))]P_{\tau_{VS}}(t|r)P'_{\tau_{VI}}(t|r)P_{\tau_{IND}}(t|r)dr + \int_0^t [g_{SV}(S(r))]P_{\tau_{VS}}(t|r)P_{\tau_{VI}}(t|r)P'_{\tau_{IND}}(t|r)dr.
\end{aligned} \tag{3.15}$$

Applying (3.5) in (3.15), and rearranging like terms, leads to the following.

$$V'(t) = g_{SV}(S(t)) - \beta_{IV}\frac{I(t)}{N(t)}V(t) - \alpha_{\tau_{VS}}(t)V(t) - \alpha_{ND}V(t), \tag{3.16}$$

where from above, $g_{SV}(S(t)) = \alpha_{\tau_{SV}}(t)S(t)$, $g_{VS}(V(t)) = \alpha_{\tau_{VS}}(t)V(t)$, $g_{VI}(V(t)) = \beta_{IV}\frac{I(t)}{N(t)}V(t)$, and $g_{VN}(V(t)) = \alpha_{\tau_{ND}}(t)V(t)$.

The equation for the $I(t)$ state is similarly derived as for $V(t)$ and $S(t)$. In (a3.-a7.), τ_{II} is lifetime until an infectious individual exists the state, i.e. either recovers from infection, or dies from disease related death, or dies naturally. The probability that the infectious individual remains infectious over the interval $(r, t]$ is defined using (3.4) by

$$P_{\tau_{II}}(t|r) = P_{\tau_{IS}}(t|r)P_{\tau_{IND}}(t|r)P_{\tau_{IDD}}(t|r), \tag{3.17}$$

where, $P_{\tau_{IS}}(t|r)$, $P_{\tau_{IND}}(t|r)$ and $P_{\tau_{IDD}}(t|r)$ are conditional survival probabilities for τ_{IS} , τ_{IND} , and τ_{IDD} over $(r, t]$ defined in (a4.-a7.), respectively. Furthermore, the infectious population at time t , given the initial amount $I(0)$ is

$$I(t) = I(0)P_{\tau_{II}}(t|0) + \int_0^t [g_{SI}(S(r)) + g_{VI}(V(r))]P_{\tau_{II}}(t|r)dr. \tag{3.18}$$

Since from Assumption 3.1 (a4.-a7.), the conditional probability in (3.17) is a product of conditional probabilities for general lifetime random variables τ_{IS} , τ_{ND} and τ_{IDD} , it follows that differentiating (3.18) with respect to time t similarly as (3.15) leads to the following.

$$\begin{aligned}
I'(t) = & I(0)P'_{\tau_{IS}}(t|0)P_{\tau_{IND}}(t|0)P_{\tau_{IDD}}(t|0) + I(0)P_{\tau_{IS}}(t|0)P'_{\tau_{IND}}(t|0)P_{\tau_{IDD}}(t|0) \\
& + I(0)P_{\tau_{IS}}(t|0)P_{\tau_{IND}}(t|0)P'_{\tau_{IDD}}(t|0) \\
& + \int_0^t [g_{SI}(S(r)) + g_{VI}(V(r))]P'_{\tau_{IS}}(t|r)P_{\tau_{IND}}(t|r)P_{\tau_{IDD}}(t|r)dr \\
& + g_{SI}(S(t)) + g_{VI}(V(t)) \\
& + \int_0^t [g_{SI}(S(r)) + g_{VI}(V(r))]P_{\tau_{IS}}(t|r)P'_{\tau_{IND}}(t|r)P_{\tau_{IDD}}(t|r)dr \\
& + \int_0^t [g_{SI}(S(r)) + g_{VI}(V(r))]P_{\tau_{IS}}(t|r)P_{\tau_{IND}}(t|r)P'_{\tau_{IDD}}(t|r)dr,
\end{aligned} \tag{3.19}$$

applying (3.5) to (3.19), for the survival lifetime random variables with no memory less property τ_{IS} and τ_{IDD} , and rearranging like terms; leads to

$$I'(t) = g_{SI}(S(t)) + g_{VI}(V(t)) - \alpha_{\tau_{IS}}(t)I(t) - \alpha_{\tau_{IDD}}(t)I(t) - \alpha_{ND}I(t), \tag{3.20}$$

where, from above it is easy to see that $g_{SI}(S(t)) = \beta_{IS}\frac{I(t)}{N(t)}S(t)$, $g_{VI}(V(t)) = \beta_{IV}\frac{I(t)}{N(t)}V(t)$, $g_{IN}(I(t)) = \alpha_{ND}I(t)$, $g_{IS}(I(t)) = \alpha_{\tau_{IS}}(t)I(t)$, and $g_{ID}(I(t)) = \alpha_{\tau_{IDD}}(t)I(t)$. Note that $\alpha_{\tau_{IDD}}(t)$ and $\alpha_{\tau_{IS}}(t)$ are HRF's of the random variables τ_{IDD} and τ_{IS} , respectively.

It follows from (3.12), (3.16) and (3.20), and substituting the derived formulas for the conversion rates $g_{ij}(i(t))$ for events from state i to j , $\forall i, j \in \{S, V, I\}$; $g_{iND}(i(t))$, $\forall i \in \{S, V, I\}$; $g_{IDD}(I(t))$ and $g_{NB}(N(t))$, that the SVIS epidemic model characterizing the *average dynamics* of the epidemic is given by the following NANLS of d.e.s, where the system coefficients are HRFs for the general interjump lifetime distributions of the underlying *renewal process*.

$$S'(t) = B + \alpha_{\tau_{VS}}(t)V(t) + \alpha_{\tau_{IS}}(t)I(t) - \beta_{IS}\frac{I(t)}{N(t)}S(t) - \alpha_{\tau_{SV}}(t)S(t) - \alpha_{\tau_{ND}}(t)S(t), \tag{3.21}$$

$$V'(t) = \alpha_{\tau_{SV}}(t)S(t) - \beta_{IV} \frac{I(t)}{N(t)} V(t) - \alpha_{\tau_{VS}}(t)V(t) - \alpha_{\tau_{ND}}(t)V(t), \quad (3.22)$$

$$I'(t) = \beta_{IS} \frac{I(t)}{N(t)} S(t) + \beta_{IV} \frac{I(t)}{N(t)} V(t) - \alpha_{\tau_{IS}}(t)I(t) - \alpha_{\tau_{IDD}}(t)I(t) - \alpha_{ND}(t)I(t). \quad (3.23)$$

Furthermore, the initial conditions of the model are given below

$$S(0) = S_0 > 0, \quad V(0) = V_0 \geq 0, \quad I(0) = I_0 > 0, \quad (3.24)$$

and the coefficients of (3.21)-(3.23) are HRFs that satisfy the conditions of Assumption 3.2 & 3.3. That is, for all $t \geq 0$, let

$$\tilde{\alpha}(t) = \{\alpha_{\tau_{SV}}(t), \alpha_{\tau_{IDD}}(t), \alpha_{\tau_{IS}}(t), \alpha_{\tau_{VS}}(t), \alpha_{\tau_{ND}}(t)\} \quad (3.25)$$

be the collection of the HRFs in (3.21)-(3.23). The following assumptions are made for the HRFs.

Assumption 3.2 From (3.25), let $\alpha_{\tau_X}(t) \in \tilde{\alpha}(t)$. Then $\alpha_{\tau_X}(t)$ satisfies the condition $\alpha_{\tau_X} \in \mathcal{C}^2([0, \infty])$, i.e. $\alpha_{\tau_X}(t)$ is twice continuously differentiable on $[0, \infty)$.

Assumption 3.3 From (3.25), let $\alpha_{\tau_X}(t) \in \tilde{\alpha}(t)$ satisfy Assumption 3.2, and there exists two constants $c_1 > 0$ and $c_2 \geq 0$, such that

$$c_2 \leq \liminf_{t \rightarrow \infty} [\alpha_{\tau_X}(t)] \leq \limsup_{t \rightarrow \infty} [\alpha_{\tau_X}(t)] \leq c_1, \forall \alpha_{\tau_X}(t) \in \tilde{\alpha}(t) \quad (3.26)$$

and

$$\alpha_X^{max} = \limsup_{t \rightarrow \infty} (\alpha_{\tau_X}(t)), \quad \alpha_X^{min} = \liminf_{t \rightarrow \infty} (\alpha_{\tau_X}(t)), \forall \alpha_{\tau_X}(t) \in \tilde{\alpha}(t). \quad (3.27)$$

For example, from (3.27), $\alpha_{SV}^{max} = \limsup_{t \rightarrow \infty} (\alpha_{\tau_{SV}}(t))$, and $\alpha_{SV}^{min} = \liminf_{t \rightarrow \infty} (\alpha_{\tau_{SV}}(t))$. That is for all $\alpha_{\tau_X}(t) \in \tilde{\alpha}(t)$, (3.27) signifies that every HRF in $\tilde{\alpha}(t)$ is ultimately bounded on $[0, \infty)$ and the inequalities below follow immediately. $0 < \alpha_{SV}^{max} \leq c_1$, $\alpha_{SV}^{min} \geq c_2$; $0 < \alpha_{IS}^{max} \leq c_1$, $\alpha_{IS}^{min} \geq c_2$; $0 < \alpha_{VS}^{max} \leq c_1$, $\alpha_{VS}^{min} \geq c_2$; $0 < \alpha_{IDD}^{max} \leq c_1$, $\alpha_{IDD}^{min} \geq c_2$, and $0 < \alpha_{ND}^{max} \leq c_1$, $\alpha_{ND}^{min} \geq c_2$.

Remark 3.2

- (1.) Note that the continuity condition in Assumption 3.2 & 3.3 is essential for the existence and uniqueness of (3.21)-(3.23). Also, since Assumption 3.2 includes all HRFs that satisfy Assumption 3.3, it follows that Assumption 3.3 will be used wherever a strict condition on boundedness is required.
- (2.) Also note that Assumption 3.2 & 3.3 form only a subset of HRFs for continuous lifetime distributions. Furthermore, the additional conditions (3.26)-(3.27) in Assumption 3.3 for the HRFs in (3.21)-(3.23), ensure the uniform convergence of the system (3.21)-(3.23) to an autonomous system. This fact is proven in the subsequent sections.
- (3.) In reference to Assumption 3.3, it is assumed without loss of generality (w.l.o.g.) that the limits of the HRFs exist, and are given by

$$(\alpha_{SV}, \alpha_{IS}, \alpha_{VS}, \alpha_{IDD}, \alpha_{ND}) = \lim_{t \rightarrow \infty} (\alpha_{\tau_{SV}}(t), \alpha_{\tau_{IS}}(t), \alpha_{\tau_{VS}}(t), \alpha_{\tau_{IDD}}(t), \alpha_{\tau_{ND}}(t)). \quad (3.28)$$

That is, from (3.27) and (3.28), it follows that

$$\begin{aligned} (\alpha_{SV}, \alpha_{IS}, \alpha_{VS}, \alpha_{IDD}, \alpha_{ND}) &= (\alpha_{SV}^{max}, \alpha_{IS}^{max}, \alpha_{VS}^{max}, \alpha_{IDD}^{max}, \alpha_{ND}^{max}) \\ &= (\alpha_{SV}^{min}, \alpha_{IS}^{min}, \alpha_{VS}^{min}, \alpha_{IDD}^{min}, \alpha_{ND}^{min}). \end{aligned} \quad (3.29)$$

- (4.) While the statistical interpretations for the conditions in Assumption 3.3 and their implications on the dynamics of the system are given in subsequent sections, it is important to note that the additional convenient assumption in (3.28) signifies that the HRFs over time become the HRF of an *exponential distribution*.

Indeed, since the HRF of the exponential distribution is the only HRF that is constant, letting $h_{Exponential(\alpha_{ij})}(t)$ denote the HRF of some exponentially distributed random variable $\tau_{ij} \sim Exponential(\alpha_{ij})$ with mean $\frac{1}{\alpha_{ij}}$, then it is written as $\alpha_{\tau_{ij}}(t) = h_{Exponential(\alpha_{ij})}(t) = \alpha_{ij}$, $\forall t > 0$. Thus, the limit (3.28) is equivalent to the following statement.

$$\begin{aligned} \alpha_{ij} = \lim_{t \rightarrow \infty} (\alpha_{\tau_{ij}}(t)) &\iff \exists t_1 > 0, \quad t_1 \text{ sufficiently large, such that,} \\ \forall t \geq t_1, \quad \alpha_{\tau_{ij}}(t) &\approx h_{Exponential(\alpha_{ij})}(t). \end{aligned} \quad (3.30)$$

Denote by

$$X(t) = (S(t), V(t), I(t)) \in \mathbb{R}_+^3, \forall t \geq 0. \quad (3.31)$$

Model validation results

It is shown below that the NANLS (3.21)-(3.23) has a solution that is unique, positive and bounded.

Theorem 4.1

- (1.) The system (3.21)-(3.23) has a unique positive solution on $t \in [0, \infty)$, whenever Assumption 3.2 & 3.3 hold.
- (2.) Also, the following are true only when Assumption 3.3 holds.
 - (a) The system (3.21)-(3.23) is asymptotically autonomous, and the asymptotic autonomous system is given by

$$\left\{ \begin{array}{l} S'(t) = B + \alpha_{VS}V(t) + \alpha_{IS}I(t) - \beta_{IS}\frac{I(t)}{N(t)}S(t) - \alpha_{SV}S(t) - \alpha_{ND}S(t), \\ V'(t) = \alpha_{SV}S(t) - \beta_{IV}\frac{I(t)}{N(t)}V(t) - \alpha_{VS}V(t) - \alpha_{ND}V(t), \\ I'(t) = \beta_{IS}\frac{I(t)}{N(t)}S(t) + \beta_{IV}\frac{I(t)}{N(t)}V(t) - \alpha_{IS}I(t) - \alpha_{IDD}I(t) - \alpha_{ND}I(t). \end{array} \right. \quad (4.1)$$

(b.) Moreover, from (3.27) and (4.1), let

$$\alpha_{IDD}^{max} = \limsup_{t \rightarrow \infty} [\alpha_{\tau_{IDD}}(t)], \quad \alpha_{max} = \max(\alpha_{IDD}^{max}, \alpha_{ND}). \quad (4.2)$$

If $N(0) \leq \min\left(\frac{1}{\alpha_{max}}B, \frac{1}{\alpha_{ND}}B\right)$, then

$$\frac{1}{\alpha_{max}}B \leq \liminf_{t \rightarrow \infty} N(t) \leq \lim_{t \rightarrow \infty} N(t) \leq \limsup_{t \rightarrow \infty} N(t) \leq \frac{1}{\alpha_{ND}}B. \quad (4.3)$$

Proof

- (1.) The existence and uniqueness of a positive solution results for the system (3.21)-(3.23) follow trivially by extending the local Lipschitz continuity results to a global solution over $t \in [0, \infty)$.
- (2.) When Assumption 3.3 and (3.28) hold, to show that the trajectories of (3.21)-(3.23) ultimately behave like the trajectories of (4.1), all that is required is to show that the rate functions of (3.21)-(3.23) converge uniformly to the rate functions of (4.1) as $t \rightarrow \infty$ (cf.^{27,28}). Indeed, from (3.21)-(3.23) define the functions

$$G_1(S(t), V(t), I(t)) = B + \alpha_{\tau_{VS}}(t)V(t) + \alpha_{\tau_{IS}}(t)I(t) - \beta_{IS}\frac{I(t)}{N(t)}S(t) - \alpha_{\tau_{SV}}(t)S(t) - \alpha_{\tau_{ND}}(t)S(t), \quad (4.4)$$

$$G_2(S(t), V(t), I(t)) = \alpha_{\tau_{SV}}(t)S(t) - \beta_{IV}\frac{I(t)}{N(t)}V(t) - \alpha_{\tau_{VS}}(t)V(t) - \alpha_{\tau_{ND}}(t)V(t), \quad (4.5)$$

$$G_3(S(t), V(t), I(t)) = \beta_{IS}\frac{I(t)}{N(t)}S(t) + \beta_{IV}\frac{I(t)}{N(t)}V(t) - \alpha_{\tau_{IS}}(t)I(t) - \alpha_{\tau_{IDD}}(t)I(t) - \alpha_{ND}(t)I(t). \quad (4.6)$$

From (3.28), it is easy to see that as $t \rightarrow \infty$, then $G_i(S(t), V(t), I(t))$, $i = 1, 2, 3$ converges uniformly to the functions below, $\forall (S(t), V(t), I(t)) \in \mathbb{R}_+^3$.

$$\left\{ \begin{array}{l} G_1(S(t), V(t), I(t)) \rightarrow B + \alpha_{VS}V(t) + \alpha_{IS}I(t) - \beta_{IS}\frac{I(t)}{N(t)}S(t) - \alpha_{SV}S(t) - \alpha_{ND}S(t), \\ G_2(S(t), V(t), I(t)) \rightarrow \alpha_{SV}S(t) - \beta_{IV}\frac{I(t)}{N(t)}V(t) - \alpha_{VS}V(t) - \alpha_{ND}V(t), \\ G_3(S(t), V(t), I(t)) \rightarrow \beta_{IS}\frac{I(t)}{N(t)}S(t) + \beta_{IV}\frac{I(t)}{N(t)}V(t) - \alpha_{IS}I(t) - \alpha_{IDD}I(t) - \alpha_{ND}I(t). \end{array} \right. \quad (4.7)$$

Hence, (3.21)-(3.23) converges asymptotically to (4.1) (see^{27,28} for more details about asymptotic autonomous systems). Furthermore, from (4.1) and (3.26), it is easy to see that $N(t) = S(t) + V(t) + I(t)$, satisfies

$$N'(t) = B - \alpha_{ND}N(t) - \alpha_{IDD}I(t). \quad (4.8)$$

Observe from (4.8) that

$$B - \alpha_{max}N(t) \leq N'(t) \leq B - \alpha_{ND}N(t), \quad (4.9)$$

and

$$\frac{B}{\alpha_{max}} - \frac{1}{\alpha_{max}}[B - \alpha_{max}N(0)]e^{-\alpha_{max}t} \leq N(t) \leq \frac{B}{\alpha_{ND}} - \frac{1}{\alpha_{ND}}[B - \alpha_{ND}N(0)]e^{-\alpha_{ND}t}. \quad (4.10)$$

Clearly, if $N(0) \leq \min\left(\frac{1}{\alpha_{max}}B, \frac{1}{\alpha_{ND}}B\right)$, then (4.3) follows immediately.

□

Remark 4.1 The result in Theorem 4.1 (2) signifies that if the initial state $(S(0), V(0), I(0)) \in \mathfrak{B}(\vec{0}, r)$, then over longtime, the maximum spread of the disease in the SVIS model (3.21)-(3.23) is bounded in the phase space for the asymptotic ANLS system (4.1), given by

$$\mathbb{C} = \bar{\mathfrak{B}}(\vec{0}, r_1) - \mathfrak{B}(\vec{0}, r_2) = \bar{\mathfrak{B}}(\vec{0}, r_1) \cap (\mathfrak{B}(\vec{0}, r_2))^c, \quad (4.11)$$

where $\bar{\mathfrak{B}}(\vec{0}, r_1)$ is the closed ball in \mathbb{R}_+^3 centered at the origin and radius $r_1 = \frac{1}{\alpha_{ND}}B$ given by

$$\bar{\mathfrak{B}}(\vec{0}, r_1) = \left\{ (S(t), V(t), I(t)) \in \mathbb{R}_+^3 \mid \|X(t)\|_1^2 = S(t) + V(t) + I(t) \leq r_1; r_1 = \frac{B}{\alpha_{ND}} \right\}, \quad (4.12)$$

and $\mathfrak{B}(\vec{0}, r_2)$ is the open ball in \mathbb{R}_+^3 centered at the origin and radius $r_2 = \frac{1}{\alpha_{max}}B$ given by

$$\mathfrak{B}(\vec{0}, r_2) = \left\{ (S(t), V(t), I(t)) \in \mathbb{R}_+^3 \mid \|X(t)\|_1^2 = S(t) + V(t) + I(t) < r_2; r_2 = \frac{B}{\alpha_{max}} \right\}. \quad (4.13)$$

In other words, every trajectory of the system (3.21)-(3.23) that evolves and over longtime enters the phase space \mathbb{C} for (4.1), continues to evolve and remain bounded in \mathbb{C} i.e. \mathbb{C} is asymptotically a *positive self-invariant space* for the system.

Types of HRF behaviors in a dynamic system

This study focuses to analyze the existence of the *asymptotic disease-free equilibria (ADFE)* for the NANLS (3.21)-(3.23), under the influence of the HRFs that satisfy Assumption 3.3, which characterize risk behaviors of biological and physical systems overtime; and exhibit one of the common shapes of HRFs for real lifetime continuous data. Indeed, there are several shapes of HRFs commonly exhibited by different types of lifetime distributions e.g. the *exponential, gamma, Weibull, Lognormal, normal, Birnbaum-Saunders, inverse normal, Lindley and Raleigh* distributions (cf^{22,23}). Examples of the HRF shapes include: *a constant, monotonic decreasing, monotonic increasing, unimodal, bathtub shapes, and so on* (cf^{22,23}).

In this study, four common shapes (namely: *bathtub, unimodal, monotonic (increasing or decreasing) and constant*) are considered for the HRFs: $\alpha_{\tau_{IDD}}(t)$, $\alpha_{\tau_{IS}}(t)$, $\alpha_{\tau_{VS}}(t)$, $\alpha_{\tau_{SV}}(t)$, and $\alpha_{\tau_{ND}}(t)$ in the NANLS (3.21)-(3.23). Taking into account the conditions of Assumption 3.3, the shapes are characterized mathematically in Hypothesis 5.1.

Hypothesis 5.1 Suppose Assumption 3.3 holds. Also, for any constant real number $c \geq 0$, let $h(t) \in \{\alpha_{\tau_{IDD}}(t), \alpha_{\tau_{IS}}(t), \alpha_{\tau_{VS}}(t), \alpha_{\tau_{SV}}(t), \alpha_{\tau_{ND}}(t)\}$, $\forall t \in [0, \infty)$ satisfy one of the following.

- (H1.) The HRF $h(t)$ has a bathtub shape that becomes bounded asymptotically i.e. $h'(t) < 0, h''(t) > 0$, for all $t \geq 0; \limsup_{t \rightarrow \infty} h(t) = c$.
- (H2.) The HRF $h(t)$ has a unimodal or reverse-bathtub shape, that becomes bounded asymptotically i.e. $h'(t) > 0, h''(t) < 0$, for all $t \geq 0; \liminf_{t \rightarrow \infty} h(t) = c$.
- (H3.) The HRF $h(t)$ has a monotonically decreasing shape that becomes bounded asymptotically i.e. $h'(t) < 0$, for all $t \geq 0; \liminf_{t \rightarrow \infty} h(t) = c$.
- (H4.) The HRF $h(t)$ has a monotonically increasing shape that becomes bounded asymptotically i.e. $h'(t) \geq 0$, for all $t \geq 0; \limsup_{t \rightarrow \infty} h(t) = c$.

The Figure 5 shows some examples of the different shapes of the HRFs given in the Hypothesis 5.1.

Remark 5.1 Observe that the model (3.21)-(3.23) satisfies Theorem 4.1, whenever Hypothesis 5.1[(H1.)-(H4.)] holds, for any of the HRFs $h(t) \in (\alpha_{\tau_{SV}}(t), \alpha_{\tau_{IS}}(t), \alpha_{\tau_{VS}}(t), \alpha_{\tau_{IDD}}(t), \alpha_{\tau_{ND}}(t))$, $t \in [0, \infty)$.

- (1.) Also, the HRF $h(t)$ in Hypothesis 5.1[(H1.)] and Figure 5(a), represents the conditional failure rate for a system, where the failure risk is initially high; decreases over time to a minimum value; then rises later, but remains bounded over time.

An example of a lifetime distribution with a HRF that satisfies Hypothesis 5.1[(H1.)] is the **Exponentiated half-logistic distribution (EHL)** with shape parameters $\lambda = 0.55$, and scale parameter $\theta = 0.15$ (see the HRF in Figure 5(a)) (cf³²). The Figure 5(a) indicates that initially the failure risk is high, then decreases to a minimum point, rises and remains bounded over time.

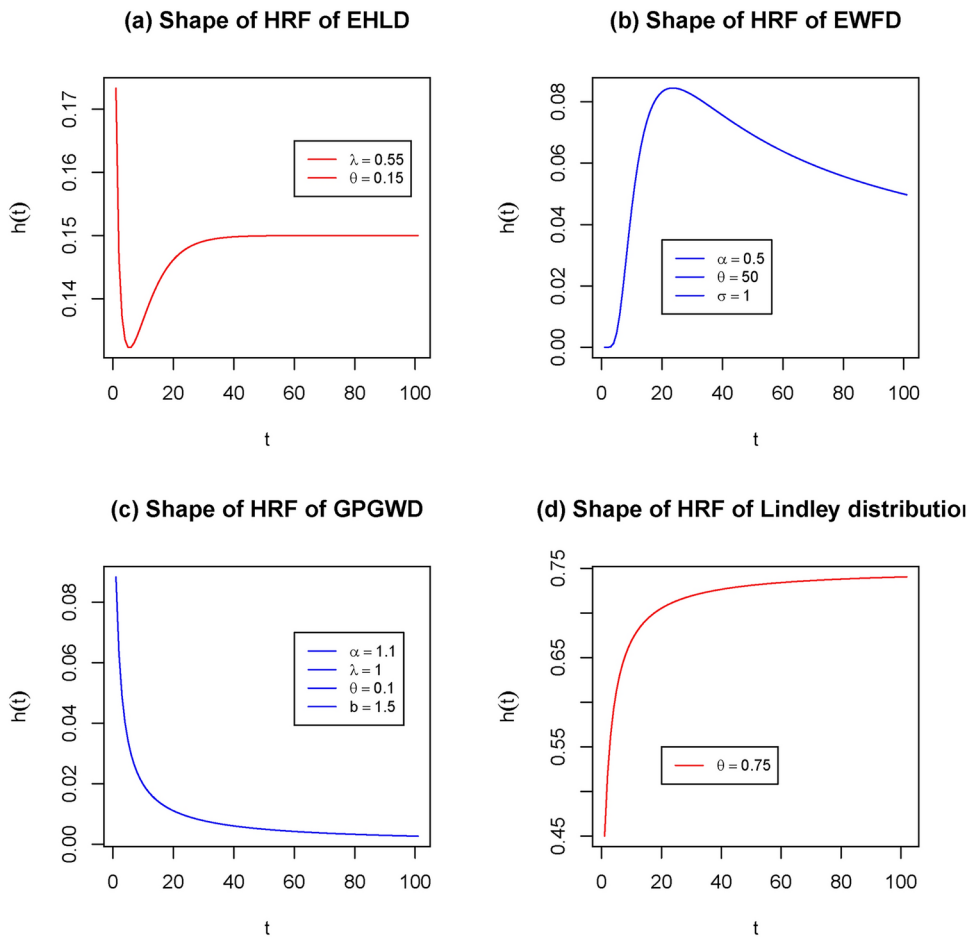


Fig. 5. Shows examples of the different shapes of the HRFs in Hypothesis 5.1. Note, (a) shows the shape of the HRF of the *EHLD* with shape parameters $\lambda = 0.55$, and scale parameter $\theta = 0.15$, which has a bathtub shape that becomes bounded over time; (b) shows the shape of the HRF of the *EWFD* with shape parameters $\alpha = 0.5$, $\theta = 50$, and scale parameter $\sigma = 1$, which has a reverse bathtub shape that becomes bounded over time; (c) shows the shape of the HRF of the *GPGWD* with shape parameters $\alpha = 1.1$, $\theta = 0.1$, and scale parameters $\lambda = 1$, $b = 1.5$, which has a monotonically decreasing shape; and (d) shows the shape of the HRF of the *Lindley distribution* with shape parameters $\theta = 0.75$, which has a monotonically increasing shape.

- (2.) The HRF $h(t)$ in Hypothesis 5.1[(H2.)] and Figure 5(b), represents the conditional failure rate for a system that has a low risk initially, which rises to a maximum value, and decrease slightly in a concave manner, and remains bounded over time. This behavior for the HRF in Hypothesis 5.1[(H2.)] is opposite to the bathtub behavior for the HRF $h(t)$ in Hypothesis 5.1[(H1.)] and Figure 5(a). An example of a lifetime distribution with a HRF that satisfies Hypothesis 5.1[(H2.)] is the **Exponentiated Weibull family distribution (EWFD)** with shape parameters $\alpha = 0.5$, $\theta = 50$, and scale parameter $\sigma = 1$ (cf.³¹), depicted in Figure 5(b). The Figure 5(b) indicates that initially the failure is low, then rises to a peak point, then decreases steadily, and remains bounded to a horizontal asymptote.
- (3.) The HRF $h(t)$ in Hypothesis 5.1[(H3.)] and Figure 5(c), represents the conditional failure rate for a system that has a high risk initially, which decreases monotonically to a minimum value, but remains bounded over time. An example of a lifetime distribution with a HRF that satisfies Hypothesis 5.1[(H3.)] is the **Generalized power generalized Weibull distribution (GPGWD)** with shape parameters $\alpha = 1.1$, $\theta = 0.1$, and scale parameters $\lambda = 1$, $b = 1.5$ (cf.³³), depicted in Figure 5(c).
- (4.) The HRF $h(t)$ in Hypothesis 5.1[(H4.)] and Figure 5(d), represents the conditional failure rate for a system that has a low risk initially, which increases monotonically to a maximum value, and remains bounded over time. An example of a lifetime distribution with a HRF that satisfies Hypothesis 5.1[(H4.)] is the *Lindley distribution* with shape parameters $\theta = 0.75$ (cf.¹⁷), depicted in Figure 5(d).

Interpretation of the HRF behaviors in the SVIS model

As shown in the next section, the existence of the asymptotic disease-free equilibrium (ADFE) depends only on the HRFs $\alpha_{\tau_{SV}}(t)$, $\alpha_{\tau_{VS}}(t)$, and $\alpha_{\tau_{ND}}(t)$. In the following remark, an interpretation for the four common behaviors of the HRFs in Hypothesis 5.1 are given for these HRFs.

Remark 5.2 Recall $\alpha_{\tau_{SV}}(t)$, $\alpha_{\tau_{VS}}(t)$, and $\alpha_{\tau_{ND}}(t)$ are the HRFs for the random times until a susceptible person is vaccinated; the random time until a vaccinated person loses immunity and return to the susceptible state; and the random time until an individual dies naturally in the population, respectively.

- (1.) Hence, the shape of the HRF $\alpha_{\tau_{SV}}(t)$ reflects the rate that susceptible persons get vaccinated. For example, a monotonic decreasing hazard rate for $\alpha_{\tau_{SV}}(t)$ reflects a continuously growing hesitation to get vaccinated e.g. influenced by false rumors about the vaccine. A monotonically increasing hazard rate for $\alpha_{\tau_{SV}}(t)$ reflects, for example, a growing desire for vaccination e.g. such as when there are education campaigns to promote vaccination as a control measure, and the population is well sensitized and educated about a good vaccine. A bathtub shape for $\alpha_{\tau_{SV}}(t)$ reflects that a period of growing hesitation for not getting vaccinated is followed by a period of a growing desire for vaccination.
- (2.) Similarly, the shape of the HRF $\alpha_{\tau_{VS}}(t)$ reflects the risk of using a vaccine with low efficacy, or reflects the failure rate of the vaccine to confer protection, or reflects the rate at which the artificial immunity obtained from the vaccine wanes over time. For example, a monotonically decreasing hazard rate for $\alpha_{\tau_{VS}}(t)$ reflects that a more potent and effective vaccine is used that confers long lasting artificial immunity with a low failure rate. On the contrary, a monotonically increasing hazard rate for $\alpha_{\tau_{VS}}(t)$ reflects that a less potent vaccine is used that has a higher failure rate over time. The bathtub shape for the hazard rate for $\alpha_{\tau_{VS}}(t)$ reflects the lifetime of the immunity conferred by a vaccine, where a period of high potency of the vaccine is followed by a period of a high failure rate of the vaccine.
- (3.) Also, the shape of the HRF $\alpha_{\tau_{ND}}(t)$ reflects the risk of natural death in the population, or the rate that individuals die naturally in the population over time. A monotonic decreasing shape for $\alpha_{\tau_{ND}}(t)$ reflects a decreasing risk of natural death over time, e.g. when there are better living standards that promote better self-care. A monotonic increasing shape for $\alpha_{\tau_{ND}}(t)$ reflects an increasing natural death rate over time, e.g. when poverty rates are high leading to poor living conditions, and high vulnerability to infection by diseases. A bathtub shape for $\alpha_{\tau_{ND}}(t)$ reflects a period of high risk of natural death that decreases to a minimum over time; and it is followed by a period of increasing natural death rate. A unimodal or reverse bathtub shape for $\alpha_{\tau_{ND}}(t)$ reflects the opposite of the bathtub shape described above.

The following theorem for the HRFs will be very useful to interpret the results for the ADDE for the NANLS (3.21)-(3.23). Let τ_{S0} , τ_{V0} and τ_{I0} be the respective random times until the next susceptible, or vaccinated, or infectious individual leaves their respective states i.e. from (2.2)-(2.3), τ_{S0} , τ_{V0} and τ_{I0} are random interjump times. The theorem below follows from the characterization of the jump process in Section 2.

Theorem 5.1 Suppose Assumption 3.3 holds. For the HRFs $\alpha_\tau(t) \in \{\alpha_{\tau_{SV}}(t), \alpha_{\tau_{VS}}(t), \alpha_{\tau_{ND}}(t)\}$ in the NANLS (3.21)-(3.23) with the limits given in (3.25), let τ_{S0} , τ_{V0} and τ_{I0} be the interjump times defined above. Then the following are true.

$$1.) \quad \tau_{S0} = \min(\tau_{SV}, \tau_{ND}), \quad \tau_{V0} = \min(\tau_{VS}, \tau_{ND}), \quad \tau_{I0} = \text{---} \quad (5.1)$$

and from (2.2)-(2.3), the distributions are given by

$$\begin{aligned} \mathbb{P}(\tau_{S0} > t) &= \mathbb{P}(\tau_{SV} > t)\mathbb{P}(\tau_{ND} > t) = e^{-\int_0^t (\alpha_{\tau_{SV}}(u) + \alpha_{\tau_{ND}}(u))du} \\ \mathbb{P}(\tau_{V0} > t) &= \mathbb{P}(\tau_{VS} > t)\mathbb{P}(\tau_{ND} > t) = e^{-\int_0^t (\alpha_{\tau_{VS}}(u) + \alpha_{\tau_{ND}}(u))du} \\ \mathbb{P}(\tau_{I0} > t) &= \mathbb{P}(\tau_{IS} > t)\mathbb{P}(\tau_{ND} > t) = e^{-\int_0^t (\alpha_{\tau_{IS}}(u) + \alpha_{\tau_{ND}}(u))du}. \end{aligned} \quad (5.2)$$

That is, the CDFs of τ_{S0} , τ_{V0} and τ_{I0} are equivalent to an exponential distributed random variable with a non-homogeneous intensity given as follows.

$$\begin{aligned} F_{\tau_{S0}}(t) &\sim F_{Exp(\lambda_{S0}(t))}(t), \quad \lambda_{S0}(t) = \int_0^t (\alpha_{\tau_{SV}}(u) + \alpha_{\tau_{ND}}(u))du \\ F_{\tau_{V0}}(t) &\sim F_{Exp(\lambda_{V0}(t))}(t), \quad \lambda_{V0}(t) = \int_0^t (\alpha_{\tau_{VS}}(u) + \alpha_{\tau_{ND}}(u))du, \\ F_{\tau_{I0}}(t) &\sim F_{Exp(\lambda_{I0}(t))}(t), \quad \lambda_{I0}(t) = \int_0^t (\alpha_{\tau_{IS}}(u) + \alpha_{\tau_{ND}}(u))du \end{aligned} \quad (5.3)$$

2.) Moreover, the conditional expected values over $[s, t]$, $s, t > 0$ satisfy the following.

$$\begin{aligned} \mathbb{E}[\tau_{S0}|s < \tau_{S0} \leq t] &= \frac{1}{\lambda_{S0}(t) - \lambda_{S0}(s)}, \quad \mathbb{E}[\tau_{V0}|s < \tau_{V0} \leq t] = \frac{1}{\lambda_{V0}(t) - \lambda_{V0}(s)}, \\ \mathbb{E}[\tau_{I0}|s < \tau_{I0} \leq t] &= \frac{1}{\lambda_{I0}(t) - \lambda_{I0}(s)}, \end{aligned} \quad (5.4)$$

and

$$\begin{aligned}\lambda_{S0} &= \lim_{t \rightarrow \infty} \frac{1}{t} \lambda_{S0}(t) = \alpha_{SV} + \alpha_{ND} \quad \text{and} \quad \lambda_{V0} = \lim_{t \rightarrow \infty} \frac{1}{t} \lambda_{V0}(t) = \alpha_{VS} + \alpha_{ND}, \\ \lambda_{I0} &= \lim_{t \rightarrow \infty} \frac{1}{t} \lambda_{I0}(t) = \alpha_{IS} + \alpha_{ND}.\end{aligned}\tag{5.5}$$

Proof The result in (5.2) follows simply by applying the interrelationship between the **survival function** and **cumulative hazard rate function** explained in (2.2)-(2.3).

Also, since the HRFs satisfy (3.25), it is easy to see that the time averages of $\lambda_{S0}(t)$, $\lambda_{V0}(t)$ and $\lambda_{I0}(t)$ satisfy (5.5). □

Remark 5.3 Theorem 5.1 signifies that the probabilities for the interjump times τ_{S0} , τ_{V0} and τ_{I0} in (5.1) can be evaluated by using equivalent exponential random variables with intensities in (5.3) given over the interval $[0, t]$, with means in (5.4). Also, since the HRFs have a limit in (3.28), the result in (5.5) suggests that the averages of the non-homogeneous Poisson rates $\lambda_{S0}(t)$, $\lambda_{V0}(t)$ and $\lambda_{I0}(t)$ become homogeneous over long time, with rates given by

$$\begin{aligned}\lambda_{S0} &= \lim_{t \rightarrow \infty} \frac{1}{t} \lambda_{S0}(t) = \alpha_{SV} + \alpha_{ND} \quad \text{and} \quad \lambda_{V0} = \lim_{t \rightarrow \infty} \frac{1}{t} \lambda_{V0}(t) = \alpha_{VS} + \alpha_{ND}, \\ \lambda_{I0} &= \lim_{t \rightarrow \infty} \frac{1}{t} \lambda_{I0}(t) = \alpha_{IS} + \alpha_{ND},\end{aligned}\tag{5.6}$$

i.e. the interjump times τ_{S0} , τ_{V0} and τ_{I0} over sufficiently longtime become identically distributed as an exponentially distributed random variable with homogeneous rates, and with means given by $\frac{1}{\lambda_{S0}}$, $\frac{1}{\lambda_{V0}}$ and $\frac{1}{\lambda_{I0}}$, respectively.

Asymptotic steady states of the SVIS model

Note that in general, for the given HRF coefficients of the NANLS (3.26)-(3.27), there are no equilibrium states at all times $t \geq 0$. However, since asymptotically, (3.26)-(3.27) becomes (4.1), whenever Assumption 3.3 holds, it is possible to characterize the steady states of the system over sufficiently long time. Note further that since HRFs have various behaviors and shapes overtime, e.g. *a constant, a monotonic decreasing, a monotonic increasing, a unimodal, a bathtub shape, and so on* (cf. 22), the specific asymptotic equilibria for (3.26)-(3.27) are not just trivially obtained by finding the steady states of (4.1). It is shown subsequently that the asymptotic equilibria have bearings on the behaviors of the HRFs in the system. Some definitions will be useful to achieve these results.

Definition 6.1 A zero-rate solution function (ZRSF):

(1.) For at any time $t \geq 0$, let

$$X^*(t) = (S^*(t), V^*(t), I^*(t)),\tag{6.1}$$

be in $X^* \in C^1([0, \infty))$ and satisfies the system (3.21)-(3.23), whenever

$$\frac{dS(t)}{dt} = 0; \quad \frac{dV(t)}{dt} = 0; \quad \frac{dI(t)}{dt} = 0.\tag{6.2}$$

The solution $X^*(t)$ in (6.1) is called a **zero-rate solution function (ZRSF)**. Thus, $X^*(t)$, $t \geq 0$ defines a path for the system (3.21)-(3.23) in the phase space \mathbb{C} in (4.11), where in the underlying random jump processes (i.e. the birth- and-death processes characterized by the general system (2.10)) for the states $S(t)$, $V(t)$ and $I(t)$, the aggregate non-homogeneous birth and death rates for single transitions between the states of the renewal processes continuously remain the same over time $t \geq 0$. In other words, the function $X^*(t)$, $\forall t \geq 0$ obtained from (6.2) is the trajectory for the SVIS epidemic dynamics, where at each time $t \geq 0$, the non-homogeneous birth rate for a susceptible or vaccinated or infectious individual is equal to the death rate. And $X^*(t)$, $t \geq 0$ becomes a constant $X^*(t) = X^*$, $t \geq 0$, whenever the birth and death rates become homogeneous.

Clearly, in the absence of disease in the system (3.21)-(3.23), i.e., for $I(t) = 0$, $\forall t \in [0, \infty)$, then solution (6.1) reduces to

$$X^*(t) = (S^*(t), V^*(t), I^*(t)) = (S^*(t), V^*(t), 0), \forall t \geq 0.\tag{6.3}$$

(2.) Suppose $X_0^* = (S_0^*, V_0^*, I_0^*) \in \mathbb{R}_+^3$ is fixed non-negative real valued vector, such that, from (6.1)

$$X^* = (S_0^*, V_0^*, I_0^*) = \lim_{t \rightarrow \infty} X^*(t), \quad (6.4)$$

then X_0^* is called an **asymptotic equilibrium state** for (3.21)-(3.23). The limit $X_0^* = (S_0^*, V_0^*, 0)$ is called an **asymptotic disease-free equilibrium state (ADFE)**. For $I_0^* > 0$, the limit (S_0^*, V_0^*, I_0^*) is called an **asymptotic endemic equilibrium state (AEE)**.

Existence of the asymptotic disease-free equilibrium (ADFE)

The existence of a disease-free equilibrium serves as a prelude for investigating disease eradication for the system (cf.²⁵). Since asymptotically, (3.26)-(3.27) becomes (4.1), whenever Assumption 3.3 holds, and the coefficients of the NANLS (3.21)-(3.23) are HRFs with various shapes in Hypothesis 5.1(H1.- H4.), it is necessary to characterize the ADFE for the NANLS, under the influence of the different behaviors of the HRFs over time. Note that the existence of (4.1) is sufficient and not necessary for the existence of the ADFE. Indeed, it is shown in some special cases for the HRFs without the strict bounded conditions in Assumption 3.2 that there exists an ADFE.

From (3.21)-(3.23) in the absence of disease, i.e. $I(t) = 0, \forall t$, the NANLS reduces to

$$\begin{cases} S'(t) = B + \alpha_{\tau_{VS}}(t)V(t) - [\alpha_{\tau_{SV}}(t) + \alpha_{\tau_{ND}}(t)]S(t); \\ V'(t) = \alpha_{\tau_{SV}}(t)S(t) - [\alpha_{\tau_{VS}}(t) + \alpha_{\tau_{ND}}(t)]V(t); \\ I'(t) = 0; \end{cases} \quad (6.5)$$

and the ZRSF in (6.3) obtained from (6.2) is given as the solution of the system

$$\begin{cases} B + \alpha_{\tau_{VS}}(t)V_0^*(t) - \alpha_{\tau_{SV}}S_0^*(t) - \alpha_{\tau_{ND}}(t)S_0^*(t) = 0, \\ \alpha_{\tau_{SV}}S_0^*(t) - \alpha_{\tau_{VS}}(t)V_0^*(t) - \alpha_{\tau_{ND}}(t)V_0^*(t) = 0. \end{cases} \quad (6.6)$$

Solving (6.6), leads to

$$\begin{aligned} S_0^*(t) &= \left(\frac{B}{\alpha_{\tau_{SV}}(t) + \alpha_{\tau_{ND}}(t)} \right) \frac{1}{1 - \frac{\alpha_{\tau_{SV}}(t)}{\alpha_{\tau_{SV}}(t) + \alpha_{\tau_{ND}}(t)} \frac{\alpha_{\tau_{VS}}(t)}{\alpha_{\tau_{SV}}(t) + \alpha_{\tau_{ND}}(t)}}, \\ V_0^*(t) &= \frac{\alpha_{\tau_{SV}}(t)}{\alpha_{\tau_{VS}}(t) + \alpha_{\tau_{ND}}(t)}S_0^*(t), \quad I_0^*(t) = 0, \quad \forall t \geq 0. \end{aligned} \quad (6.7)$$

Observe that $S_0^*(t) > 0$, for all $t \geq 0$, since

$$0 < \frac{\alpha_{\tau_{SV}}(t)}{\alpha_{\tau_{SV}}(t) + \alpha_{\tau_{ND}}(t)} \frac{\alpha_{\tau_{VS}}(t)}{\alpha_{\tau_{VS}}(t) + \alpha_{\tau_{ND}}(t)} < 1, \forall \alpha_{\tau_{ij}}(t) > 0, \quad i, j \in \{S, V, N, D\}. \quad (6.8)$$

Also, since the NANLS (3.21)-(3.23) is nonlinear, and explicit analytical solutions are intractable, the rest of this paper is focused to characterize the limits of the ZRSF (6.7), with respect to the behaviors of the HRFs $\alpha_{\tau_{SV}}(t)$, $\alpha_{\tau_{VS}}(t)$, and $\alpha_{\tau_{ND}}(t)$ in Hypothesis 5.1(H1. - H4.). It is easy to see from (6.7) that when the ADFE exists, it is given by the limit

$$(S_0^*, V_0^*, 0) = \lim_{t \rightarrow \infty} (S_0^*(t), V_0^*(t), I_0^*(t)). \quad (6.9)$$

Remark 6.1

- (1.) The ZRSF in (6.7) depends on the combined HRFs $[\alpha_{\tau_{SV}}(t) + \alpha_{\tau_{ND}}(t)]$ and $[\alpha_{\tau_{VS}}(t) + \alpha_{\tau_{ND}}(t)]$ in the disease free system (6.5), which represent the respective rates that a susceptible and a vaccinated individual exits the susceptible and the vaccinated states. Note that the asymptotic behavior of these HRFs has been given in Theorem 5.1 and Remark 5.3.
- (2.) Also, since the HRFs $\alpha_{\tau_{SV}}(t), \alpha_{\tau_{ND}}(t), \alpha_{\tau_{VS}}(t)$ can take any of the shapes in Hypothesis 5.1 over time, and from (3.30), there is a point $t_1 > 0$ sufficiently large, such that for $t \geq t_1$, $\alpha_{\tau_{ij}}(t) \approx h_{\text{Exponential}}(\alpha_{ij})(t)$, $\forall \alpha_{\tau_{ij}}(t) \in \{\alpha_{\tau_{SV}}(t), \alpha_{\tau_{ND}}(t), \alpha_{\tau_{VS}}(t)\}$, this implies that the qualitative behavior of the ZRSF in (6.7) must depend on the behavior of the HRFs $\alpha_{\tau_{ij}}(t)$ for $t \in [0, t_1]$, and the behavior of $\alpha_{\tau_{ij}}(t)$ for $t \in [t_1, \infty)$.

Furthermore, from a biological perspective, the growth orders of the HRFs $\alpha_{\tau_{SV}}(t), \alpha_{\tau_{ND}}(t), \alpha_{\tau_{VS}}(t)$ have different implications on the disease dynamics. For example, if $\alpha_{\tau_{SV}}(t)$ tends to grow larger than $\alpha_{\tau_{VS}}(t)$ over time, this reflects a scenario where vaccination is highly motivated, and a more effective vaccine with longer immunity life is used in the population. Clearly, this scenario will lead to a unique val-

ue for the ADFE, than a different scenario for the HRFs $\alpha_{\tau_{SV}}(t), \alpha_{\tau_{ND}}(t), \alpha_{\tau_{VS}}(t)$. Some scenarios for the growth orders of the HRFs are considered subsequently.

Note, while there are numerous scenarios for the growth orders of the HRFs $\alpha_{\tau_{SV}}(t), \alpha_{\tau_{ND}}(t), \alpha_{\tau_{VS}}(t)$ remarked above in Remark 6.1[(2.)] that represent various distributions for the lifetimes in the epidemic dynamics, only a few special cases will be characterized in this section. The following definition of growth orders in Wanduku⁴⁰ will be useful to characterize the growth orders for the HRFs.

Definition 6.2 Given two real valued functions f and g ,

1. If $\exists k > 0$, and n_0 , such that $\forall n > n_0, |f(n)| \leq k|g(n)|$, then it is said that f is big-o of g , and is denoted by $f(n) = O(g(n))$ or $f = O(g)$. If $f(n) \rightarrow 0$, as $n \rightarrow \infty$, that is, f turns in the limit to a zero function for sufficiently large n , then it is written as $f = O(\epsilon)$ or $f(n) = O\left(\frac{1}{n}\right)$, for $\epsilon > 0$. If $f(n)$ is a constant function as $n \rightarrow \infty$, then it is written $f(n) = O(1)$
2. if $\exists k_1, k_2 > 0$, and n_0 , such that $\forall n > n_0, k_1|g(n)| \leq |f(n)| \leq k_2|g(n)|$, then it is said that f is big-theta of g , and is denoted by $f(n) = \theta(g(n))$. If $f(n) \rightarrow \infty$ as $n \rightarrow \infty$, then it is written $f(n) = \theta(n)$ or $f = \theta\left(\frac{1}{\epsilon}\right)$, for $\epsilon > 0$.

Remark 6.2 Observe from Remark 6.1[(2.)] that

comparing the growth rate of the HRF $\alpha_{\tau_{ij}}(t) \in \{\alpha_{\tau_{SV}}(t), \alpha_{\tau_{ND}}(t), \alpha_{\tau_{VS}}(t)\}$ to that of a constant function using the $O(1)$ notation, i.e., $\alpha_{\tau_{ij}}(t) = O(1)$ is equivalent to comparing the growth rate of $\alpha_{\tau_{ij}}(t)$ to that of a function of the HRF $h_{exponential}(t), \forall t \geq t_1$.

Suppose $g : \mathbb{R}_+ \rightarrow \mathbb{R}_+$ is a positive real valued function, and $g \circ h_{exponential}(t) = g(h_{exponential}(t))$ is a composition of g and $h_{exponential}(t)$, then by Definition 6.2

$$\alpha_\tau(t) = O(1) \iff \alpha_\tau(t) = O(g \circ h_{exponential}(t)),$$

and this signifies that after $t > t_1$, the behavior of $\alpha_{\tau_{ij}}(t) \approx g \circ h_{exponential}(t)$, and over $t \in (0, t_1)$, the HRF $\alpha_{\tau_{ij}}(t)$ may display any other behavior e.g. a monotonic, bathtub, unimodal, or a constant shape etc. in Hypothesis 5.1.

The scenarios for the growth orders of the HRFs $\alpha_{\tau_{SV}}(t), \alpha_{\tau_{VS}}(t)$, and $\alpha_{\tau_{ND}}(t)$ are summarized in the following hypotheses.

Hypothesis 6.1 Let $g : \mathbb{R}_+ \rightarrow \mathbb{R}_+$ is a positive real valued function. Applying Definition 6.2, let $\tilde{\alpha}(t) = \{\alpha_{\tau_{SV}}(t), \alpha_{\tau_{ND}}(t), \alpha_{\tau_{IS}}(t), \alpha_{\tau_{VS}}(t), \alpha_{\tau_{ND}}(t)\}$ be a collection of HRFs.

H_1 : The HRFs $\alpha_{\tau_{SV}}(t), \alpha_{\tau_{ND}}(t), \alpha_{\tau_{VS}}(t)$ and $\alpha_{\tau_{ND}}(t)$ satisfy the conditions in Assumption 3.3 and $\alpha_{\tau_{SV}}(t) = O(g \circ h_{exponential}(t)), \alpha_{\tau_{ND}}(t) = O(g \circ h_{exponential}(t))$, $\alpha_{\tau_{IS}}(t) = O(g \circ h_{exponential}(t)), \alpha_{\tau_{VS}}(t) = O(g \circ h_{exponential}(t))$, and $\alpha_{\tau_{ND}}(t) = O(g \circ h_{exponential}(t)) \iff \limsup_{t \rightarrow \infty} \tilde{\alpha}(t) < \infty$.

H_2 : The HRFs $\alpha_{\tau_{SV}}(t), \alpha_{\tau_{VS}}(t)$ and $\alpha_{\tau_{ND}}(t)$ satisfy the conditions in Assumption 3.3 and $\alpha_{\tau_{SV}}(t) = O(g \circ h_{exponential}(t)), \alpha_{\tau_{VS}}(t) = O(\epsilon)$ and $\alpha_{\tau_{ND}}(t) = O(g \circ h_{exponential}(t)) \iff \limsup_{t \rightarrow \infty} \alpha_{\tau_{SV}}(t) < \infty, \limsup_{t \rightarrow \infty} \alpha_{\tau_{VS}}(t) = 0$, and $\limsup_{t \rightarrow \infty} \alpha_{\tau_{ND}}(t) < \infty$.

H_3 : The HRFs $\alpha_{\tau_{SV}}(t)$, and $\alpha_{\tau_{ND}}(t)$ satisfy the conditions in Assumption 3.3; while $\alpha_{\tau_{VS}}(t)$ satisfies Assumption 3.2; and $\alpha_{\tau_{SV}}(t) = O(g \circ h_{exponential}(t)), \alpha_{\tau_{VS}}(t) = \Theta\left(\frac{1}{\epsilon}\right)$ and $\alpha_{\tau_{ND}}(t) = O(g \circ h_{exponential}(t)) \iff \limsup_{t \rightarrow \infty} \alpha_{\tau_{SV}}(t) < \infty, \limsup_{t \rightarrow \infty} \alpha_{\tau_{VS}}(t) = \infty$, and $\limsup_{t \rightarrow \infty} \alpha_{\tau_{ND}}(t) < \infty$.

H_4 : The HRF $\alpha_{\tau_{ND}}(t)$ and $\alpha_{\tau_{SV}}(t)$ satisfies the conditions in Assumption 3.3; while and $\alpha_{\tau_{VS}}(t)$ sat-
isfy Assumption 3.2; and there exists constants $k_1, k_2 > 0$ such that $\alpha_{\tau_{SV}}(t) = k_1 \left(\frac{1}{\alpha_{\tau_{VS}}(t)}\right)^{k_2}$; $\limsup_{t \rightarrow \infty} \alpha_{\tau_{VS}}(t) = \infty$; and $\limsup_{t \rightarrow \infty} \alpha_{\tau_{ND}}(t) < \infty \iff$ there exists constants $k_1, k_2 > 0$ such that $\alpha_{\tau_{SV}}(t) = k_1 \left(\frac{1}{\alpha_{\tau_{VS}}(t)}\right)^{k_2}, \alpha_{\tau_{VS}}(t) = \Theta\left(\frac{1}{\epsilon}\right)$, and $\alpha_{\tau_{ND}}(t) = O(g \circ h_{exponential}(t))$.

Remark 6.3 Since Hypothesis 6.1 (H_1) asserts that all HRFs $\alpha_\tau(t) \in \{\alpha_{\tau_{SV}}(t), \alpha_{\tau_{VS}}(t), \alpha_{\tau_{ND}}(t)\}$ satisfy the growth condition $\alpha_\tau(t) = O(g \circ h_{exponential}(t))$, i.e. all lifetime distributions tend to behave like the exponential distribution asymptotically, the results for Hypothesis 6.1(H_1) in the system (3.21)-(3.23) are utilized as the baseline for comparison with the results for the other hypotheses in Hypothesis 6.1(H_2-H_4), to determine how the ADFE changes whenever the HRFs change their asymptotic behaviors.

The results that follow characterize the ADFE (6.9), whenever Hypothesis 6.1 holds.

Theorem 6.1 Baseline ADFE result:

Let the HRFs $\alpha_{\tau_{ij}}(t) \in \{\alpha_{\tau_{SV}}(t), \alpha_{\tau_{VS}}(t), \alpha_{\tau_{ND}}(t)\}$ satisfy Hypothesis 5.1 ($H_1 - H_4$); and also let Hypothesis 6.1 (H_1) and (3.28) hold. The ADFE for (3.21)-(3.23) is given by $X_0^* = (S_0^*, V_0^*, 0)$, where

$$\begin{aligned} S_0^* &= B \left(\frac{1}{\alpha_{\tau_{SV}} + \alpha_{\tau_{ND}}} \right) \left[\frac{1}{1 - \frac{\alpha_{\tau_{SV}}}{\alpha_{\tau_{SV}} + \alpha_{\tau_{ND}}} \frac{\alpha_{\tau_{VS}}}{\alpha_{\tau_{VS}} + \alpha_{\tau_{ND}}}} \right] \\ &\propto \frac{1}{\alpha_{\tau_{SV}} + \alpha_{\tau_{ND}}} B; \end{aligned} \quad (6.10)$$

or equivalently

$$\begin{aligned} S_0^* &= \left[\frac{\alpha_{\tau_{VS}} + \alpha_{\tau_{ND}}}{\alpha_{\tau_{SV}} + \alpha_{\tau_{VS}} + \alpha_{\tau_{ND}}} \right] \frac{1}{\alpha_{\tau_{ND}}} B \\ &\propto \frac{1}{\alpha_{\tau_{ND}}} B; \end{aligned} \quad (6.11)$$

and

$$V_0^* = \alpha_{\tau_{SV}} \frac{1}{\alpha_{\tau_{VS}} + \alpha_{\tau_{ND}}} S_0^*; \quad I_0^* = 0. \quad (6.12)$$

Proof Clearly, when Hypothesis 6.1 (H_1) and (3.28) hold, then it follows from (6.9) that the ADFE is given by (6.10)-(6.12). \square

Remark 6.4 Theorem 6.1 signifies that when the HRFs $\alpha_{\tau_{VS}}(t)$, $\alpha_{\tau_{SV}}(t)$ and $\alpha_{\tau_{ND}}(t)$ grow over time and become constant like the HRF $h_{exponential}(t)$, $\forall t \geq 0$, (1) the NANLS (3.21)-(3.23) is approximated asymptotically by the corresponding autonomous system (4.1), with exponential coefficients given by (3.28). (2) There exists an ADFE for the system given by (6.10).

From Theorem 5.1 and Remark 5.3, it is easy to see from (6.10) that S_0^* is a constant multiple of the influx B in the system, over the average lifetime in the susceptible state $\mathbb{E}[\tau_{S0}] = \frac{1}{\lambda_{S0}}$; and $V_0^* = \alpha_{\tau_{SV}} \frac{1}{\alpha_{\tau_{VS}} + \alpha_{\tau_{ND}}} S_0^*$ is the susceptibles S_0^* that are vaccinated at the exponential rate $\alpha_{\tau_{SV}}$, over the lifetime in the vaccinated state $\mathbb{E}[\tau_{V0}] = \frac{1}{\lambda_{V0}}$.

Theorem 6.2 Let the HRFs $\alpha_{\tau_{ij}}(t) \in \{\alpha_{\tau_{SV}}(t), \alpha_{\tau_{VS}}(t), \alpha_{\tau_{ND}}(t)\}$ satisfy Hypothesis 5.1 ($H_1 - H_4$); and let Hypothesis 6.1 (H_2) and (3.28) hold. The ADFE for the system (3.21)-(3.23) is given by

$$S_0^* = \frac{1}{\alpha_{\tau_{SV}} + \alpha_{\tau_{ND}}} B; \quad V_0^* = \alpha_{\tau_{SV}} \frac{1}{\alpha_{\tau_{ND}}} S_0^*; \quad I_0^* = 0. \quad (6.13)$$

Proof Clearly, when Hypothesis 6.1 (H_2) and (3.28) hold, where $\lim_{t \rightarrow \infty} \alpha_{\tau_{VS}}(t) = 0$ (since $\alpha_{\tau_{VS}}(t) = O(\epsilon)$), then it follows from (6.9) that the ADFE is given by (6.13). \square

Remark 6.5 It is clear from (6.11) and (6.13) that

$$\begin{aligned} [S_0^* \text{ in (6.10)}] &= B \left(\frac{1}{\alpha_{\tau_{SV}} + \alpha_{\tau_{ND}}} \right) \left[\frac{1}{1 - \frac{\alpha_{\tau_{SV}}}{\alpha_{\tau_{SV}} + \alpha_{\tau_{ND}}} \frac{\alpha_{\tau_{VS}}}{\alpha_{\tau_{VS}} + \alpha_{\tau_{ND}}}} \right] \gg B \left(\frac{1}{\alpha_{\tau_{SV}} + \alpha_{\tau_{ND}}} \right) \\ &= [S_0^* \text{ in (6.13)}], \end{aligned} \quad (6.14)$$

this is because from (6.8), $\left[\frac{1}{1 - \frac{\alpha_{\tau_{SV}}}{\alpha_{\tau_{SV}} + \alpha_{\tau_{ND}}} \frac{\alpha_{\tau_{VS}}}{\alpha_{\tau_{VS}} + \alpha_{\tau_{ND}}}} \right] \gg 1$.

Thus, the magnitude of S_0^* in the ADFE, in the baseline Theorem 6.1 is larger than the corresponding values of S_0^* in (6.13). However, from (6.11) and (6.12), it is easy to see that

$$[V_0^* \text{ in (6.12)}] = \alpha_{\tau_{SV}} \frac{1}{\alpha_{\tau_{VS}} + \alpha_{\tau_{ND}}} S_0^* \leq \alpha_{\tau_{SV}} \frac{1}{\alpha_{\tau_{VS}} + \alpha_{\tau_{ND}}} \frac{1}{\alpha_{\tau_{ND}}} B = [V_0^* \text{ in (6.13)}].$$

This suggests that when Hypothesis 6.1 (H_2) holds, i.e. asymptotically, if both the rates at which susceptible individuals are vaccinated, and die naturally become exponential rates (i.e. $\alpha_{\tau_{SV}}(t) = O(g \circ h_{exponential}(t))$, and $\alpha_{\tau_{ND}}(t) = O(g \circ h_{exponential}(t))$); and the vaccine efficacy is strong, so as to confer immunity against infection lasting over sufficiently long time, which results to a continuously decreasing rate of losing immunity (i.e. $\alpha_{\tau_{VS}}(t) = O(\epsilon)$), then more people remain in the asymptotic vaccinated steady state, whenever the autonomous system (4.1) is achieve.

Theorem 6.3 Let the HRFs $\alpha_\tau(t) \in \{\alpha_{\tau_{SV}}(t), \alpha_{\tau_{ND}}(t)\}$ satisfy Hypothesis 5.1 (H1. – H4.); and let Hypothesis 6.1 (H_3) and (3.28) hold (i.e. $\alpha_{\tau_{VS}}(t) = \Theta(\frac{1}{\epsilon})$). The ADFE for the system (3.21)-(3.23) is given by

$$S_0^* = \frac{1}{\alpha_{\tau_{ND}}} B; \quad V_0^* = 0; \quad I_0^* = 0. \quad (6.15)$$

Proof Clearly, when Hypothesis 6.1 (H_3) holds, and the limits for the HRFs are given in (3.28), where $\alpha_{\tau_{VS}}(t) = \theta(\frac{1}{\epsilon})$, then it follows from (6.9) that the ADFE is given by (6.15). \square

Remark 6.6 It clear from (6.11) and (6.15) that $[S_0^* \text{ in}(6.11)] \leq [S_0^* \text{ in}(6.15)]$, and $[V_0^* \text{ in}(6.12)] > [V_0^* \text{ in}(6.15)]$. While Theorem 6.3 cannot be used to inform vaccination policies for disease control, the results reflect the outcome of attempting to further mitigate the impacts of the disease epidemic using a poorly developed vaccine, meanwhile other more effective control measures are in place. In fact, Theorem 6.3 suggests that when Hypothesis 6.1 (H_3) holds, that is, the rate at which vaccinated individuals lose immunity continuously grows significantly larger than both the rates at which susceptible individuals are vaccinated, or die naturally (i.e. $\alpha_{\tau_{SV}}(t) = O(g \circ h_{\text{exponential}}(t))$, $\alpha_{\tau_{VS}}(t) = \Theta(\frac{1}{\epsilon})$ and $\alpha_{\tau_{ND}}(t) = O(g \circ h_{\text{exponential}}(t))$), then over longtime when the system becomes autonomous, only the susceptible individuals remain in steady state. And the vaccination strategy would be utterly waste of effort and resources.

Theorem 6.4 Let the HRF $\alpha_{\tau_{ND}}(t)$ satisfy Hypothesis 5.1 (H1. – H4.); and let Hypothesis 6.1 (H_4) and (3.28) hold in the case where there exists $k_2 \geq 1$ and $k_1 > 0$ (i.e. $\alpha_{\tau_{SV}}(t) = O(\epsilon)$, whenever $\alpha_{\tau_{VS}}(t) = \Theta(\frac{1}{\epsilon})$). The ADFE for the system (3.21)-(3.23) is given by

$$S_0^* = \frac{1}{\alpha_{\tau_{ND}}} B; \quad V_0^* = 0; \quad I_0^* = 0. \quad (6.16)$$

Proof Clearly, when Hypothesis 6.1 (H_4) holds, and the limits for the HRFs are given in (3.28), where $\alpha_{\tau_{SV}}(t) = k_1 \frac{1}{(\alpha_{\tau_{VS}}(t))^{k_2}}$, $\exists k_1 > 0, k_2 \geq 1$, then it follows from (6.9) that the ADFE is given by (6.16). \square

Remark 6.7 Observe that the conditions of Hypothesis 6.1 (H_4) that $\alpha_{\tau_{SV}}(t)$ is inversely proportional to $\alpha_{\tau_{VS}}(t)$ (i.e. $\alpha_{\tau_{SV}}(t) = k_1 \frac{1}{(\alpha_{\tau_{VS}}(t))^{k_2}}$, $\exists k_1 > 0, k_2 \geq 1$), and that $\alpha_{\tau_{VS}}(t)$ continuously grows sufficiently large (i.e. $\alpha_{\tau_{VS}}(t) = \Theta(\frac{1}{\epsilon})$) reflects the outcome of another poorly planned disease control strategy attempting to further ameliorate the effects of a disease epidemic using a poorly developed vaccine, meanwhile other more effective control measures are in place. In this case the failure of the vaccine (i.e. $\alpha_{\tau_{VS}}(t) = \Theta(\frac{1}{\epsilon})$) leads to a drastic dissuasion of vaccination (i.e. $\alpha_{\tau_{SV}}(t) = O(\epsilon)$). Similarly to Theorem 6.3 and Remark 6.6, this vaccination strategy would be a waste of effort and resources.

Sensitivity of the ZRSF and HRFs over time

Recall, Section 6.1, the the ZRSF (6.9) of the system (3.21)-(3.23) characterizes the state of the system, at any instant $t > 0$ when the system growth rate is zero. And the asymptotic behavior of (6.9) is given in Theorem 6.1-6.4. It is also important to characterize simultaneously, how the ZRSF (6.9) and the HRFs change over time together. This information gives insights on how the nonlinear behaviors of the HRFs in Hypothesis 5.1 affect the ZRSF over time leading to the results in Theorem 6.1-6.4.

For the HRFs $\alpha_\tau(t) \in \{\alpha_{\tau_{SV}}(t), \alpha_{\tau_{VS}}(t), \alpha_{\tau_{ND}}(t)\}$, denote by

$$\begin{aligned} y_\alpha(t) &= \frac{\alpha_{\tau_{SV}}(t)}{\alpha_{\tau_{SV}}(t) + \alpha_{\tau_{ND}}(t)}, \quad z_\alpha(t) = \frac{\alpha_{\tau_{VS}}(t)}{\alpha_{\tau_{VS}}(t) + \alpha_{\tau_{ND}}(t)} \\ x_\alpha(t) &= \left[1 - \frac{\alpha_{\tau_{SV}}(t)}{\alpha_{\tau_{SV}}(t) + \alpha_{\tau_{ND}}(t)} \frac{\alpha_{\tau_{VS}}(t)}{\alpha_{\tau_{VS}}(t) + \alpha_{\tau_{ND}}(t)} \right] = 1 - y_\alpha(t)z_\alpha(t). \end{aligned} \quad (7.1)$$

Then from (6.7), it is easy to see that

$$S_0^*(t) = \left(\frac{B}{\alpha_{\tau_{SV}}(t)} \right) \frac{y_\alpha(t)}{[1 - y_\alpha(t)z_\alpha(t)]}, \quad V_0^*(t) = \frac{\alpha_{\tau_{SV}}(t)}{\alpha_{\tau_{VS}}(t)} z_\alpha(t) S_0^*(t), \quad I_0^*(t) = 0, \quad \forall t \geq 0. \quad (7.2)$$

It is easy to see from (7.2) that the following derivatives hold.

$$\begin{aligned} \frac{\partial S_0^*(t)}{\partial \alpha_{\tau_{SV}}(t)} &= \frac{B}{(\alpha_{\tau_{SV}}(t))^2} \frac{y_\alpha^2(t)}{x_\alpha(t)} \left[\frac{y_\alpha(t)z_\alpha(t)}{1 - y_\alpha(t)z_\alpha(t)} \frac{\alpha_{\tau_{ND}}(t)}{\alpha_{\tau_{SV}}(t)} - 1 \right] \\ &= \frac{B}{(\alpha_{\tau_{SV}}(t))^2} \frac{y_\alpha^2(t)}{x_\alpha(t)} \left[\frac{\alpha_{\tau_{VS}}(t)}{\alpha_{\tau_{SV}}(t) + \alpha_{\tau_{VS}}(t) + \alpha_{\tau_{ND}}(t)} - 1 \right], \end{aligned} \quad (7.3)$$

and

$$\frac{\partial V_0^*(t)}{\partial \alpha_{\tau_{SV}}(t)} = \frac{\alpha_{\tau_{ND}}(t)}{(\alpha_{\tau_{SV}}(t))^2} \frac{z_\alpha^2(t)}{y_\alpha(t)} S_0^*(t) \left[\frac{y_\alpha(t)z_\alpha(t)}{1 - y_\alpha(t)z_\alpha(t)} + 1 \right]. \quad (7.4)$$

Similarly,

$$\frac{\partial S_0^*(t)}{\partial \alpha_{\tau_{VS}}(t)} = B \left(\frac{\alpha_{\tau_{ND}}(t)}{\alpha_{\tau_{SV}}(t)} \right) \frac{1}{(\alpha_{\tau_{VS}}(t))^2} \frac{y_\alpha^2(t)z_\alpha^2(t)}{x_\alpha^2(t)}, \quad (7.5)$$

and

$$\frac{\partial V_0^*(t)}{\partial \alpha_{\tau_{VS}}(t)} = B \cdot \frac{z_\alpha^2(t) \cdot y_\alpha(t)}{x_\alpha^2(t)} \cdot \frac{1}{(\alpha_{\tau_{VS}}(t))^2} \left[-x_\alpha(t) + y_\alpha(t)z_\alpha(t) \frac{\alpha_{\tau_{ND}}(t)}{\alpha_{\tau_{VS}}(t)} \right]. \quad (7.6)$$

Also, define

$$\begin{aligned} f_\alpha(t) &= y_\alpha(t)z_\alpha(t) + \frac{\alpha_{\tau_{ND}}(t)}{\alpha_{\tau_{VS}}(t)} z_\alpha^2(t). \\ &= \frac{\alpha_{\tau_{SV}}(t)}{\alpha_{\tau_{SV}}(t) + \alpha_{\tau_{ND}}(t)} \frac{\alpha_{\tau_{VS}}(t)}{\alpha_{\tau_{VS}}(t) + \alpha_{\tau_{ND}}(t)} + \frac{\alpha_{\tau_{ND}}(t)}{\alpha_{\tau_{VS}}(t) + \alpha_{\tau_{ND}}(t)} \frac{\alpha_{\tau_{VS}}(t)}{\alpha_{\tau_{VS}}(t) + \alpha_{\tau_{ND}}(t)}. \end{aligned} \quad (7.7)$$

The following result characterizes the behavior of the ZRSF of the system (3.21)-(3.23) with respect to the HRFs $\alpha_{\tau_{SV}}(t)$ and $\alpha_{\tau_{VS}}(t)$.

Theorem 7.1 Let the HRFs $\alpha_\tau(t) \in \{\alpha_{\tau_{SV}}(t), \alpha_{\tau_{VS}}(t), \alpha_{\tau_{ND}}(t)\}$ satisfy any of Hypothesis 5.1 (H1. – H4.); and let $f_\alpha(t)$ be as defined in (7.7). The ZRSF (6.7) of the system (3.21)-(3.23) satisfies the following.

$$(1.) \quad \begin{cases} \frac{\partial S_0^*(t)}{\partial \alpha_{\tau_{SV}}(t)} \geq 0, & \text{if } \alpha_{\tau_{SV}}(t) + \alpha_{\tau_{ND}}(t) \geq 1, \\ \frac{\partial S_0^*(t)}{\partial \alpha_{\tau_{SV}}(t)} < 0, & \text{otherwise,} \end{cases} \quad (7.8)$$

and

$$\begin{cases} \frac{\partial V_0^*(t)}{\partial \alpha_{\tau_{SV}}(t)} \geq 0, & \text{if } y_\alpha(t)z_\alpha(t) \geq \frac{1}{2}, \\ \frac{\partial V_0^*(t)}{\partial \alpha_{\tau_{SV}}(t)} < 0, & \text{otherwise.} \end{cases} \quad (7.9)$$

$$(2.) \quad \frac{\partial S_0^*(t)}{\partial \alpha_{\tau_{VS}}(t)} \geq 0; \text{ and}$$

$$\begin{cases} \frac{\partial V_0^*(t)}{\partial \alpha_{\tau_{VS}}(t)} \geq 0, & \text{if } f_\alpha(t) \geq 1, \\ \frac{\partial V_0^*(t)}{\partial \alpha_{\tau_{VS}}(t)} < 0, & \text{otherwise;} \end{cases} \quad (7.10)$$

Proof The results follow from (7.3)-(7.6), and applying trivial differentiation rules, algebraic manipulations and simplifications. \square

Remark 7.1

1. Theorem 7.1 (1.) signifies that in the absence of disease, the ZRSF $S_0^*(t)$ and $V_0^*(t)$ increase monotonically with respect to the HRF $\alpha_{\tau_{SV}}(t)$, whenever the conditions $\alpha_{\tau_{SV}}(t) + \alpha_{\tau_{ND}}(t) \geq 1$ and $y_\alpha(t)z_\alpha(t) \geq \frac{1}{2}$ hold, respectively, otherwise $S_0^*(t)$ and $V_0^*(t)$ decrease monotonically.

Similarly, Theorem 7.1 (2.) signifies that in the absence of disease, the ZRSF $S_0^*(t)$ always increases monotonically with respect to the HRF $\alpha_{\tau_{VS}}(t)$; and given that $S_0^*(t)$ increases with respect to $\alpha_{\tau_{VS}}(t)$, the ZRSF $V_0^*(t)$ increases monotonically, whenever the condition $f_\alpha(t) \geq 1$ holds, otherwise $V_0^*(t)$ decreases.

Recall Remark 6.2, the results of Theorems 6.1-6.4 suggest that asymptotically, after some sufficiently large time $t \geq t_1 > 0$, there exists an ADFE for (3.21)-(3.23), whenever the HRFs satisfy the conditions in Hypothesis 6.1. That is, the results in Theorems 6.1-6.4 give light to the behavior of the ZRSFs $S_0^*(t)$ and $V_0^*(t)$ in the later half-time interval $[t_1, \infty)$.

The new results in Theorem 7.1 now give light on the behavior of the ZRSFs $S_0^*(t)$ and $V_0^*(t)$ as both the ZRSFs and the HRFs $\alpha_{\tau_{VS}}(t)$ and $\alpha_{\tau_{SV}}(t)$ change together over the first half-time interval $t \in (0, t_t)$. Clearly, Theorem 7.1 (1-2) signifies that the ZRFs $S_0^*(t)$ and $V_0^*(t)$, for the susceptible and the vaccinated states, respectively, will rise and fall simultaneously as HRFs $\alpha_{\tau_{SV}}$ (t) and $\alpha_{\tau_{VS}}(t)$, in the same time intervals, wherever the HRFs take the four shapes monotonic, bathtub, unimodal and constant, provided the conditions of Theorem 7.1 (1-2) hold. This result is exhibited in the numerical simulation results in Section 9, that describe the relationships better.

Exponential stability and disease eradication

In this section exponential stability is investigated and comparative results are given for the extinction of the disease in the NANLS (3.21)-(3.23) for the general HRFs in Assumption 3.2, and for the traditional Markovian model in (4.1) with exponential lifetimes. The basic reproduction number for the disease in both systems are obtained.

Theorem 8.1 For the HRFs $\alpha_\tau(t) \in \tilde{\alpha}(t) = \{\alpha_{\tau_{SV}}(t), \alpha_{\tau_{IDD}}(t), \alpha_{\tau_{IS}}(t), \alpha_{\tau_{VS}}(t), \alpha_{\tau_{ND}}(t)\}$ in the NANLS (3.21)-(3.23), let Assumption 3.2 hold. Define $\tau_{I0} = \min(\tau_{IS}, \tau_{IDD}, \tau_{ND})$ i.e. τ_{I0} is the interjump time until every infected individual either recovers from infection or dies from disease related or natural causes. The following statistical and mathematical properties are true.

- (1.) The HRF of τ'_{I0} at anytime $t \geq 0$ is $\alpha_{\tau'_{I0}}(t) = \alpha_{\tau_{IS}}(t) + \alpha_{\tau_{IDD}}(t) + \alpha_{\tau_{ND}}(t)$; the CDF of τ'_{I0} is equivalent to an exponential random variable with non-homogeneous intensity $\lambda'_{I0}(t)$ i.e. $F_{\tau'_{I0}}(t) \sim F_{Exp(\lambda'_{I0}(t))}$, where $\lambda'_{I0}(t)$ is the CHRF of τ'_{I0} given by $\lambda'_{I0}(t) = \int_0^t \alpha_{\tau'_{I0}}(u)du$.
- (2.) The parameters

$$\lambda'_{I0} = \lim_{t \rightarrow \infty} \frac{1}{t} \lambda'_{I0}(t) = \lim_{t \rightarrow \infty} \frac{1}{t} \int_0^t \alpha_{\tau'_{I0}}(u)du, \quad (8.1)$$

and $\frac{1}{\lambda'_{I0}}$ are respectively, the instantaneous exit rate from state I at any time $t \geq 0$, and the average holding time in state I until the individual jumps into either state S , or dies from disease, or from natural causes.

- (3.) The NANLS (3.21)-(3.23) does not have a steady state, however, the basic reproduction number (BRN) of the disease over a finite time interval $[0, t)$ of length t is given by

$$\mathfrak{R}_0(t) = \frac{\beta_{IS}}{\frac{1}{t} \lambda'_{I0}(t)} + \frac{\beta_{IV}}{\frac{1}{t} \lambda'_{I0}(t)}, \quad (8.2)$$

and over a sufficiently long time interval (i.e. $t \rightarrow \infty$) the instantaneous basic reproduction number is given by

$$\mathfrak{R}_0 = \lim_{t \rightarrow \infty} \mathfrak{R}_0(t) = \frac{\beta_{IS}}{\lambda'_{I0}} + \frac{\beta_{IV}}{\lambda'_{I0}}. \quad (8.3)$$

In addition, when $\mathfrak{R}_0 < 1$, there exists $\gamma > 0$ such that

$$\lim_{t \rightarrow \infty} \frac{1}{t} \log(I(t)) < -\gamma. \quad (8.4)$$

That is, $I(t) \rightarrow 0$ exponentially, as $t \rightarrow 0$.

Proof (1.)-(2.) The proofs for (1.) & (2.) are similar to the proof of Theorem 5.1, and omitted.
 (3) Define the Lyapunov function

$$V(t) = \log(I(t)). \quad (8.5)$$

Differentiating (8.5) with respect to the system (3.21)-(3.23) leads to the following.

$$\begin{aligned} dV(t) &= \frac{1}{I(t)} dI(t) = \left[\beta_{IS} \frac{S(t)}{I(t)} + \beta_{IV} \frac{V(t)}{I(t)} - \alpha_{\tau'_{I0}}(t) \right] dt \\ &\leq \left[\beta_{IS} + \beta_{IV} - \alpha_{\tau'_{I0}}(t) \right] dt. \end{aligned} \quad (8.6)$$

It follows from (8.6) it follows that

$$\begin{aligned} \lim_{t \rightarrow \infty} \frac{1}{t} V(t) &\leq \lim_{t \rightarrow \infty} \frac{1}{t} V(0) + \left[\beta_{IS} + \beta_{IV} - \lim_{t \rightarrow \infty} \frac{1}{t} \int_0^t \alpha_{\tau'_{I0}}(u) du \right] \\ &= -\lambda'_{I0} [1 - \mathfrak{R}_0]. \end{aligned} \quad (8.7)$$

Take $\gamma = \lambda'_{I0} [1 - \mathfrak{R}_0] > 0$, whenever $\mathfrak{R}_0 > 0$.

□

Corollary 8.1 Assume that the HRFs $\alpha_\tau(t) \in \tilde{\alpha}(t) = \{\alpha_{\tau_{SV}}(t), \alpha_{\tau_{IDD}}(t), \alpha_{\tau_{IS}}(t), \alpha_{\tau_{VS}}(t), \alpha_{\tau_{ND}}(t)\}$ in the NANLS (3.21)-(3.23) are constants or satisfy Assumption 3.3, i.e. every $\alpha_\tau(t)$ is the HRF of an exponentially distributed random variable with homogeneous rates in (3.28). Then the system (3.21)-(3.23) reduces to the traditional Markovian SVIS model in (4.1). Moreover, the following properties are true.

- (1.) $\tau'_{I0} = \min(\tau_{IS}, \tau_{IDD}, \tau_{ND})$ i.e. τ'_{I0} is the interjump time until every infected individual either recovers from infection or dies from disease related or natural causes, and the HRF of τ'_{I0} at anytime $t \geq 0$ is the constant $\alpha_{\tau'_{I0}} = \alpha_{IS} + \alpha_{IDD} + \alpha_{ND}$; the CDF of τ'_{I0} is the exponential random variable with non-homogeneous intensity $\lambda'_{I0}(t)$ i.e. $F_{\tau'_{I0}}(t) \sim F_{Exp(\lambda'_{I0}(t))}$, where $\lambda'_{I0}(t)$ is the CHRF of τ'_{I0} given by $\lambda'_{I0}(t) = \alpha_{\tau'_{I0}} t$.
- (2.) The parameters

$$\lambda'_{I0} = \lim_{t \rightarrow \infty} \frac{1}{t} \lambda'_{I0}(t) = \alpha_{IS} + \alpha_{IDD} + \alpha_{ND}, \quad (8.8)$$

and $\frac{1}{\lambda'_{I0}}$ are respectively, the instantaneous exit rate from state I at any time $t \geq 0$, and the average holding time in state I until the individual jumps into either state S , or dies from disease, or from natural causes.

- (3.) The system (4.1) has a disease-free equilibrium $(S^*, V^*, 0)$ given by Theorems 6.1-6.4. Furthermore, the instantaneous basic reproduction number (BRN) of the disease is given by

$$\mathfrak{R}_0 = \frac{\beta_{IS}}{\lambda'_{I0}} + \frac{\beta_{IV}}{\lambda'_{I0}}, \quad (8.9)$$

and when $\mathfrak{R}_0 < 1$, there exists $\gamma > 0$ such that

$$\lim_{t \rightarrow \infty} \frac{1}{t} \log(I(t)) < -\gamma. \quad (8.10)$$

That is, $I(t) \rightarrow 0$ exponentially, as $t \rightarrow 0$.

Proof The proof follows immediately from the proof of Theorem 8.1 for the special case of the exponential lifetime. □

Remark 8.1 Theorem 8.1 characterizes the path for disease elimination in the system (3.21)-(3.23). Indeed, the expressions in (8.2)-(8.3) provide the formulas for computing the BRN over finite and sufficiently longtime. And (8.4) asserts that when the BRN is less than one, the disease is eliminated from the population. Similar interpretation of (8.9)-(8.10) is obtained for the Markovian system (3.28). However, important contrasts are drawn

between the two systems and in the results in Theorem 8.1 and Corollary 8.1. (a) By oversimplifying a complex disease dynamics approximating HRFs that have nonlinear hazard shapes by corresponding constant hazard shapes of the exponential distribution in (3.28), it is impossible to obtain insights on how the BRN changes over time as in (8.2)-(8.3). Secondly, while the result for $\mathfrak{R}_0 < 1$ is exciting, it only in the result (8.2)-(8.3) and Theorem 8.1 (1) that one gathers perspective about the underlying factors affecting the decline in the state $I(t)$ over time. In fact, if $\mathfrak{R}_0 < 1$ and in Theorem 8.1 (1), for instance, it follows that $\alpha_{\tau_{IS}}(t)$ is monotonic decreasing while $\alpha_{\tau_{TDD}}(t)$ is monotonic increasing, then from (8.2), one concludes that the decline in $I(t)$ overtime is a result of a rising mortality rate of the disease, and not because of increased recovery over time. In this scenario, the decline of $I(t)$ overtime in (8.4) is a cause for concern and not an advantage for disease eradication. Other advantages of the NANLS (3.21)-(3.23) over the Markovian system (4.1) are given subsequently in the example in Subsection 8.1.

Theoretical example

Theorem 8.1 and Corollary 8.1 illuminate the major differences in disease eradication mechanisms, and disadvantages of the inflexible Markovian SVIS model (4.1) to represent complex disease dynamics compared to the SVIS epidemic model (3.21)-(3.23) with general lifetime distributions. The following example simultaneously shows a step-by-step approach (a.) to identify and model the non-MAC transition event lifetime distributions for τ_{IS} , τ_{TDD} , and τ_{ND} in (3.21)-(3.23) defined in Assumption 3.1; and (b.) to compare disease eradication conditions in NANLS (3.21)-(3.23) and ANLS (4.1) to determine the extend that the lifetime distributions affect the SVIS dynamics from the dynamics in (4.1).

Description of data

Consider an arbitrary disease epidemic with (1.) a significantly high risk of death without vaccination e.g. SARS-CoV-2 COVID-19 with median time from onset of symptom until death under 20 days (cf.⁴¹); and HIV/AIDS with 90% mortality rate without ART (cf.⁴²) (note that no information in this example reflects COVID19 or HIV/AIDS epidemics). This suggests that the HRF for the time until death $\alpha_{\tau_{TDD}}(t)$ is monotonically increasing. Suppose 50 non-survivors of the disease in the population are observed, and Figure 6 (c) is a summary for uncensored time after symptoms emerge until death from the disease in years.

(2.) Assume that the vaccinated yields some positive response to a single dose vaccine which offers some protection from infection, and also promotes recovery from infection for those who catch infection after vaccination. However, both the artificial immunity and influence on recovery diminish overtime. This suggests that the risk of vaccine failure rises i.e. $\alpha_{\tau_{VS}}(t)$ increases monotonically; and the HRF for recovery $\alpha_{\tau_{IS}}(t)$ decreases monotonically overtime. Figure 6(a) is a summary for an independent sample of 60 subjects containing simulated data of uncensored time for τ_{IS} after symptoms emerge until recovery from infection; and Figure 6(b) is a summary for an independent sample of 40 subjects containing simulated data of uncensored time for τ_{VS} after vaccination until no antibodies from the vaccine can be detected.

(3.) Assume that the risk of natural death remains constant overtime and the average lifespan is 77.5 years. This implies the HRF for natural death is for the exponential distribution with rate $\alpha_{\tau_{ND}}(t) = \alpha_{ND} = \frac{1}{77.5}$ per year.

(4.) For simplicity assume there are ongoing vaccination campaigns to educate about the vaccine, but the population responds slowly to the education at a steady rate. Individuals seek vaccination on average 13 months after training so that the HRF $\alpha_{\tau_{SV}}(t)$ is for the exponential distribution with rate $\alpha_{\tau_{SV}}(t) = \alpha_{SV} = \frac{1}{13/12}$ per year.

(5.) For the MAC contact rates, to allow different scenarios for the disease, it is assumed that the disease has an average yearly incidence between 0.77 and 42.5 per 50 people, i.e. $\beta_{IS} \in [0.77/50 = 0.0154, 42.5/50 = 0.85]$ per year. Furthermore, the protection conferred by the vaccine leads to between 0.2% to 98% reduction in the disease transmission rate, i.e. $\beta_{IV} \in [0.02 \times \beta_{IS}, 0.98 \times \beta_{IS}]$ per year. Also, it is assumed that there is a slow steady influx of $B = 0.55/52$ per year who are susceptible.

(6.) The population initially is composed of the states: $S(0) = 280$, $I(0) = 15$, $V(0) = 5$, and $N(0) = S(0) + V(0) + I(0) = 300$.

Statistical Analysis of the non-MAC transition event lifetime models

The uncensored data in Figure 6 is used to determine the exact distributions of the random variables τ_{IS} , τ_{VS} and τ_{TDD} . Since the histograms are right skewed, a plausible starting point is to verify members of the *Exponential family*¹³ such as the *gamma* distribution subfamily that includes *gamma*, *Weibull* and *exponential* distributions^{13,23}, and other mixture distributions such as the *Lindley* distribution⁴³. Figure 7 shows the *Quantile-Quantile (Q-Q) plot*⁴⁴ for the observations of τ_{IS} , τ_{VS} in Figure 6 (a)-(b) compared to the corresponding theoretical quantiles of two gamma distributions with shape and rate parameters: $(shape(\beta), rate(\alpha)) = (0.5, 0.75)$ in Figure 6 (a), and $(shape(\beta), rate(\alpha)) = (2, 0.3)$ in Figure 6 (b). The moderate to strong linear correlation in the Q-Q plots provide significant evidence that $\tau_{IS} \sim Gamma(shape = 0.5, rate = 0.75)$ and $\tau_{VS} \sim Gamma(shape = 2, rate = 0.3)$. Also, applying *Kolmogorov-Smirnov test*⁴⁵ on the observations for τ_{TDD} in Figure 6(c), comparing the data against 50 randomly simulated quantiles from *Lindley*($\theta = 0.1$) yields a $p - value = 0.8693$. Hence, there is no reason to doubt that $\tau_{TDD} \sim Lindley(\theta = 0.1)$.

Thus, based on the conclusions of the statistical analysis that $\tau_{IS} \sim Gamma(shape = 0.5, rate = 0.75)$, $\tau_{VS} \sim Gamma(shape = 2, rate = 0.3)$ and $\tau_{TDD} \sim Lindley(\theta = 0.1)$, the following give a proper interpretation of the parameters of the non-MAC transition events lifetime distributions in the SVIS disease dynamics.

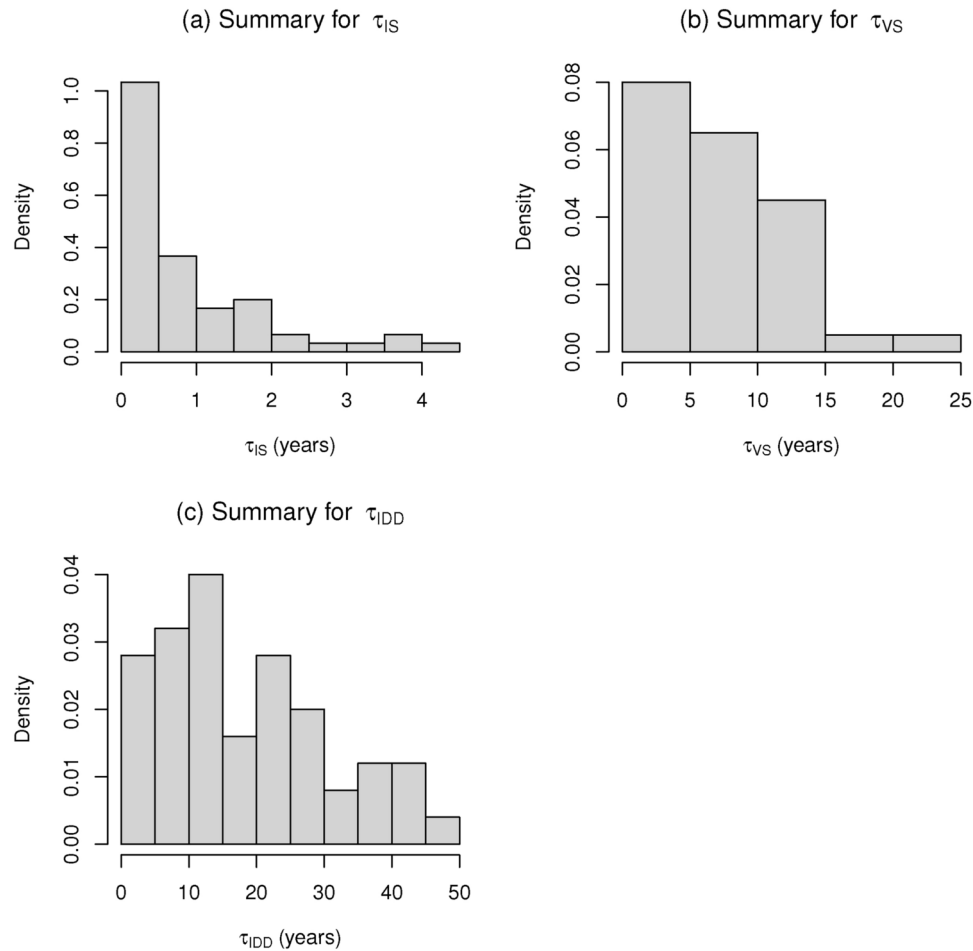


Fig. 6. (a) is a histogram for an independent sample of 60 subjects containing simulated data of uncensored time τ_{IS} , after symptoms emerge until recovery from infection; and Figure (b) is a summary for an independent sample of 40 subjects containing simulated data of uncensored time for τ_{VS} , after vaccination until no antibodies from the vaccine can be detected. Figure (c) is a summary for uncensored time τ_{IDD} after symptoms emerge until death from the disease in years.

- (i) The mean and variance time after symptoms emerge until recovery in the population based on $\tau_{IS} \sim \text{Gamma}(\text{shape}(\beta) = 0.5, \text{rate}(\alpha) = 0.75)$ are $\mathbb{E}[\tau_{IS}] = \alpha\beta = 0.375$ years (19.5 weeks), and $\text{Var}[\tau_{IS}] = \alpha\beta^2 = 0.1875$.
- (ii) The mean and variance time after vaccination until the vaccine wanes based on $\tau_{VS} \sim \text{Gamma}(\text{shape} = 2, \text{rate} = 0.3)$ are $\mathbb{E}[\tau_{VS}] = \alpha\beta = 0.6$ years (31.2 weeks), and $\text{Var}[\tau_{VS}] = \alpha\beta^2 = 0.24$.
- (iii) The mean and mode time after symptoms emerge until disease related death based on $\tau_{IDD} \sim \text{Lindley}(\text{shape}(\theta) = 0.1)$ are $\mathbb{E}[\tau_{IDD}] = \frac{\theta+2}{\theta(\theta+1)} = 19.09$ years; and $\text{mode} = \frac{1-\theta}{\theta} = 9$ years.

Furthermore, for the given values of the shape, rate and scale parameters of the gamma and Lindley distributions above, the HRFs in the SVIS model over a period $t \in [0, 40]$ years, are shown in Figure 8. Observe that the behaviors of the HRFs $\alpha_{\tau_{IS}}(t)$, $\alpha_{\tau_{VS}}(t)$, and $\alpha_{\tau_{IDD}}(t)$ reflect the monotonic decreasing, increasing and increasing behaviors, respectively, as suggested in Subsection 8.1. In addition, these HRFs satisfy the general assumptions in Assumption 3.2.

Recall^{13,23,43}, for $\tau_1 \sim \text{Gamma}(\text{shape}(\beta), \text{rate}(\alpha))$, $\tau_2 \sim \text{Exponential}(\alpha)$, and $\tau_3 \sim \text{Lindley}(\theta)$, the CHRFs are denoted by

$$\begin{aligned} H_{\tau_1}^{\text{gamma}}(t, \alpha, \beta) &= -\log \left(1 - \frac{\Gamma(\alpha, t/\beta)}{\Gamma(\alpha)} \right), t > 0; \quad H_{\tau_2}^{\text{exponential}}(t, \alpha) = \alpha t, t > 0, \\ H_{\tau_3}^{\text{Lindley}}(t, \theta) &= -\log \left(\frac{(\theta + 1 + \theta t)e^{-\theta t}}{\theta + 1} \right), t > 0, \end{aligned} \quad (8.11)$$

where $\Gamma(\alpha, t/\beta)$ is the lower incomplete gamma function (cf.²³).

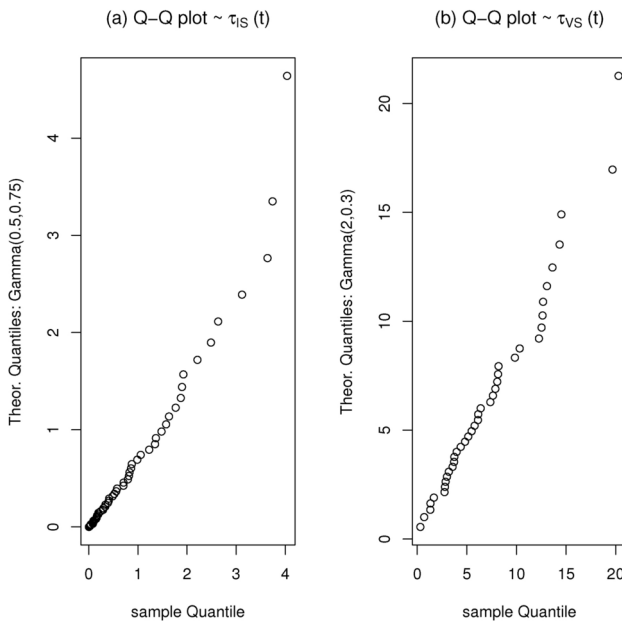


Fig. 7. (a) shows the *Quantile-Quantile (Q-Q) plot* for the observed τ_{IS} in Figure 6 (a) with the corresponding theoretical quantiles of gamma distributions with shape and rate parameters $(\beta, \alpha) = (0.5, 0.75)$; and (b) shows the *Quantile-Quantile (Q-Q) plot* for the observed τ_{VS} in Figure 6 (b) with the corresponding theoretical quantiles of gamma distributions with shape and rate parameters $(\beta, \alpha) = (2, 0.3)$.

Results for the mathematical analysis in Theorem 8.1 and Corollary 8.1

The results in Theorem 8.1 and Corollary 8.1 for the given data in Subsections 8.1 & 8.1 are examined.

Results for the NANLS SVIS model (3.21)-(3.23) : In Theorem 8.1 (1), observe from (8.11) that the HRF and CHRF of τ_{I0} are given as follows.

$$\begin{aligned} \alpha_{\tau'_{I0}}(t) &= \alpha_{\tau_{IS}}(t) + \alpha_{\tau_{IID}}(t) + \alpha_{\tau_{ND}}(t); \\ \lambda'_{I0}(t) &= \int_0^t \alpha_{\tau'_{I0}}(u) du = H_{\tau_1}^{gamma}(t, \alpha = 0.75, \beta = 0.5) + H_{\tau_3}^{Lindley}(t, \theta = 0.1) \\ &\quad + H_{\tau_1}^{gamma}(t, \alpha = 0.3, \beta = 2) + H_{\tau_2}^{exponential}(t, \alpha = 1/77.5). \end{aligned} \quad (8.12)$$

From (8.2), (8.12), and the data in Subsection 8.1 (3), the BRN at any time $t \in (0, 40]$ is computed for any selected value of $\beta_{IS} \in [0.0154, 0.85]$ and $\beta_{IV} = 0.02 \times \beta_{IS}$ using

$$\mathfrak{R}_0(t) = \frac{\beta_{IS}}{\frac{1}{t}\lambda'_{I0}(t)} + \frac{0.02 \times \beta_{IS}}{\frac{1}{t}\lambda'_{I0}(t)}. \quad (8.13)$$

Figure 9 depicts discrete values of $\mathfrak{R}_0(t)$ over $t \in (0, 40]$, whenever $\beta_{IS} = 0.85$. This figure shows that $\mathfrak{R}_0(t) < 1, \forall t \in (0, 40]$, and while $\mathfrak{R}_0(t)$ increases initially during the first 20 years, it drops suddenly, and hence, the disease is expected to die out over time.

The remark of the disease dying out over time is evident in the trajectories of the system (3.21)-(3.23) given in Figure 10. Indeed, in Figure 10 (b) the disease state $I(t)$ dies out over time. The behaviors of the HRFs in Figure 8 have created an oscillatory behavior in the state $S(t)$ in Figure 10 (a) which typically does not occur in traditional autonomous o.d.e systems such as the (4.1)(cf.⁴⁶). In fact, the initial decline in $S(t)$ is due mostly to vaccination and also due to infection at the exponential rates, α_{SV} and β_{IS} ; however, the declining potency of the vaccine overtime exhibited in Figure 8 (b) results in a rise in $S(t)$. Coupled with less recovery from infection over time in Figure 8 (a), ongoing infection at constant rate β_{IS} , and a rise in fatality rate of the disease in Figure 8 (c) (owing to the expiring implicit benefits, such as the power of the vaccine to reduce severity of infection for those that vaccinated before infection), the susceptible state $S(t)$ continues to decline overtime. Similarly, $V(t)$ in Figure 10 (c) rises initially due to the steady vaccination at exponential rate β_{IV} coupled with the initial high potency of the vaccine to block infection (i.e. $\beta_{IV} = 0.02 \times \beta_{IS}$). However, the decline in $V(t)$ overtime is due

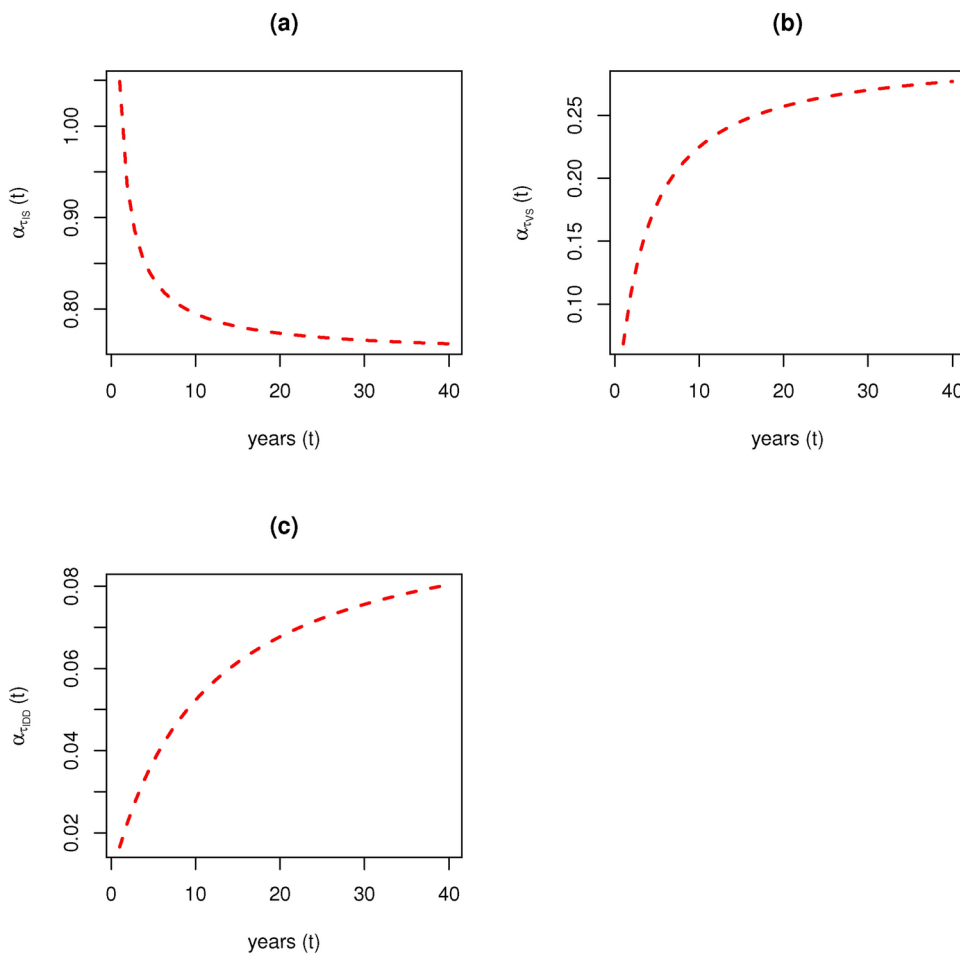


Fig. 8. (a) shows the monotonic decreasing HRF for $\alpha_{\tau_{IS}}(t)$ based on gamma distributions with shape and rate parameters $(\beta, \alpha) = (0.5, 0.75)$; (b) shows the monotonic increasing HRF $\alpha_{\tau_{VS}}(t)$, based on gamma distributions with shape and rate parameters $(\beta, \alpha) = (2, 0.3)$; and (c) shows the monotonic increasing HRF $\alpha_{\tau_{IDD}}(t)$ based on $\tau_{IDD} \sim Lindley(shape(\theta) = 0.1)$ in the SVIS model over a period $t \in [0, 40]$ years, respectively.

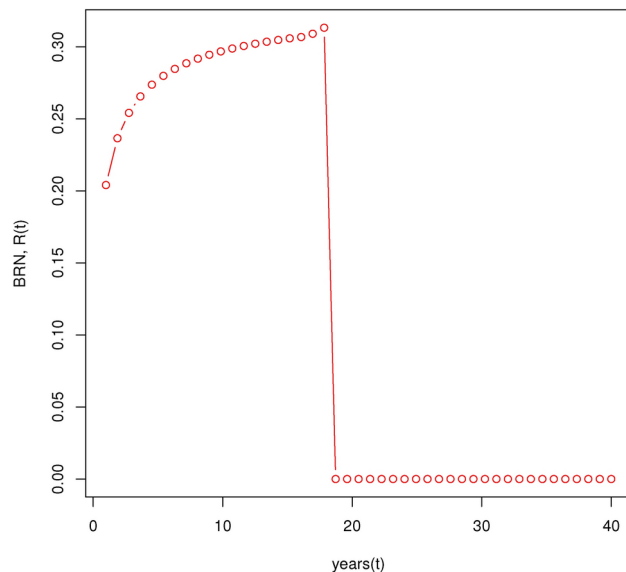


Fig. 9. Shows the discrete values of $\mathfrak{R}_0(t)$ over $t \in (0, 40]$ with $\beta_{IS} = 0.85$, and here $\mathfrak{R}_0(t) < 1, \forall t \in (0, 40]$.

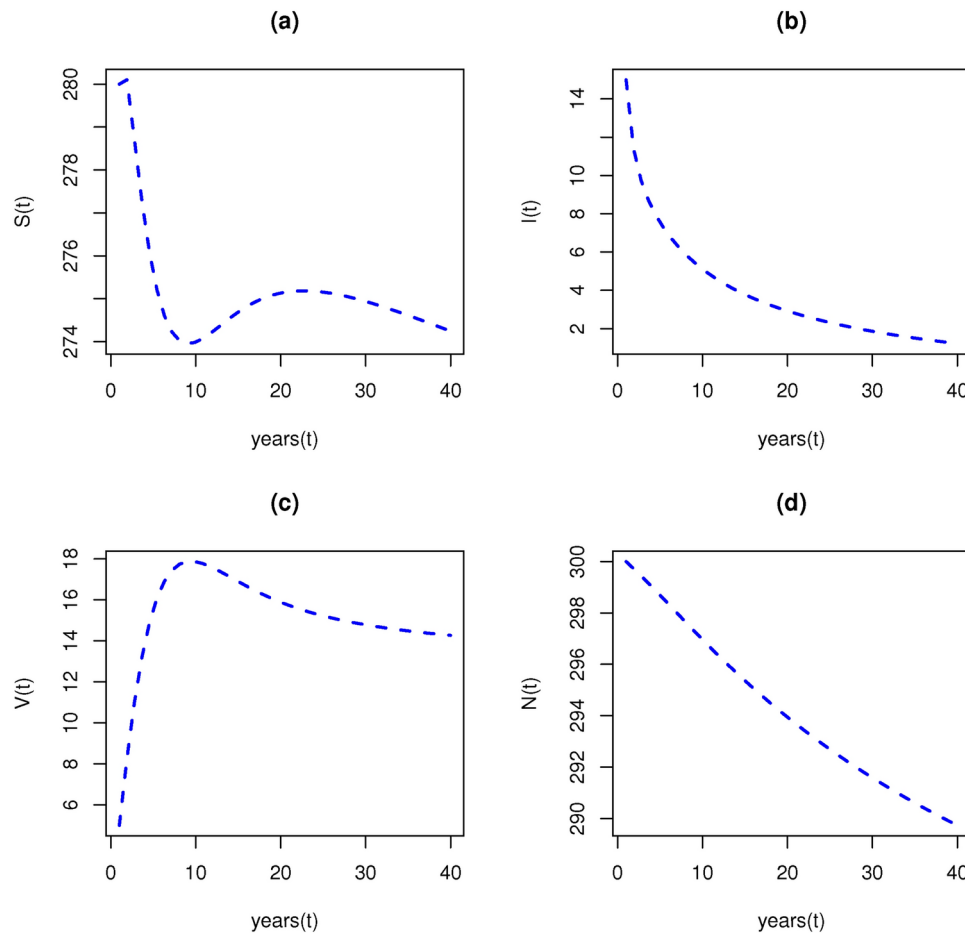


Fig. 10. Shows the trajectories of the system (3.21)–(3.23) under the influence of the HRFs in Figure 8. (a) shows the trajectory of the $S(t)$, (b) shows the trajectory of the $I(t)$, (c) shows the trajectory of the $V(t)$, and (d) shows the trajectory of the $N(t)$ over $t \in (0, 40]$.

to artificial immunity waning over time in Figure 8 (b). While the decline in the state $I(t)$ overtime can indicate disease eradication, it should be noted in Figure 10 (b) that the decline over time is not matched by a rise in recovery in Figure 8 (a). Also, the rise in disease related death in Figure 8 (c) indicates clearly that the decline in $I(t)$ overtime is due to a rising mortality rate of the disease. Thus, the condition $\mathfrak{R}_0 < 1$ in this scenario tells only half the story about the decline of disease in the population.

Results for the SVIS ANLS (4.1): The results from the above analysis elucidate the disadvantages of using the Markovian SVIS ANLS (4.1) for a complex disease dynamics. In fact, to examine the results for (4.1) in Corollary 8.1, the averages in Subsection 8.1 (i.)–(iii.) are used to estimate the HRFs $\alpha_{\tau_{IS}}(t) \approx 1/0.375$, $\alpha_{\tau_{VS}}(t) \approx 1/0.6$ and $\alpha_{\tau_{IDD}}(t) \approx 1/19.09$. In addition to the other parameter estimates in Subsection 8.1, the BRN in (8.8) is given for the same value of $\beta_{IS} = 0.85$ by

$$\begin{aligned}\lambda'_{I0} &= \lim_{t \rightarrow \infty} \frac{1}{t} \lambda'_{I0}(t) = \alpha_{IS} + \alpha_{IDD} + \alpha_{ND} \approx 4.386, \\ \mathfrak{R}_0 &= \frac{\beta_{IS}}{\lambda'_{I0}} + \frac{0.02 \times \beta_{IS}}{\lambda'_{I0}} \approx 0.19.\end{aligned}\tag{8.14}$$

Unfortunately, despite the fact that the BRN $\mathfrak{R}_0 < 1$, the system (4.1) under the given set of parameter estimates and assumption of exponential lifetime for both MAC and non-MAC transition events violates the existence of a unique positive solution in Theorem 4.1. Therefore, the trajectories for the system (4.1) are omitted. This clearly indicates the disadvantage of over simplifying a complex disease dynamics such as (3.21)–(3.23) by approximating important HRFs that have nonlinear hazard shapes overtime by the constant hazard shape of an exponential distribution.

Numerical simulations

In this section, numerical simulation results for the NANLS SVIS epidemic model in (3.21)-(3.23) subject to various specific lifetime distributions (cf.^{47–50}), are given, to elucidate the behaviors of the trajectories of the system relative to the ZRSF in (6.7), whenever the HRFs of the distributions satisfy the shapes in Hypothesis 5.1 (H1.–H4.). Moreover, the ADFE for each case in Theorem 6.1–6.4 is given.

Trajectories based on the Equation (6.7) and ADFE based on the Theorem 6.1

Consider the random time until a susceptible person is vaccinated, $\tau_{SV} \sim Lindley(\theta > 0)$ with a scale parameter θ , that represents the rate of vaccination in a population. The hazard rate of the *Lindley distribution* (cf.¹⁷) is defined as,

$$\alpha_{\tau_{SV}}(t) = h(t)|_{Lindley(\theta)} = \frac{\theta^2(1+t)}{1+\theta+\theta t}, t \geq 0. \quad (9.1)$$

It can be shown that $\limsup_{t \rightarrow \infty} \alpha_{\tau_{SV}}(t) = \theta$. Let, the rate of vaccination in a population is $\theta = 0.3$. Hence, the initial value of $\alpha_{\tau_{SV}}(0) = \frac{0.3^2}{1+0.3} = 0.0692308$, then the HRF $\alpha_{\tau_{SV}}(t)|_{Lindley(\theta)}$ increases monotonically, remains bounded at $\theta = 0.3$ over time, satisfies the shape of the Hypothesis 5.1(H4.), and is depicted in Figure 11(a). Which suggests a growing desire for vaccination, the population is well sensitized, and educated about a good vaccine. Again, consider the random time until each vaccine dose of type i wanes, $\tau_{v_i} \sim EWFD$ ($\alpha_i > 0, \theta_i > 0, \sigma_i > 0$), $i = 1, 2, \dots, n$, where α_i represents the rate of vaccine efficacy changes over time, θ_i indicates the vaccine immunity wane rate, and σ_i represents the time scale over which the vaccine remain effective (cf.³¹). Here, the reliability of the vaccine immunity is a competing risk with a *parallel competitive lifetime arrangement for all n doses* (cf.²²). This implies that the time until the system wanes, is given by $\tau_{VS}(t) = \max(\tau_{v_1}, \tau_{v_2}, \dots, \tau_{v_n})$. Furthermore, it is easy to show that the HRF for $\tau_{VS}(t)$ is given by the sum of the HRF of the lifetime of the components i.e.,

$$\alpha_{\tau_{VS}}(t) = \sum_{i=1}^n h(t)|_{EWFD(\alpha_i, \theta_i, \sigma_i)} = \sum_{i=1}^n \frac{\left(\frac{\alpha_i \theta_i}{\sigma_i}\right) \left(\frac{t}{\sigma_i}\right)^{\alpha_i-1} e^{-(\frac{t}{\sigma_i})^{\alpha_i}} \left(1 - e^{-(\frac{t}{\sigma_i})^{\alpha_i}}\right)^{\theta_i-1}}{1 - \left(1 - e^{-(\frac{t}{\sigma_i})^{\alpha_i}}\right)^{\theta_i}}, t \geq 0. \quad (9.2)$$

If three different vaccine doses are considered in the model, i.e. $n = 3$, then for the parallel system,

$$\alpha_{\tau_{VS}}(t)|_{EWFD(\alpha_i, \theta_i, \sigma_i)} = \sum_{i=1}^3 \frac{\left(\frac{\alpha_i \theta_i}{\sigma_i}\right) \left(\frac{t}{\sigma_i}\right)^{\alpha_i-1} e^{-(\frac{t}{\sigma_i})^{\alpha_i}} \left(1 - e^{-(\frac{t}{\sigma_i})^{\alpha_i}}\right)^{\theta_i-1}}{1 - \left(1 - e^{-(\frac{t}{\sigma_i})^{\alpha_i}}\right)^{\theta_i}}, i = 1, 2, 3. \quad (9.3)$$

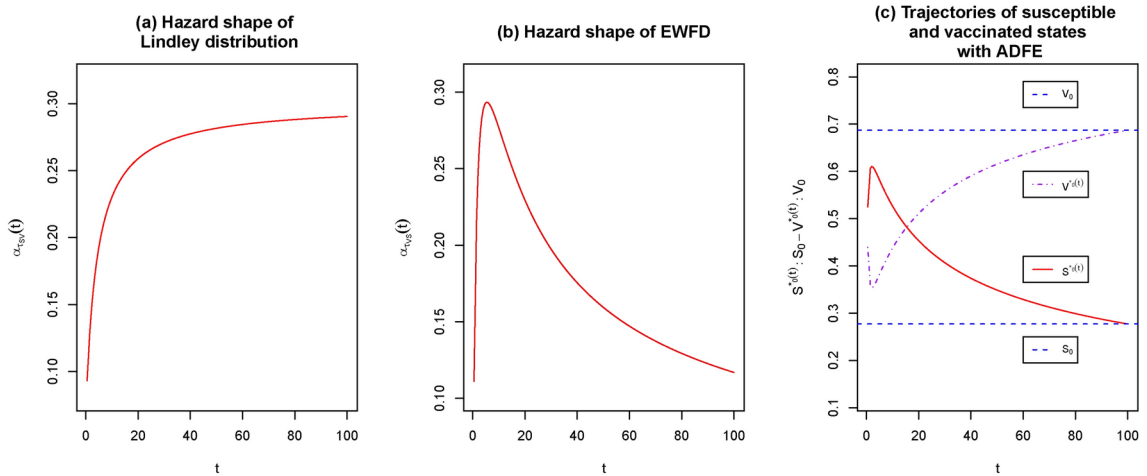


Fig. 11. Shows the different shapes of the HRFs, trajectories, and ADFE of subsection 9.1. Note, (a) shows the shape of the HRF of the *Lindley distribution* with shape parameter $\theta = 0.3$, which has a monotonically increasing shape over time for τ_{SV} in (9.1), (b) shows the shape of the HRF of the *EWFD* with three different sets of parameters as $(\alpha_1 = 0.4, \theta_1 = 5, \sigma_1 = 2)$, $(\alpha_2 = 0.5, \theta_2 = 5, \sigma_2 = 2)$, and $(\alpha_3 = 0.6, \theta_3 = 5, \sigma_3 = 2)$, which increases initially, reaches to a pick point, then start decreasing for τ_{VS} in (9.3), (c) shows the trajectory of the susceptible state based on the equation (6.7) with corresponding ADFE line based on the equation (6.11), and the trajectory of the vaccinated state based on the equation (6.7) with corresponding ADFE line based on the equation (6.12).

Based on the three different sets of parameters for the EWFD as $(\alpha_1 = 0.4, \theta_1 = 5, \sigma_1 = 2)$, $(\alpha_2 = 0.5, \theta_2 = 5, \sigma_2 = 2)$, and $(\alpha_3 = 0.6, \theta_3 = 5, \sigma_3 = 2)$; the HRF is computed, satisfies the shape of the Hypothesis 5.1(H2.), and is depicted in Figure 11(b). The HRF represents low risk initially, rises to a peak point over time, then start decreasing, but remains bounded over time. This suggests that initially, the vaccine is effective, but its efficacy begins to decrease over time, leading to an increasing failure rate.

For the other parameters of the model (3.21)-(3.23) that do not depend on time, it is assumed that the average influx rate, $B = 0.00024525$. For simplicity, it is assumed that the lifetime until natural death is exponentially distributed i.e. $\tau_{ND} \sim \text{Exponential}(\lambda = 0.0132275132)$. This implies that based on the lifespan of 75.6 years, the HRF $\alpha_{\tau_{ND}} = 1/75.6 = 0.0132275132$ per year. By using these HRFs, and the equation (6.7), the trajectories of $S_0^*(t), V_0^*(t)$ against time t are computed, and depicted in Figure 11(c). The corresponding ADFE based on the Theorem 6.1 is given into the figure, denoted by dashed line. Note that, no trajectory for the infectious state, $I_0^*(t)$ is presented due to the 0 value in the equation (6.7). Here, the trajectory of the susceptible state, $S_0^*(t)$ in the Figure 11(c), denoted by solid line, increases initially, reaches to a peak point, then decreases over time into the ADFE S_0^* . Which suggests that, if the system remains in a zero-rate over time (i.e. ZRSFs exist), then initially due to, for instance, false rumors, and low vaccine efficacy, susceptible people remain unwilling to receive vaccinations, and over time, the number of susceptible people who are without immunity remain in a maximum point. Later over time, susceptible people become sensitized, learn about good vaccines, get vaccinated, and gradually leave the susceptible state into the vaccinated state as they receive effective vaccination to develop immunity. This results in a decreasing trend for the susceptible state, that becomes bonded in the ADFE. Again, the trajectory of the vaccinated state, $V_0^*(t)$ in the Figure 11(c), denoted by dotdash line, decreases initially due to use of low effective vaccines, and reach to a minimum point. Later over time, the vaccine efficacy grows and more people remain immune; as a result, the number of persons with vaccine immunity rises and the trend grows and remains bounded in the ADFE.

Trajectories based on the Equation (6.7) and ADFE based on the Theorem 6.2

Consider, the random time until a susceptible person is vaccinated, $\tau_{SV} \sim \text{Lindley}(\theta > 0)$ with scale parameter θ , which represents the rate of vaccination in a population. The hazard rate of the *Lindley distribution* (cf. 17) is defined in (9.1). It can be shown that $\limsup_{t \rightarrow \infty} \alpha_{\tau_{SV}}(t) = \theta$. Let, the rate of vaccination in a population is $\theta = 0.03$. Hence, the initial value of $\alpha_{\tau_{SV}}(0) = \frac{0.03}{1+0.03} = 0.0008737864$, then the HRF $\alpha_{\tau_{SV}}(t)|_{\text{Lindley}(\theta)}$ increases monotonically, remains bounded at $\theta = 0.03$ over time, satisfies the shape of the Hypothesis 5.1(H4.), and is depicted in Figure 12(a). Which suggests a growing desire for vaccination, the population is well sensitized, and educated about a good vaccine. Again, consider the random time until each vaccine dose of type i wanes, $\tau_{v_i} \sim \text{Gamma}(\alpha_i > 0, \lambda_i > 0)$, $i = 1, 2, \dots, n$, where α_i represents the number of stages of the immune response, λ_i affects the duration of vaccine efficacy (cf. 30). Here, the reliability of the vaccine immunity is a competing risk with a *parallel competitive lifetime arrangement* for all n doses (cf. 22). This implies that the time until the immunity in the system wanes is given by $\tau_{VS}(t) = \max(\tau_{v_1}, \tau_{v_2}, \dots, \tau_{v_n})$. Furthermore, it is easy to show that the HRF for the $\tau_{VS}(t)$ is given by the sum of the HRF of the lifetime of the components i.e.,

$$\alpha_{\tau_{VS}}(t) = \sum_{i=1}^n h(t)|_{\text{Gamma}(\alpha_i, \lambda_i)} = \sum_{i=1}^n \frac{\lambda_i^{\alpha_i} t^{\alpha_i-1} e^{-\lambda_i t}}{\Gamma(\alpha_i) - \gamma(\alpha_i, \lambda_i t)}, t \geq 0. \quad (9.4)$$

If three different vaccine doses are considered in the model, i.e. $n = 3$, then for the parallel system,

$$\alpha_{\tau_{VS}}(t)|_{\text{Gamma}(\alpha_i, \lambda_i)} = \sum_{i=1}^3 \frac{\lambda_i^{\alpha_i} t^{\alpha_i-1} e^{-\lambda_i t}}{\Gamma(\alpha_i) - \gamma(\alpha_i, \lambda_i t)}, i = 1, 2, 3. \quad (9.5)$$

Based on the three different sets of parameters for the *Gamma distribution* as $(\alpha_1 = 3, \lambda_1 = 0.2)$, $(\alpha_2 = 3, \lambda_2 = 0.3)$, and $(\alpha_3 = 3, \lambda_3 = 0.4)$; the HRF is computed, satisfies the shape of the Hypothesis 5.1(H2.), and is depicted in Figure 12(b). The HRF represents moderate risk initially, rises to a peak point, then start decreasing, but remain bounded over time. Which suggests that, initially the vaccine works, but vaccine's efficacy start decreasing against the disease, failure rate rises to a maximum value; the failure rate of the vaccine decreases eventually. For the others parameters of the model (3.21)-(3.23) that do not depend on time, it is assumed that the average influx rate, $B = 0.00024525$. For simplicity, it is assumed that the lifetime until natural death is exponentially distributed i.e. $\tau_{ND} \sim \text{Exponential}(\lambda = 0.0132275132)$. This implies that the HRF is $\alpha_{\tau_{ND}} = 0.0132275132$ per year. By using the above HRFs and the equation (6.7), the trajectories of $S_0^*(t), V_0^*(t)$ against time t are computed, and depicted in Figure 12(c). The corresponding ADFE based on the Theorem 6.2 is depicted into the figures, denoted by the dashed line. Note that, no trajectory for the infectious state, $I_0^*(t)$ is presented due to the 0 value in equation (6.7).

Here, the trajectory of the susceptible state, $S_0^*(t)$ in the Figure 12(c), denoted by solid line, is nearly constant initially, then decreases over time into the ADFE $S_0^*(t)$. Which suggests that if the system remains in a zero-rate over time (i.e. ZRSFs exist), then initially due to, for instance, hesitation and uncertainty about vaccine efficacy, fewer susceptible people receive the vaccine and leave the susceptible state. Later over time, susceptible people become sensitized, learn about a good vaccine, get vaccinated, and gradually leave the susceptible state into the vaccinated state, as they receive effective vaccination to develop immunity. This results is a decreasing

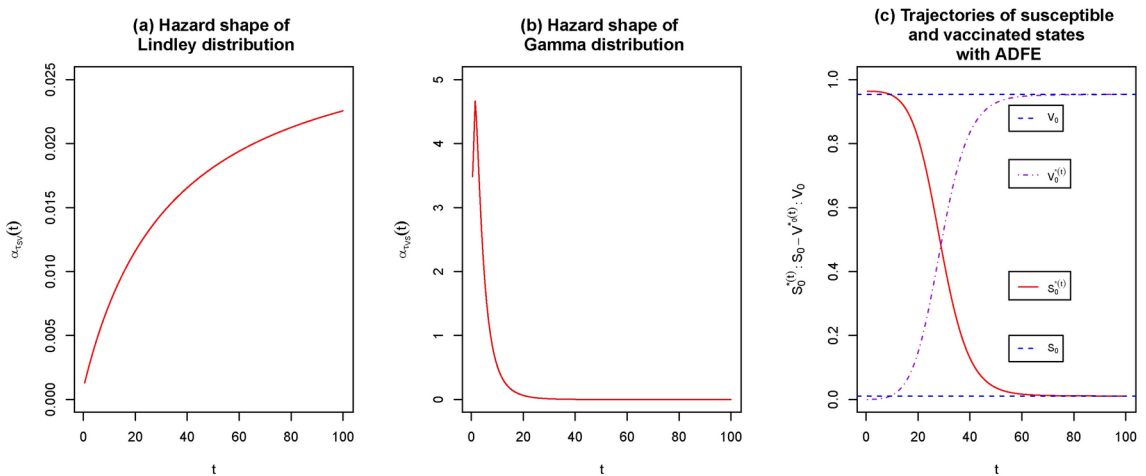


Fig. 12. Shows the different shapes of the HRFs, trajectories, and ADFE of subsection 9.2. Note, (a) shows the shape of the HRF of the *Lindley distribution* with shape parameter $\theta = 0.03$, which has a monotonically increasing shape over time for τ_{SV} in (9.1), (b) shows the shape of the HRF of the *Gamma distribution* with three different sets of parameters as $(\alpha_1 = 3, \theta_1 = 0.2)$, $(\alpha_2 = 3, \theta_2 = 0.3)$, and $(\alpha_3 = 3, \theta_3 = 0.4)$, which increases initially, reaches to a pick point, then start decreasing and saturates over time for τ_{VS} in (9.5), (c) shows the trajectory of the susceptible state based on the equation (6.7) with corresponding ADFE line based on the equation (6.13), and the trajectory of the vaccinated state based on the equation (6.7) with corresponding ADFE line based on the equation (6.13).

trend for the susceptible state, that becomes bounded in the ADFE. Again, in Figure 12(c), the trajectory of the vaccinated state, $V_0^*(t)$, denoted by dotdash line, stables initially due to hesitation to take a vaccine. Later over time, the vaccine efficacy grows and more people remain immune; as a result, the number of persons with vaccine immunity rises and the trend grows and remains bounded in the ADFE.

Trajectories based on the Equation (6.7) and ADFE based on the Theorem 6.3

Consider, the random time until a susceptible person is vaccinated, $\tau_{SV} \sim Lindley(\theta > 0)$ with scale parameter θ ; and the hazard rate of the *Lindley distribution* (cf.¹⁷) is defined in (9.1). It can be shown that $\limsup_{t \rightarrow \infty} \alpha_{\tau_{SV}}(t) = \theta$. Let, the rate of vaccination in a population is $\theta = 0.03$. Hence, the initial value of $\alpha_{\tau_{SV}}(0) = \frac{0.03^2}{1+0.03} = 0.0008737864$, then the HRF $\alpha_{\tau_{SV}}(t)|_{Lindley(\theta)}$ increases monotonically, remains bounded at $\theta = 0.03$ over time, satisfies the shape of the Hypothesis 5.1(H4.), and is depicted in Figure 13(a). Which suggests a growing desire for vaccination, the population is well sensitized, and educated about a good vaccine. Again, consider the random time until each vaccine dose of type i wanes, $\tau_{v_i} \sim GPGWD(\alpha_i > 0, \lambda_i > 0, \theta_i > 0, b_i > 0)$, $i = 1, 2, \dots, n$, where, α_i represents the initial biological responses to the vaccine, λ_i represents the time scale and affects the duration of vaccine efficacy, θ_i indicates the vaccine efficacy declines rate, b_i affects the modulation of the hazard rate over time (cf.³³). Here, the reliability of the vaccine immunity is a competing risk with a *parallel competitive lifetime arrangement* for all n doses (cf.²²). This implies that the time until the system wanes, is given by $\tau_{VS}(t) = \max(\tau_{v_1}, \tau_{v_2}, \dots, \tau_{v_n})$. Furthermore, it is easy to show that the HRF for $\tau_{VS}(t)$ is given by the sum of the HRF of the lifetime of the components i.e.,

$$\alpha_{\tau_{VS}}(t) = \sum_{i=1}^n h(t)|_{GPGWD(\alpha_i, \lambda_i, \theta_i, b_i)} = \sum_{i=1}^n \alpha_i \lambda_i \theta_i b_i t^{\alpha_i - 1} (1 + \lambda_i t^{\alpha_i})^{\theta_i - 1}, t \geq 0. \quad (9.6)$$

If three different vaccine doses are considered in the model, i.e. $n = 3$, then for the parallel system,

$$\alpha_{\tau_{VS}}(t)|_{GPGWD(\alpha_i, \lambda_i, \theta_i, b_i)} = \sum_{i=1}^3 \alpha_i \lambda_i \theta_i b_i t^{\alpha_i - 1} (1 + \lambda_i t^{\alpha_i})^{\theta_i - 1}, i = 1, 2, 3. \quad (9.7)$$

Based on the three different sets of parameters for the GPGWD as $(\alpha_i = 1.2, \lambda_i = 0.01, \theta_i = 1.8, b_i = 1.5)$, $(\alpha_i = 1.3, \lambda_i = 0.01, \theta_i = 1.8, b_i = 1.5)$, and $(\alpha_i = 1.4, \lambda_i = 0.01, \theta_i = 1.8, b_i = 1.5)$; the HRF is computed, satisfies the shape of the Hypothesis 5.1(H4.), and is depicted in Figure 13(b). The HRF represents low risk initially, and it rises monotonically over time. Which suggests that, initially the vaccine works well, but the vaccine's efficacy starts decreasing against the disease; the failure rate of the vaccine rises over time. For the other parameters of the model (3.21)-(3.23) that do not depend on time, it is assumed that the average influx rate, $B = 0.00024525$. For simplicity, it is assumed that the lifetime until natural death is exponentially distributed i.e. $\tau_{ND} \sim Exponential(\lambda = 0.0132275132)$. This implies that the HRF is $\alpha_{\tau_{ND}} = 0.0132275132$ per year. By using the above HRFs and the equation (6.7),

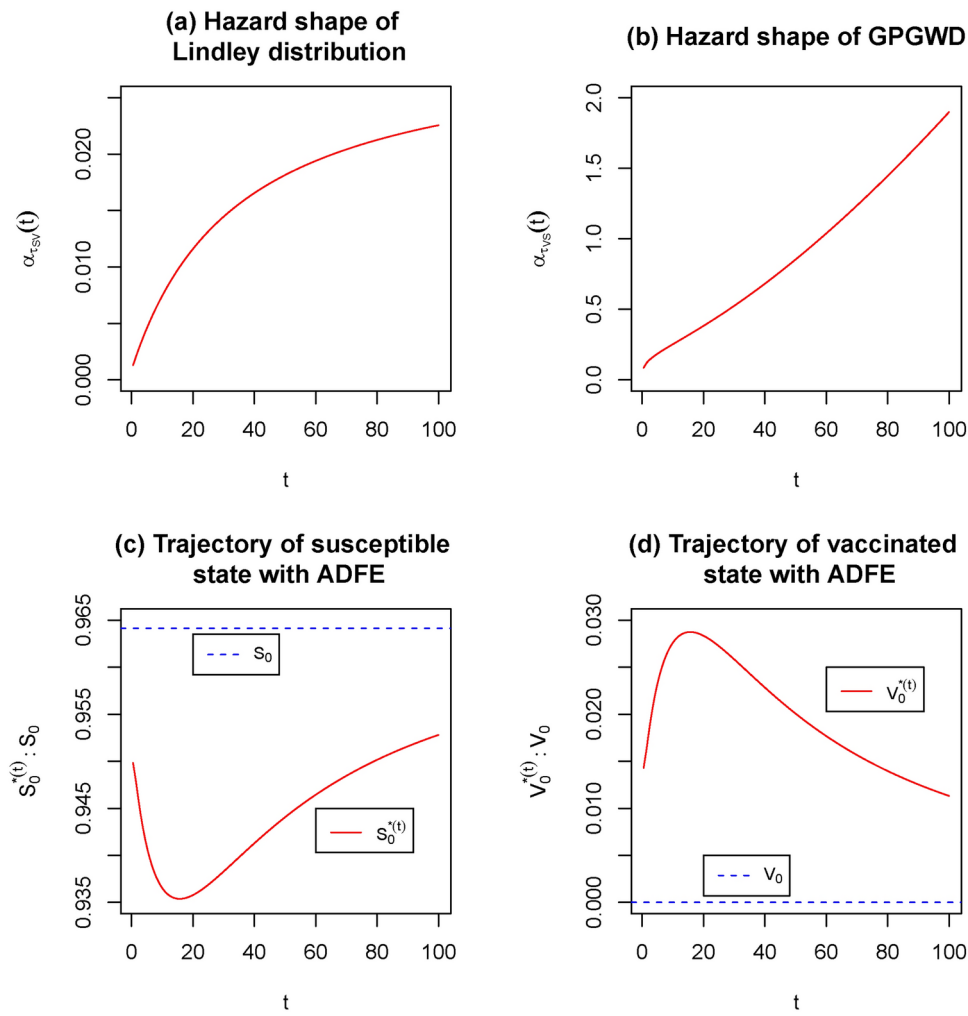


Fig. 13. Shows the different shapes of the HRFs, trajectories, and ADFE of subsection 9.3. Note, (a) shows the shape of the HRF of the *Lindley distribution* with shape parameter $\theta = 0.03$, which has a monotonically increasing shape over time for τ_{SV} in (9.1), (b) shows the shape of the HRF of the *GPGWD* with three different sets of parameters as $(\alpha_1 = 1.2, \lambda_1 = 0.01, \theta_1 = 1.8, b_1 = 1.5)$, $(\alpha_2 = 1.3, \lambda_2 = 0.01, \theta_2 = 1.8, b_2 = 1.5)$, and $(\alpha_3 = 1.4, \lambda_3 = 0.01, \theta_3 = 1.8, b_3 = 1.5)$, which has an increasing shape over time for τ_{VS} in (9.7), (c) shows the trajectory of the susceptible state based on the equation (6.7) with corresponding ADFE line based on the equation (6.15), and (d) shows the trajectory of the vaccinated state based on the equation (6.7) with corresponding ADFE line based on the equation (6.15).

the trajectories of $S_0^*(t)$, $V_0^*(t)$ against time t are computed, and depicted in Figure 13(c), and Figure 13(d), respectively. The corresponding ADFE based on the Theorem 6.3 is depicted into the figures, denoted by the dashed line. Note that, no trajectory for the infectious state, $I_0^*(t)$ is presented due to 0 value in (6.7).

Here, the trajectory of the susceptible state, $S_0^*(t)$ in the Figure 13(c), denoted by solid line, decreases initially, reaches to a minimum point, then increases over time into the ADFE S_0^* . Which suggests that if the system remains in a zero-rate over time (i.e. ZRSFs exist), then initially due to, for instance, good vaccination education, and high vaccine efficacy, susceptible people are willing to receive vaccinations, and over time, the number of susceptible people who are without immunity remain in a minimum point. Later over time, more vaccinated people lose immunity due to failure of vaccine efficacy, and the number of the susceptible people rises. This results in an increasing trend for the susceptible state, that becomes bonded in the ADFE. Again, in Figure 13(d), the trajectory of the vaccinated state, $V_0^*(t)$, denoted by solid line, increases initially due to use of effective vaccine, and reaches to a peak point. Later over time, the vaccine efficacy becomes low and more people lose immunity; as a result, the number of persons with vaccine immunity decreases and the decreasing trend remains bounded in the ADFE.

Trajectories based on the Equation (6.7) and ADFE based on the Theorem 6.4

Consider, the random time until a susceptible person is vaccinated, $\tau_{SV} \sim EWFD(\alpha > 0, \theta > 0, \sigma > 0)$ (cf.³¹), and the hazard rate of the *EWFD* is defined as,

$$\alpha_{\tau_{SV}}(t) = h(t)|_{EWFD(\theta)} = \frac{\left(\frac{\alpha\theta}{\sigma}\right)\left(\frac{t}{\sigma}\right)^{\alpha-1}e^{-(\frac{t}{\sigma})^\alpha}\left(1-e^{-(\frac{t}{\sigma})^\alpha}\right)^{\theta-1}}{1-\left(1-e^{-(\frac{t}{\sigma})^\alpha}\right)^\theta}, t \geq 0. \quad (9.8)$$

Let, the parameters value as ($\alpha = 0.2$, $\theta = 0.5$, and $\sigma = 2$). Hence, the initial value of $\alpha_{\tau_{SV}}(0) = 0.359510424$, then the HRF $\alpha_{\tau_{SV}}|_{EWFD}$ decreases monotonically, remains bounded at 0.004544480 over time, satisfies the shape of the Hypothesis 5.1(H3.), and is depicted in Figure 14(a). Which suggests a declining trend in vaccination, the population hesitant due to false rumors, and low vaccine efficacy. Again, consider the random time until each vaccine dose of type i wanes, $\tau_{v_i} \sim GPGWD(\alpha_i > 0, \lambda_i > 0, \theta_i > 0, b_i > 0)$, $i = 1, 2, \dots, n$ (cf.³³), and the reliability of the vaccine immunity is a competing risk with a *parallel competitive lifetime arrangement for all n doses* (cf.²²). This implies that the time until the system wanes, is given by $\tau_{VS}(t) = \max(\tau_{v_1}, \tau_{v_2}, \dots, \tau_{v_n})$. Furthermore, it is easy to show that the HRF for $\tau_{VS}(t)$ is given by the sum of the HRF of the lifetime of the components i.e.,

$$\alpha_{\tau_{VS}}(t) = \sum_{i=1}^n h(t)|_{GPGWD(\alpha_i, \lambda_i, \theta_i, b_i)} = \sum_{i=1}^n \alpha_i \lambda_i \theta_i b_i t^{\alpha_i-1} (1 + \lambda_i t^{\alpha_i})^{\theta_i-1}, t \geq 0. \quad (9.9)$$

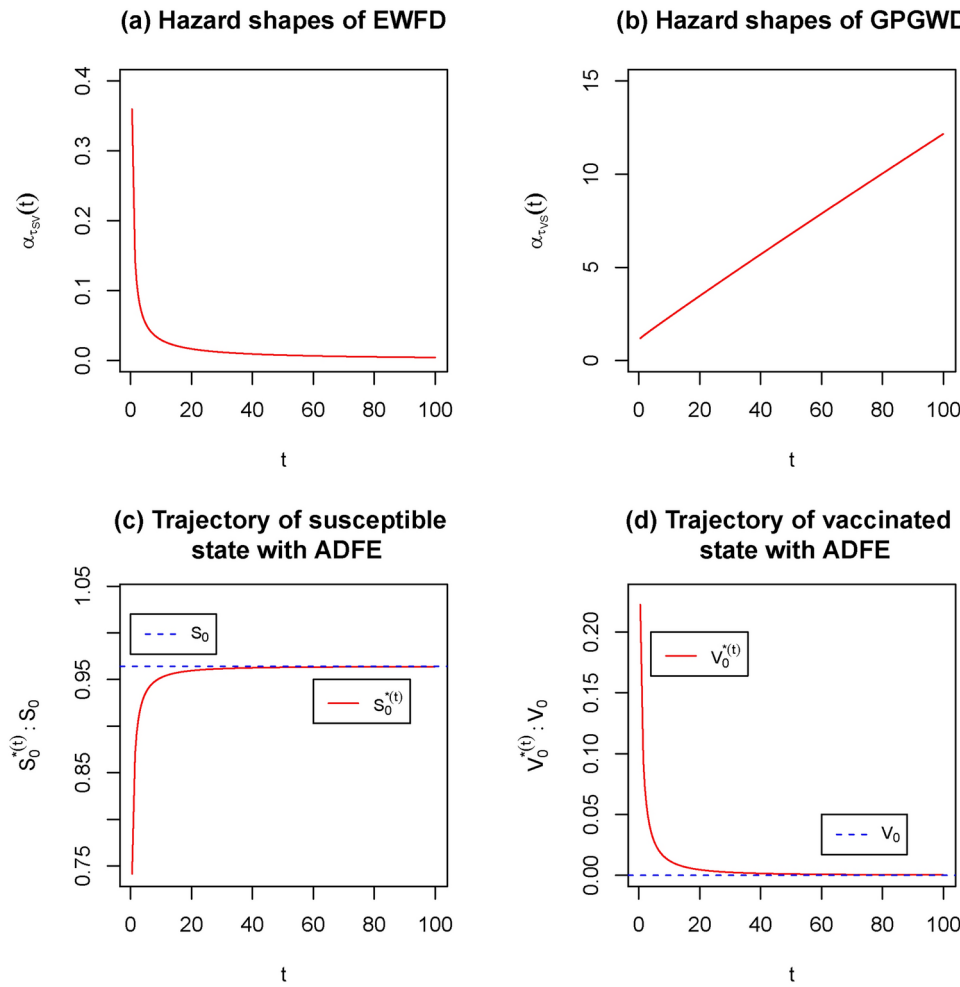


Fig. 14. Shows the different shapes of the HRFs, trajectories, and ADFE of subsection 9.4. Note, (a) shows the shape of the HRF of the EWFD with parameters value as ($\alpha = 0.2$, $\theta = 0.5$, and $\sigma = 2$), which has a monotonically decreasing shape, and saturates over time for τ_{SV} in (9.8), (b) shows the shape of the HRF of the GPGWD with three different sets of parameters as $(\alpha_1 = 1, \lambda_1 = 0.1, \theta_1 = 1.9, b_1 = 2)$, $(\alpha_2 = 1.01, \lambda_2 = 0.1, \theta_2 = 1.9, b_2 = 2)$, and $(\alpha_3 = 1.05, \lambda_3 = 0.1, \theta_3 = 1.9, b_3 = 2)$, which has a monotonically increasing shape for over time for τ_{VS} in (9.10), (c) shows the trajectory of the susceptible state based on the equation (6.7) with corresponding ADFE line based on the equation (6.16), and (d) shows the trajectory of the vaccinated state based on the equation (6.7) with corresponding ADFE line based on the equation (6.16).

If three different vaccine doses are considered in the model, i.e. $n = 3$, then for the parallel system,

$$\alpha_{\tau_{VS}}(t)|_{GPGWD(\alpha_i, \lambda_i, \theta_i, b_i)} = \sum_{i=1}^3 \alpha_i \lambda_i \theta_i b_i t^{\alpha_i - 1} (1 + \lambda_i t^{\alpha_i})^{\theta_i - 1}, i = 1, 2, 3. \quad (9.10)$$

Based on the three different sets of parameters for the GPGWD as, $(\alpha_1 = 1, \lambda_1 = 0.1, \theta_1 = 1.9, b_1 = 2), (\alpha_2 = 1.01, \lambda_2 = 0.1, \theta_2 = 1.9, b_2 = 2),$ and $(\alpha_3 = 1.05, \lambda_3 = 0.1, \theta_3 = 1.9, b_3 = 2)$, the HRF is computed, satisfies the shape of the Hypothesis 5.1(H4.), and is depicted in Figure 14(b). The HRF represents low risk initially, rises monotonically over time. Which suggests that, initially the vaccine works well, but vaccine's efficacy start decreasing against the disease; the failure rate of the vaccine rises over time. For the other parameters of the model (3.21)-(3.23) that do not depend on time, it is assumed that the average influx rate, $B = 0.00024525$. For simplicity, it is assumed that the lifetime until natural death is exponentially distributed i.e. $\tau_{ND} \sim \text{Exponential}(\lambda = 0.0132275132)$. This implies that the HRF is $\alpha_{\tau_{ND}} = 0.0132275132$ per year. By using the above HRFs and the equation (6.7), the trajectories of $S_0^*(t), V_0^*(t)$ against time t are computed, and depicted in Figure 14(c), and Figure 14(d), respectively. The corresponding ADFE based on Theorem 6.4 is given into the figures, denoted by the dashed line. Note that, no trajectory for the infectious state, $I_0^*(t)$ is presented due to the 0 value in equation (6.7).

Here, the trajectory of the susceptible state, $S_0^*(t)$ in the Figure 14(c), denoted by solid line, is monotonically increasing, and over time it remains bounded into the ADFE S_0^* . Which suggests that if the system remains in a zero-rate over time (i.e. ZRSFs exist), then due to, for instance, false rumors, and low vaccine efficacy, susceptible people are unwilling to receive vaccination, and over time, the number of susceptible people who are without immunity remain in the susceptible state. This results in an increasing trend for the susceptible state, that becomes bounded in the ADFE. Again, in Figure 14(d), the trajectory of the vaccinated state $V_0^*(t)$, denoted by solid line, is monotonically decreasing due to the use of the low effective vaccine, rumors, and hesitation to receive the vaccine. As a result, the number of vaccinated persons with vaccine immunity decreases over time and the trend remains bounded in the ADFE.

Numerical simulation to characterizes the behavior of the ZRSF of the system (3.21)-(3.23) with respect to the HRFs

If the HRF $\alpha_\tau(t) \in \{\alpha_{\tau_{SV}}(t), \alpha_{\tau_{VS}}(t), \alpha_{\tau_{ND}}(t)\}$ satisfy any of the assumptions in Hypothesis 5.1 (H1.) – (H4.); then the ZRSFs in (6.7) of the system (3.21)-(3.23) satisfy the conditions in (7.8), and (7.9) in the absence of disease.

According to the conditions in (7.8), the ZRSF $S_0^*(t)$ increase monotonically if $\alpha_{\tau_{SV}}(t) + \alpha_{\tau_{ND}}(t) \geq 1$ holds, otherwise decreases monotonically with respect to the HRF $\alpha_{\tau_{SV}}(t)$. Figure 15(a) depicts the condition of $\alpha_{\tau_{SV}}(t) + \alpha_{\tau_{ND}}(t)$ in (7.8), and Figure 16(c) depicts the trajectory of the susceptible state, $S_0^*(t)$. The Figure 15(a) makes it evident that the requirement $\alpha_{\tau_{SV}}(t) + \alpha_{\tau_{ND}}(t) < 1$ holds, hence the Figure 16(c) displays a monotonically decreasing shape of $S_0^*(t)$, validating one of the criteria in (7.8). In addition, according to the condition in (7.9), the ZRSF $V_0^*(t)$ increases monotonically if $y_\alpha(t)z_\alpha(t) \geq \frac{1}{2}$ holds, otherwise decreases monotonically with respect to the HRF $\alpha_{\tau_{SV}}(t)$. Figure 15(b) shows the condition of $y_\alpha(t)z_\alpha(t)$ in (7.9), and Figure 16(d) shows the trajectory of the vaccinated state $V_0^*(t)$. The Figure 15(b) makes it evident that the condition $y_\alpha(t)z_\alpha(t) \geq \frac{1}{2}$ holds, hence the Figure 16(d) displays a monotonically increasing shape of $V_0^*(t)$, validating one of the conditions in (7.9).

Moreover, if the HRF $\alpha_\tau(t) \in \{\alpha_{\tau_{SV}}(t), \alpha_{\tau_{VS}}(t), \alpha_{\tau_{ND}}(t)\}$ satisfy any of the assumptions in Hypothesis 5.1 (H1.) – (H4.), and $f_\alpha(t)$ is defined in (7.7), then the ZR solutions in (6.7) of the system (3.21)-(3.23) satisfy the conditions in (7.10) in the absence of disease.

Now, according to the conditions in (7.10), the ZRSF $S_0^*(t)$ always increases monotonically if the HRF $\alpha_{\tau_{VS}}(t)$ increases, otherwise the result gives the opposite. Figure 16(b) depicts the HRF $\alpha_{\tau_{VS}}(t)$ in (7.10), and the Figure 16(c) depicts the trajectory of the susceptible state, $S_0^*(t)$. The Figure 16(c) depicts a monotonically decreasing shape since the Figure 16(b) shows a decreasing shape of the HRF $\alpha_{\tau_{VS}}(t)$, which validates one of the condition in (7.10).

Finally, according to the conditions in (7.10), the ZRSF $V_0^*(t)$ increases monotonically if $f_\alpha(t) \geq 1$ holds, otherwise decreases monotonically with respect to the HRF $\alpha_{\tau_{VS}}(t)$. Figure 15(c) depicts the condition of $f_\alpha(t)$ in (7.10), and Figure 16(d) depicts the trajectory of the vaccinated state, $V_0^*(t)$. The Figure 15(c) makes it evident that the condition $f_\alpha(t) < 1$ holds, hence the Figure 16(d) depicts an increasing shape of the ZRSF $V_0^*(t)$, while the Figure 16(b) shows a decreasing shape of the HRF $\alpha_{\tau_{VS}}(t)$, validating one of the conditions in (7.10).

Discussion

The development of compartmental models with underlying renewal processes in Section 2 represents a significant advancement in the modeling of general dynamic processes such as disease dynamics, particularly in the context of the SVIS (Susceptible-Vaccinated-Infected-Susceptible) epidemic model. This study addresses the limitations of traditional compartmental models that assume exponentially distributed lifetime stages, which are often unrealistic due to the constant hazard rate assumption. The theoretical framework for the SVIS model in Section 3 introduces a non-autonomous nonlinear system (NANLS) of ordinary differential equations (ODEs), where the coefficients are hazard rate functions (HRFs) for the non-MAC transition event interjump times. This approach includes more realistic lifetime distributions that better represent the complexities of disease transmission and vaccine efficacy. The exploration of different HRF shapes- monotonic, bathtub,

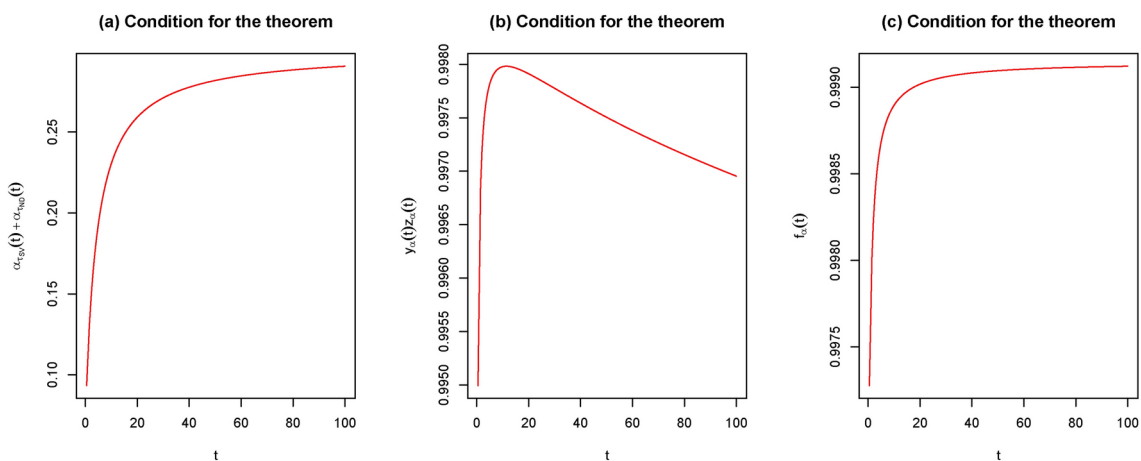


Fig. 15. Shows the conditions of the Theorem 7.1. Note, (a) shows the condition of (7.8), where $\alpha_{\tau_{SV}}(t) + \alpha_{\tau_{ND}}(t) < 1$, (b) shows the condition of (7.9), where $y_\alpha(t)z_\alpha(t) \geq \frac{1}{2}$, and (c) shows the condition of (7.10), where $f_\alpha(t) < 1$.

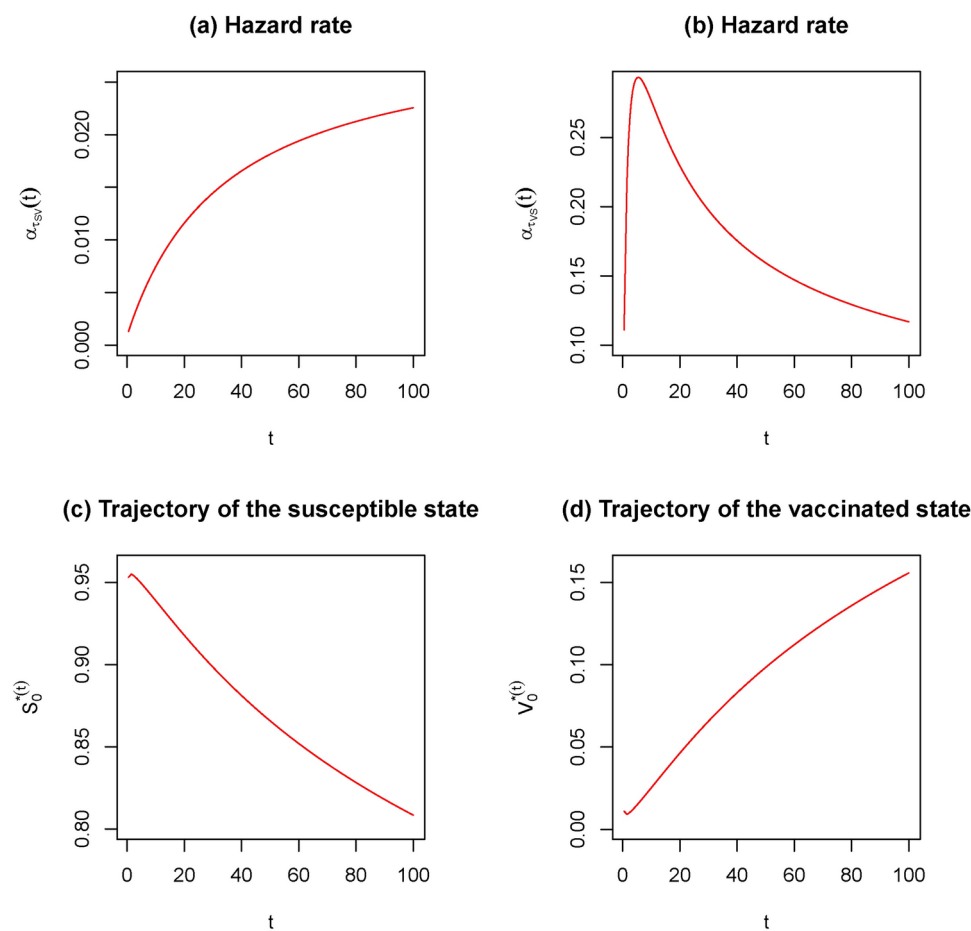


Fig. 16. Shows the different shapes of the HRFs, and trajectories to describe the Theorem 7.1. Note, (a) shows the shape of the HRF $\alpha_{\tau_{SV}}(t)$, which has a monotonically increasing shape over time, (b) shows the shape of the HRF $\alpha_{\tau_{VS}}(t)$, which increases initially, reaches to a pick point, then start decreasing, (c) shows the trajectory of the susceptible state, $S_0^*(t)$, which increases initially, then starts decreasing over time, and (d) shows the trajectory of the vaccinated state, $V_0^*(t)$, which decreases initially, then starts increasing over time.

reverse bathtub, and constant in Sections 5 & 6 leads to insights on how the hazard behaviors affect disease control strategies. In fact, the time dependent BRN $\mathfrak{R}_0(t)$, $t > 0$ and other control parameters in the theoretical model in Section 8 bear on the HRFs that reflect the asymptotic behaviors of the disease dynamics i.e. disease eradication $\mathfrak{R}_0(t) < 1$ or persistence $\mathfrak{R}_0(t) \geq 1$. Furthermore, for a family of HRFs that asymptotically behave as the exponential distribution, the proposed theoretical NANLS becomes asymptotically ANLS, and there exists a time $t_1 > 0$, sufficiently large, where for $t \in [0, t_1]$ the disease dynamics evolves in the path strongly influenced by the nonlinear characters of the HRFs; and notwithstanding the Markovian behavior of the system for $t \in [t_1, \infty)$, there are multiple ADFEs possible. The analytical results are substantiated by a practical example and numerical simulation results in Sections 8 & 9 that exhibit the superior advantages of the proposed model to represent complex risk behaviors for non-MAC transition events in the disease dynamics, specifically for a vaccine with low efficacy with a marginal positive effect on recovery. For instance, it is shown that the monotonic increasing HRF of the Lindley distribution offers a more plausible representation of vaccine immunity waning over time, compared to the constant exponential rate assumed in Markovian models. The monotonic decreasing and increasing HRFs, respectively, for the gamma distribution depict the declining recovery rate and rising fatality of the disease overtime. More examples with more advanced and flexible lifetime distributions are given in Section 9.

Nevertheless, the sensitivity analysis of the SVIS model to different HRF behaviors in Section 7 reveals critical insights into the asymptotic properties of the epidemic system. Indeed, by examining the ZRSF of the NANLS SVIS model, insights are obtained on the long-term outcomes of various vaccination strategies and their impact to achieve disease-free equilibrium. It is observed that the effectiveness of vaccination strategies/programs are influenced by numerous factors, such as vaccine type lifetimes, multiple dosage lifetimes, and population behavior. The proposed model offers a framework to evaluate these factors and optimize vaccination strategies for better disease management. This study contributes to epidemic modeling and survival analysis providing a more realistic and detailed framework for the integration of renewal processes in compartmental models. Future research should focus on empirical validation of these models by using real-world data and exploring the application of this framework to other compartmental infectious diseases. By bridging the gap between theoretical models and practical applications, there is effective and efficient response and management of future epidemics.

Note that the assumptions for memory and memoryless properties for lifetime distributions in Remark 3.1 have important consequences for a disease dynamics. This necessitates more advanced tools for analyzing multiscales and fractional derivatives^{51–53} to investigate the impacts of memory in the system as a future work.

Conclusion

In this study, a general model for the transition rates between jumps in a renewal process for a dynamic epidemic process is derived. The model is applied to study the impacts of the HRFs (hazard rate functions) of the interjump times in a SVIS disease epidemic dynamics. The newly obtained SVIS model characterizing the average dynamics of the underlying renewal process is a NANLS (non-autonomous nonlinear system) of o.d.e.s., where the system coefficients are HRFs. Moreover, the NANLS is asymptotically autonomous. The importance of the HRFs to determine disease eradication outcomes is investigated by studying the impacts of the asymptotic behavior of the HRFs on the existence of an ADFE (asymptotic disease-free equilibrium). Four qualitative behaviors of the HRFs over time - *a monotonic, bathtub, reverse bathtub, and constant shapes* are explored to determine the outcome of the ADFE. The results indicate that HRFs play a crucial role in determining the outcomes of epidemic dynamics in both the short-term and long-term. Moreover, an ANLS (autonomous nonlinear system) of o.d.e epidemic model is very limited to explain disease dynamics over short-term. Numerical simulation results are given for several lifetime distributions exhibiting various shapes for their HRFs, that represent different lifetimes for vaccine efficacy and artificial immunity; random time until vaccination, and also survival until death.

Data availability

All data generated or analysed during this study are included in this published article. There was no specific dataset used in this study. All data is based on simple mathematical simulations in R, and easily replicated.

Received: 3 January 2024; Accepted: 15 November 2024

Published online: 14 January 2025

References

1. Bailey, Norman T.J. *The mathematical theory of infectious diseases and its applications*. Charles Griffin & Company Ltd, 5a Crendon Street, High Wycombe, Bucks HP13 6LE., (1975).
2. Wanduku, Divine. A novel complex social network rumor stochastic model: Convergence in distribution to a final rumor size. *Heliyon* **9**(4), e15125 (2023).
3. Allen, L. An introduction to stochastic epidemic models. In *Mathematical Epidemiology* (eds Wu, J. et al.) 81–130 (Springer, Berlin, Heidelberg, 2008).
4. Voit, E. O., Martens, H. A. & Omholt, S. W. 150 years of the mass action law. *PLOS Computational Biology* **11**, e1004012 (2015).
5. Komorowski, M., Costa, M. J., Rand, D. A. & Stumpf, M. P. Sensitivity, robustness, and identifiability in stochastic chemical kinetics models. *Proc. Natl. Acad. Sci. USA* **108**, 8645–8650 (2011).
6. Jiang, R., Singh, P., Wrede, F., Hellander, A. & Petzold, L. Identification of dynamic mass-action biochemical reaction networks using sparse bayesian methods. *PLoS Comput Biol.* **18**, e1009830 (2022).
7. Greenwood, Priscilla E., & Gordillo, Luis F. *Stochastic Epidemic Modeling*, pages 31–52. Springer Netherlands, Dordrecht, (2009).
8. Saha, Sangeeta, Dutta, Protimsha & Samanta, Guruprasad. Dynamical behavior of sirs model incorporating government action and public response in presence of deterministic and fluctuating environments. *Chaos, Solitons & Fractals* **164**, 112643 (2022).
9. Dutta, P., Samanta, G. & Nieto, J. J. Periodic transmission and vaccination effects in epidemic dynamics: a study using the svivis model. *Nonlinear Dyn* **112**, 2381–2409 (2024).

10. Shim, Eunha. A note on epidemic models with infective immigrants and vaccination. *Mathematical Biosciences & Engineering* **3**(3), 557–566 (2006).
11. Wanduku, Divine. The multilevel hierarchical data em-algorithm. applications to discrete-time markov chain epidemic models. *Heliyon* **8**(12), e12622 (2022).
12. Wanduku, Divine, Jegede, Omotomilola, Rahul, Chinmoy, Oluyede, Broderick, & Farotimi, Oluwaseun. 4 - on a novel seirs markov chain epidemic model with multiple discrete delays and infection rates: modeling and sensitivity analysis to determine vaccination effects. In Hemen Dutta and Khalid Hattaf, editors, *Advances in Epidemiological Modeling and Control of Viruses*, pages 95–143. Academic Press, (2023).
13. Casella, George, & Berger, L. Roger. *Statistical Inference*. cengage, Belmont, CA, (2002).
14. Feng, Z., Xu, D. & Zhao, H. Epidemiological models with non-exponentially distributed disease stages and applications to disease control. *Bull Math Biol.* **69**, 1511–36 (2007).
15. Francesco, Di Lauro et al. Dynamic survival analysis for non-markovian epidemic models. *J. R. Soc. Interface* **19**, 20220124 (2022).
16. Sherborne, N., Miller, J. C., Blyuss, K. B. & Kiss, I. Z. Mean-field models for non-markovian epidemics on networks. *Journal of mathematical biology* **76**, 755–778 (2018).
17. Ghitany, M. E., Atieh, B. & Nadarajah, S. Lindley distribution and its application. *ScienceDirect* **78**, 493–506 (2007).
18. Pang, Guodong & Pardoux, Étienne. Functional limit theorems for non-Markovian epidemic models. *The Annals of Applied Probability* **32**(3), 1615–1665 (2022).
19. Franco, E., Diekmann, O. & Gyllenberg, M. Modelling physiologically structured populations: renewal equations and partial differential equations. *J. Evol. Equ.* **23**, 46 (2023).
20. Hethcote, H. & Tudor, D. Integral equation models for endemic infectious diseases. *J. Math. Biol.* **9**, 37–47 (1980).
21. Lloyd, A. Realistic distributions of infectious periods in epidemic models. *Theor. Pop. Biol.* **60**, 59–71 (2001).
22. Rausand, Marvin. *SYSTEM RELIABILITY THEORY Models, Statistical Methods, and Applications*. John Wiley & Sons, Inc., second edition edition, (2004).
23. Lee, E. T. & Wang, J. W. *Statistical Methods for Survival Data Analysis*. A John Willy & Sons, Inc, third edition, (2003).
24. Wanduku, Divine. Complete global analysis of a two-scale network sirs epidemic dynamic model with distributed delay and random perturbations. *Applied Mathematics and Computation* **294**, 49–76 (2017).
25. Wanduku, Divine. On the almost sure convergence of a stochastic process in a class of nonlinear multi-population behavioral models for hiv/aids with delayed art treatment. *Stochastic Analysis and Applications* **39**(5), 861–897 (2021).
26. Mateus, Joaquim P. & Silva, César. M. A non-autonomous seirs model with general incidence rate. *Applied Mathematics and Computation* **247**, 169–189 (2014).
27. Castillo-Chávez, Carlos, & Thieme, Horst R. Asymptotically autonomous epidemic models. In Ovide Arino, David E Axelrod, Marek Kimmel, and Michel Langlais, editors, *Mathematical Population Dynamics: Analysis and heterogeneity*, page 33. Wuerz Publishing Ltd., Winnipeg, Canada, (1995).
28. Markus, L. Asymptotically autonomous differential systems. contributions to the theory of nonlinear oscillations iii (s. lefschetz,ed. *Annals of Mathematics Studies*, 36:17–29, (1956).
29. Jaisingh, Lloyd R. Competing risks in parallel and series systems. *Microelectronics Reliability* **28**(3), 469–485 (1988).
30. Walck, C. *Handbook on Statistical Distributions for Experimentalists*. Particle Physics Group (Fysikum University of Stockholm, 2007).
31. Mudholkar, G. S. & Srivastava, D. K. Exponentiated weibull family for analyzing bathtub failure-rate data. *IEEE Transactions on Reliability* **42**, 299–302 (1993).
32. Seo, J. I. & Kang, S. B. Notes on the exponentiated half logistic distribution. *Elsevire* **39**, 6491–6500 (2015).
33. Selim, M.A. The generalized power generalized weibull distribution: Properties and applications. *arXiv*, 2:15, (2018).
34. Ibe, Oliver C. *Markov Processes for Stochastic Modeling*. Elsevier Inc., 2nd edition, (2013).
35. MEDHI, J. Chapter 1 - stochastic processes. In J. MEDHI, editor, *Stochastic Models in Queueing Theory (Second Edition)*, pages 1–46. Academic Press, Burlington, second edition edition, (2003).
36. Center for disease control and prevention (cdc), *Stay Up to Date with COVID-19 Vaccines Including Boosters*. <https://www.cdc.gov/coronavirus/2019-ncov/vaccines/stay-up-to-date.html>. [Page last reviewed: October 25, 2022].
37. Taboe, Hemaho B., Asare-Baah, Michael, Iboi, Enahoro A. & Ngonghala, Calistus N. Critical assessment of the impact of vaccine-type and immunity on the burden of covid-19. *Mathematical Biosciences* **360**, 108981 (2023).
38. Ngonghala, Calistus N., Taboe, Hemaho B., Safdar, Salman & Gumel, Abba B. Unraveling the dynamics of the omicron and delta variants of the 2019 coronavirus in the presence of vaccination, mask usage, and antiviral treatment. *Applied Mathematical Modelling* **114**, 447–465 (2023).
39. Wanduku, Divine. Threshold conditions for a family of epidemic dynamic models for malaria with distributed delays in a non-random environment. *International Journal of Biomathematics* **10**, 1850085 (2018).
40. Wanduku, Divine & Ladde, G. S. A two-scale network dynamic model for human mobility process. *Mathematical Biosciences* **229**(1), 1–15 (2011).
41. Zhou, Fei et al. Clinical course and risk factors for mortality of adult inpatients with covid-19 in wuhan, china: a retrospective cohort study. *Lancet* **395**, 1054–62 (2020).
42. WHO. Without treatment, how quickly can a person living with hiv become ill? Accessed on June 29, (2024).
43. Ghitany, M. E., Atieh, B. & Nadarajah, S. Lindley distribution and its application. *Mathematics and Computers in Simulation* **78**(4), 493–506 (2008).
44. Ott, R. Lyman, & Longnecker, Michael. *An Introduction to Statistical Methods and Data Analysis*. Brooks/Cole, Cengage Learning, (2015).
45. Daniel, Wayne W. *Applied Nonparametric Statistics* (PWS-Kent, Boston, 1990).
46. WANDUKU, DIVINE, & LADDE, G.S. Fundamental properties of a two-scale network stochastic human epidemic dynamic model. *Neural, Parallel, and Scientific Computations* **19**, 229–270 (2011).
47. Oluyede, Broderick, Chipepa, Fastel & Wanduku, Divine. The odd weibull-topp-leone-g power series family of dis-tributions: model, properties, and applications. *Journal of Nonlinear Sciences and Applications* **14**, 268–286 (2021).
48. Oluyede, Broderick O., Jimoh, Hameed Abiodun, Wanduku, Divine & Makubate, Boikanyo. A new generalized log-logistic erlang truncated exponential distribution with applications. *Electronic Journal of Applied Statistical Analysis (EJASA)* **13**(2), 293 (2020).
49. Chipepa, Fastel, Wanduku, Divine & Oluyede, Broderick O. Half logistic odd weibull-topp-leone-g family of distributions: Model, properties and applications. *Afrika Statistika* **15**(4), 2481 (2020).
50. Oluyede, Broderick O., Fagbamigbe, A., Makubate, B., & Wanduku, D. The exponentiated generalized power series: Family of distributions: theory, properties and applications. *Heliyon*, 6(8), (2020).
51. Hattaf, Khalid. A new mixed fractional derivative with applications in computational biology. *Computation* **12**, 7 (2024).
52. Hattaf, Khalid. A new class of generalized fractal and fractal-fractional derivatives with non-singular kernels. *Fractal and Fractional* **7**, 395 (2023).
53. Alkhazzan, Abdulwasea, Wang, Jungang, Nie, Yufeng & Hattaf, Khalid. A new stochastic split-step θ -nonstandard finite difference method for the developed svir epidemic model with temporary immunities and general incidence rates. *Vaccines* **10**, 1682 (2022).

Acknowledgements

Thanks to the editors and reviews for their suggestions that have improved the paper. The foundational ideas of this paper originated from M.M.Hasan's graduate thesis, directed by Prof. Divine Wanduku: Hasan, Md Mahmud, "Survival Lifetime Models for Competitive Vaccination Strategies, Recovery and Disease Related Death in Infectious Disease Dynamical Systems" (2022). Electronic Theses and Dissertations. 2510. Available at: <https://digitalcommons.georgiasouthern.edu/etd/2510>.

Author contributions

D.W. conceived the problems, supervised the project and wrote all proofs and remarks in the manuscript, and example in Section 8. M.M.H wrote the numerical simulation results section 9 of the manuscript. The authors give consent to publish this paper.

Funding

This paper was not supported by funding from any organization.

Declarations

Competing interests

The authors declare no competing interests.

Additional information

Correspondence and requests for materials should be addressed to D.W.

Reprints and permissions information is available at www.nature.com/reprints.

Publisher's note Springer Nature remains neutral with regard to jurisdictional claims in published maps and institutional affiliations.

Open Access This article is licensed under a Creative Commons Attribution-NonCommercial-NoDerivatives 4.0 International License, which permits any non-commercial use, sharing, distribution and reproduction in any medium or format, as long as you give appropriate credit to the original author(s) and the source, provide a link to the Creative Commons licence, and indicate if you modified the licensed material. You do not have permission under this licence to share adapted material derived from this article or parts of it. The images or other third party material in this article are included in the article's Creative Commons licence, unless indicated otherwise in a credit line to the material. If material is not included in the article's Creative Commons licence and your intended use is not permitted by statutory regulation or exceeds the permitted use, you will need to obtain permission directly from the copyright holder. To view a copy of this licence, visit <http://creativecommons.org/licenses/by-nc-nd/4.0/>.

© The Author(s) 2025